Implementation of Wide Area Protection System (WAPS) for Electrical Power System Smart Transmission Grids

By

Bright Tetteh

Supervisors: Mrs. Kehinde O. Awodele

Prof. Komla A. Folly

Dissertation submitted in partial fulfilment for the requirements of the degree of Master of Science in Electrical Engineering

Department of Electrical Engineering

University of Cape Town

South Africa

November 2020

Plagiarism Declaration

I know the meaning of plagiarism and declare that:

A. This dissertation is my unaided work, both in conception and execution, apart from the legal guidance of my supervisors. Where we have collaborated with other people, or we have used material generated by other researchers, the parties or materials are indicated in the acknowledgments or with references as appropriate.
B. The dissertation has not been submitted before for a degree at this University or any other University in part or whole.
C. I am now presenting the dissertation for examination for the MSc (Eng) Degree

Date: 11 November 2020

Name:	**Student Number**	**Signature**
Bright Tetteh	TTTBRI001	Signed by candidate

PUBLISHED RESEARCH PAPERS

These are the research papers written during this research

1. B. Tetteh and K. Awodele, "Power System Protection Evolutions from Traditional to Smart Grid Protection," *2019 IEEE 7th International Conference on Smart Energy Grid Engineering (SEGE)*, Oshawa, ON, Canada, 2019, pp. 12-16.

2. B. Tetteh, K. Awodele and K. Folly, "Real-Time Simulation of Power System Wide Area Protection," *2020 International SAUPEC/RobMech/PRASA Conference*, Cape Town, South Africa, 2020, pp. 1-6.

ABSTRACT

The planning, operation and control of the power system has been evolving since its inception. These changes are due to the advancement in science and technology, and changes in energy policy and customer demands. The envisioned power system - smart grid (SG) - is expected to have functional and operational capabilities that maximize the reliability, minimize generation deficit, and cost issues in the power system. However, many power systems in the world today still operate traditionally, with one-way communication and one-way power flow.

Transitioning to a smart grid influences the protection schemes of the power system, as the smart grid is to leverage distributed energy resources (DERs) using distributed generation (DG) units and allow for bi-directional flow of power and information. Therefore, there is a need for advanced protection schemes. Wide-area protection (WAP) techniques are proposed as one of the solutions to solve the protection challenges in the smart grid due to their reliance on wide-area information instead of local information.

This dissertation considered three WAP techniques which are differentiated based on the data used for faulted zone detection: (A) Positive sequence voltage magnitude (PSVM), (B) Gain in momentum (GIM) and (C) Sum of positive and zero sequence currents (SPZSC). The dissertation investigated their performances in terms of accuracy in detecting the faulted zones and the faulted lines, and fault clearing time. The investigation was done using three simulation platforms: MATLAB/Simulink, Real-Time (Software in the Loop (SIL)) and Hardware-in-the-Loop (HIL) implementation using Opal-RT and SEL-351A relay. The results show that, in terms of detecting the faulted zones, all the techniques investigated have 100% accuracy in all the 36 tested fault cases. However, in terms of identifying the faulted line in the faulted zone, the algorithms were not able to detect all the 36 tested cases accurately. In some cases, the adjacent line was detected instead of the actual faulted line. In those scenarios, the detected line and the faulted line present similar characteristics making the algorithms to detect the wrong line. For the faulted line detection accuracy, the algorithm (A) has an accuracy of 86%, (B) has an accuracy of 94% and (C) has an accuracy of 92%.

The fault clearing times of the algorithms were similar for both the MATLAB/Simulink and real-time simulation without the actual control hardware which was the SEL-351A relay. When the simulation was done with the control hardware through Hardware-in-the-loop, a communication

delay was introduced which increased the fault clearing times. The maximum fault clearing time for the techniques investigated through the HIL simulation are 404 ms, 256 ms, and 150 ms for the techniques (A), (B) and (C) respectively and this variation is due to the different fault detection methods used in the three algorithms. The fault clearing time includes communication between the Opal-RT real-time simulator and SEL-351A relay using RJ45 ethernet cable, these fault clearing times can change if a different communication medium is used. From the performance data presented, it is evident that these algorithms will perform better when used as backup protection since the common timer settings for backup protection schemes range from 1200 ms to 1800 ms, while primary protection is expected to respond almost instantaneously, that is, with no initial time delay.

ACKNOWLEDGMENT

First of all, I would like to thank my Lord and Savior Jesus Christ for His love and grace towards me, which has given me strength and many opportunities including the registration and funding for my master's degree, and the strength and wisdom to write this dissertation.

I would also like to thank the Mastercard foundation for the full funding support throughout my study. Your investment in the next generation of African leaders is highly appreciated, and it will yield the results that you desired.

My sincere thanks also go to my main supervisor Mrs. Awodele, for her motherly care, love, and immense support in carrying out this research. You started helping me even when I was home and have not yet registered for my degree. I came with high expectations, knowing that I will have a supportive supervisor and guess what? You exceeded those expectations. The investment you have made in me including valuable conversations we have had, and opportunities granted me are highly appreciated

I would also like to thank my co-supervisor Professor Komla Folly. Your exemplary leadership, support, and inputs are highly appreciated. I am forever grateful to have worked with you.

My sincere thanks also go to my family and friends who supported me in this journey; Emmanuel Ampomah, with whom I shared my daily life while carrying out this study and Jeff Watitwa with whom I shared my academic life while on this Journey. Your friendship and support have made this journey memorable. I would also like to thank the members of the power research group for your valuable inputs and constructive criticisms which helped in shaping this research into world-class research.

CONTENTS

LIST OF TABLES

LIST OF FIGURES

LIST OF ABBREVIATIONS

AC:	Alternating Current
ADC:	Analog to Digital converters
ADN:	Active Distribution Networks
ADSL:	Asymmetric digital subscriber line
ANM:	Active Network Management
BPZs:	Backup protection zones
CHIL:	Controller Hardware-in-the-Loop
CPP:	Critical peak pricing
CT:	Current Transformer
DAC:	Digital to Analog Converters
DC:	Direct Current
DER:	Distributed Energy Resources
DGs:	Distributed Generations
DLC:	Direct load control
DMT:	Definite minimum time
DRTS:	Digital real-time simulator
DSM:	Demand-side management
EMS:	Energy Management Systems
FAN:	Field area network
GHG:	Green House Gas
GIM:	Gain in Momentum
HDSL:	High-bit-rate digital subscriber line

HIL:	Hardware-In-the-Loop
HMI:	Human-machine interface
IDMT:	Inverse definite minimum time
IEDs:	Intelligent Electronic Devices
ILG:	Integer linear programming
LPC:	Local Protection Centre
MD:	Measuring devices
NAN:	Neighborhood area network
PDC:	Phasor Data Concentrator
PON:	Passive optical network
PDN:	Passive Distribution Networks
PHIL:	Power hardware-in-the-Loop
PLC:	Power Line Communication
PSVM:	Positive sequence voltage magnitude
PZs:	Protections zones
RER:	Renewable Energy Resources
RES:	Renewable Energy Sources
RTDS:	Real-Time Digital Simulator
RTP:	Real-time pricing
SCADA:	Supervisory Control and Data Acquisition
SDH:	Synchronous digital hierarchy
SEL:	Schweitzer Engineering Laboratories
SER:	Sequential event recorder

SG:	Smart Grid
SPZSC:	Sum of positive and zero sequence currents
SONET:	Synchronous optical networking
ToUP:	Time of use pricing
VDSL:	Very high-speed digital subscriber line
VPZ:	Vulnerable protection zone
WAC:	Wide Area Control
WADP:	Wide-area differential protection
WAMPAC:	Wide Area Monitoring, Protection and Control
WAN:	Wide area network
WAPC:	Wide Area Protection and Control
WAPS:	Wide Area Protection Systems
WDM:	Wavelength division multiplexing
XHP:	eXtra High Perfor

CHAPTER ONE: INTRODUCTION

1.1 Background

Improvement in technology has changed the operation of the power system in recent years. Demand for electrical energy for domestic and industrial purposes is on a constant rise. These make the power system equipment operate close to their system capacity limit, making them prone to failures and disturbances. Despite all these, the performance indexes for today's power system are even higher as customers demand more reliability at the minimum cost possible. These are due to the following: the introduction of electronic devices that are sensitive to power interruptions, the use of electric vehicles, the introduction of distributed generations in the form of renewable energy sources, etc. Hence the power system is required from the operator's perspective to operate more efficiently, reliably, and resiliently.

To achieve this, the term Smart Grid (SG) was introduced, referring to an electrical power grid which is smart in its operational and functional capabilities. Many utilities, institutions, and researchers came up with different kinds of definitions for the term 'Smart Grid,' the descriptions are based on the smart grid's operational and functional characteristics as well as the benefits derived from the smart grid. The flow of electrical energy and information is one–way only in the traditional grid, whereas the SG allows two - way flow of electrical power and information that will enable customer participation. For the smart grid to realize its vision, there are vital areas of the smart grid involving different technologies that must be developed, and these are the smart infrastructure system, the smart management system and the smart protection system [1].

The SG is to operate with self-healing capability, resiliency to system disturbances and natural disasters, and adaptiveness to the system operational dynamics. These functional requirements have changed the protection needs of the grid drastically, and this is the role of the smart protection in the smart grid. This intelligent grid protection requires a wide-area view of the grid in real-time, adaptiveness to the power system dynamics, and the ability to detect and clear faults. Over the years, science and technology have been advancing. Currently, we have fast communication and measuring devices. Hence, the protection requirements of the SG are achievable.

Several researchers have developed algorithms and schemes for Wide Area Protection Systems (WAPS) for smart grid applications. Most of these schemes are only applicable as backup protection due to low-speed communication and the need to process massive amounts of data, which make them not fast enough for primary protection. The Wide Area Protection (WAP) techniques have the sole purpose of preventing ***cascading failure*** caused by failure to trip and unnecessary tripping of the protection systems based on local information. Hence their role as backup protection will still serve the purpose. However, researchers have suggested that with the advancement in communication technology where we have 5G communication technology in the pipeline estimated to become operational from 2020 and there have been some pilots projects, the WAP techniques can serve the purpose of primary protection [2].

The main concern of researchers and utility companies as they seek to implement this new paradigm of protection is whether the WAP techniques have the needed accuracy and fault response time to serve their purpose of large-area blackout prevention. In this research, the performance of some selected Wide Area Protection (WAP) techniques in literature have been evaluated in terms of their accuracy and fault response time through MATLAB/Simulink simulation, real-time simulation (Software-In-the – Loop (SIL)), and Hardware-In-the-Loop (HIL) implementation.

1.2 Research Hypothesis, Questions, Aim, and Objectives

1.2.1 Research Hypothesis and Questions

Electrical engineers have always sought to operate the power system with increased reliability and efficiency, securely and safely, to reduce failures which may lead to wide-area blackouts. However, technological limitations have made it difficult. The "Smart Grid" emerged to address the limitations of the power system (generation, transmission, and distribution) [3]. An aspect of the smart grid is wide-area protection (WAP) based on a wide-area measurement system. WAP aims at preventing massive area blackout of the power system, hence improving reliability. Various WAP algorithms with different accuracies and speeds have been developed in the literature. A WAP algorithm can prevent wide area blackout, however its performance must be investigated before implementation using simulation methods that will evaluate how it will perform on the actual system. Hardware-in-the Loop simulation using real-time simulators can be used to evaluate the expected performance of different WAP algorithms on the actual power

system. Based on the above, the research hypothesis statement is "*With an advanced (fast) communication technology, WAP algorithms have the ability to serve as primary protection for the power system*". This will be investigated by answering the following questions:

1. How different is the smart grid from the traditional grid?
2. What role has WAMS in smart grid operations?
3. How can WAMS enhance the Monitoring, Protection, and Control of the smart grid?
4. How effective are WAP techniques in protecting the power system?
5. How fast can these WAP algorithms act to protect the power system?
6. With the advancement in communication technology, can these WAP techniques be used for primary protection?

1.2.2 Research Aim

To implement and evaluate wide area protection (WAP) techniques for power system transmission grids through MATLAB/Simulink simulation, real-time simulation, and Hardware-In-the-Loop (HIL) implementation.

1.2.3 Research Objectives

1. Provide Literature on Wide Area Measurement Systems.
2. Provide Literature on Smart Grid Technology.
3. Provide literature on power systems protection.
4. Simulate a standard power system in MATLAB/Simulink.
5. Evaluate selected algorithms/methods for power system wide-area protection using PMU data through MATLAB/Simulink simulation, Real-Time simulation using OPAL-RT and Hardware-In-the-Loop (HIL) simulation using SEL relays.

1.3 Research Scope and Limitations

The research is limited to investigating the use of Wide Area Measurement (WAM) data obtained from Phasor Measurement Unit (PMU) technologies for protection in power systems to enhance their reliable operation and security. The research aims at implementing and evaluating selected techniques for Wide Area Protection System (WAPS) in the power system. These techniques are evaluated based on the accuracy of fault detection and the speed of operation, thus the fault clearing

time. The research is focused on methods for transmission grids protection; hence the power system under study is the IEEE 9-bus power system.

1.4 Importance of this Research

All over the world, electrical engineers are discussing transitioning to a better power system known as the smart grid. The smart grid has different aspects which must be thoroughly investigated through research before implementation. This research seeks to provide an investigation into an important aspect of the smart grid known as the wide area protection systems (WAPS) and its feasibility for smart transmission grids protection. This research is important as it provides foundation, guidance and information to engineers considering implementing this new protection system.

1.5 Research Structure

The remaining of the chapters of this dissertation are described briefly to put the work in context:

Chapter Two reviews the literature on smart grid technology, power system protection, wide-area measurement system and wide area protection of the power system.

Chapter Three gives an overview of smart grid operation, protection, communication, and hardware-in-the-loop simulation.

Chapter Four discusses the wide area protection techniques implementation in MATLAB/Simulink.

Chapter Five discusses the wide area protection technique implementation in real-time using OPAL-RT.

Chapter Six discusses Hardware-In-the-Loop (HIL) implementation of the wide area protection techniques using SEL-351A Relay.

Chapter Seven analyses and discusses results obtained from chapters four to six.

Chapter Eight concludes the research with a summary and key finding.

CHAPTER TWO: LITERATURE REVIEW

This chapter presents comprehensive literature on smart grid technology, power system protection, Wide Area Measurement System (WAMS), Wide Area Protection System (WAPS), and the Implementation of Wide Area Protection Systems.

2.1 Overview of the Smart Grid

Over the years, many countries have faced energy deficiency, and this has had a direct impact on the development of the nations, the economy, and the society. The environment has also been affected through greenhouse gas emissions due to the use of fossil fuels. These and many others, such as policy and regulation, quality of service, and integration of Distributed Energy Resources (DER), are the major drivers for a better and more efficient power system known as the 'smart grid' (SG) [4].

Although various definitions of SG are posed by several researchers, they all point to the same idea: the SG is expected to leverage advances in information and communication technology and electrical power system technology to solve the challenges faced by the traditional power system and achieve a reliable, safe, efficient, secure, resilient, and sustainable supply of electricity.

Power system equipment manufacturing companies and utilities are shifting their focus to developing products that will serve the purpose of the SG. Also, many countries in America, Europe and Asia have been investing heavily in the SG infrastructure for some years now [5]. Countries that retain the traditional power system paradigm will soon be unable to get electrical equipment for their system maintenance. To improve the receptiveness of these countries to the SG paradigm, it is fitting to consider the question "is the smart grid completely different from the conventional one that we are used to?" The answer is: not really in terms of structure, but very different in terms of operational capabilities, functionalities and principles needed for effective management and control.

The SG can be conceptualized as a system of systems, consisting of the smart infrastructure system, the smart management system and the smart protection system. The technical requirements of these systems and the aspects of the traditional system to be adapted to realize their deployment are discussed in subsequent sections.

2.2 Smart Infrastructure System

We can subdivide the smart infrastructure system into subsystems known as energy, information, and communication subsystems; these are the infrastructure underlying the smart grid. This infrastructure system allows a two-way flow of electricity and data instead of the one-way flow in the traditional grid. The smart grid information and electricity flows allow power from the customers' side onto the main grid and the participation of the customers in decision making on how they receive and use power through a smart metering system [6].

2.2.1 Smart Energy Subsystem

The energy infrastructure system of the electrical power grid consists of the generation, transmission, and distribution systems. In the traditional power system, the flow of electricity is unidirectional: from large generating plants (mainly hydro or thermal), through transmission and distribution networks to customers. The SG replaces this unidirectional flow of power with a bi-directional power flow. The bi-directional flow of electricity and information in the SG enables customers to manage their energy consumption and generate power from RERs for self-consumption or export to the grid. On the other hand, electric utilities are able to collect data about the state of the power system for efficient operation, and optimal response to changes in the system demands, supplies, and costs. Figure 2.1 depicts the diagrammatic narrative that describes the traditional grid operation [5].

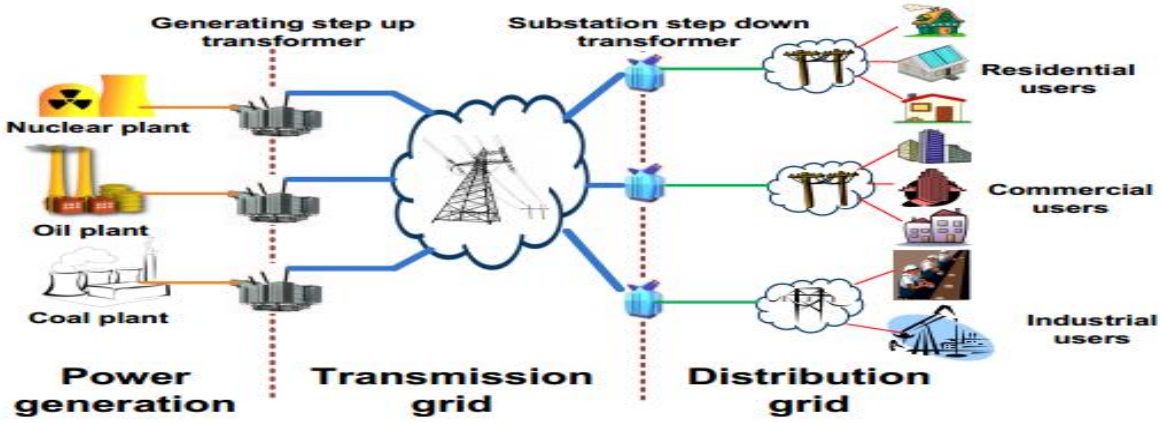

Figure 2.1: An Example of the Traditional Power System [5].

The power generation in the smart grid involves a central power station as well as an integration of Distributed Energy Resources (DERs) into the power grid at the customer ends. These DERs are predominantly Renewable Energy Resources (RERs), such as solar power, wind turbine, and in some cases, storage systems. The DERs reduce the Green House Gas (GHG) emission into the environment, provide more power generation, increase power supply reliability, and smoothen the demand profile. The DGs located at the customer ends can form part of what is known as micro-grids, which feed power to the grid and can also operate independently of the grid (i.e., in an islanded mode) during a fault on the main grid to supply only the customer loads. Figure 2.2 illustrates a generic structure of the smart grid.

One of the disadvantages of these DGs, which is under research for solutions is that their power generation patterns, which are dependent on the weather (wind, sunshine, etc.), are far from being similar to the demand patterns of the customers, and their generation patterns are unpredictable. To find out how these DGs can be beneficial to the smart grid, the authors in [7] investigated the impact of integrating renewable energy resources alone onto the power grid and then integrating renewable energy resources with storage devices.

The investigation was based on power cumulative cost and user service reliability. It was found out that the integration of renewable energy resources alone can increase customer service reliabilities and reduce costs. However, integration of the renewable energy resources with the storage devices can smoothen bulk power generation, reduce peak load, and remove the uncertainties that are caused by integrating DERs.

Also, the traditional protection of the power system is compromised when there is a greater amount of DGs incorporated onto the power system. The DGs influence the magnitude of the short circuit fault current and the direction of flow of the current, this affects the security and dependability of the protection schemes and gives false tripping. There is, therefore, the need for developing new protection schemes that will be suitable for the smart grid environment to mitigate the impact of incorporating DGs [9], [10].

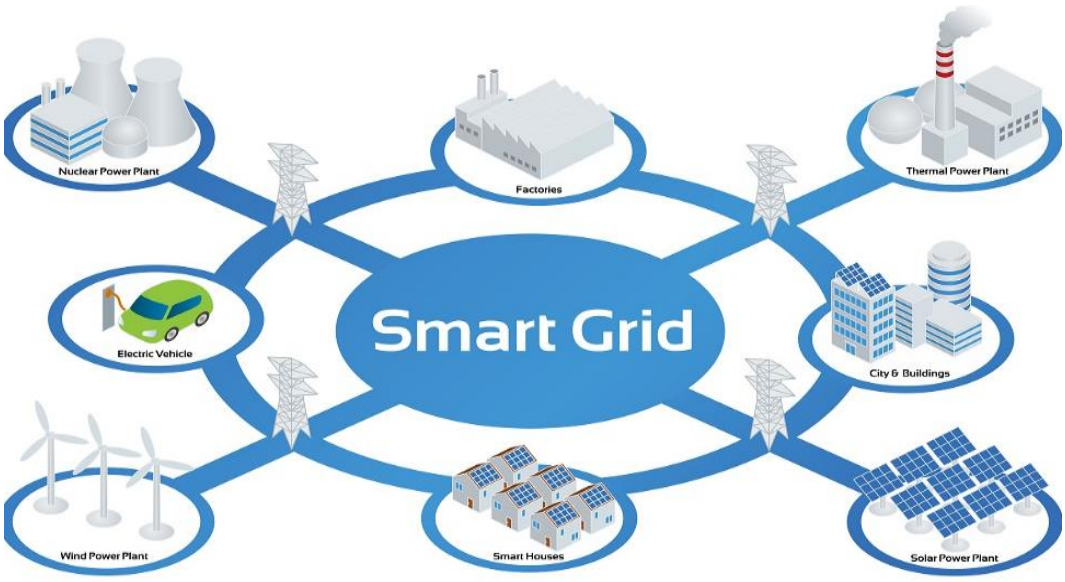

Figure 2.2. A Generic Structure of the Smart Grid [8]

Infrastructure challenges in terms of components ageing and increase in load demand have called for the need of the smart transmission grid. The transmission system of the smart grid consists of smart control centres, smart transmission networks and smart substations, this is to incorporate innovative technologies such as power electronics and advanced communications into the transmission network monitoring, protection and control. The authors of [11] did extensive work on the smart transmission system and identified some of the major features that will characterize it. The first of major features is digitalization, this is where the transmission system is going to employ a digital platform to enable system measurement for monitoring and protection of the entire transmission system. These digital platforms will also serve a purpose for sensing, computation and control, and maintenance of the system. Also, other features identified are flexibility, intelligence and resilience; these features will enable the transmission system to: expand according to customers' demands, be aware of the operation state of the network and withstand disturbances with self-healing for recovery after a fault condition. Furthermore, the paper identified sustainability where the transmission network is environmentally friendly enough with high efficiency, and customization that is, tailoring the network in accordance to the customer needs as other features of the smart transmission grid. The distribution system of the smart grid is

going to be characterized with several DGs as mentioned earlier, this is going to change the approach for management, control and protection of the distribution grid.

a) Smart Information Subsystem

The smart grid does not only depend on the improvement of the power infrastructure technology but also on the *acquisition, management and use of information*. Information about the state of the power system (voltages, currents, phasor angles) is paramount for effective monitoring control and protection purposes. With the improvement in technology, the measurement devices of the power system have also improved.

There are now Intelligent Electronic Devices (IEDs), smart meters and Phasor Measurement Units (PMU) for obtaining accurate information in the smart grid. The information subsystem of the smart grid has different levels that can be looked at separately. These include information measurement, monitoring and metering which involves smart meters, PMUs and sensors and information management which involves data modelling, analysis and optimization.

b) Smart communication Subsystem

Communication in power system is very important for proper management, control and operation of the power system and equipment. The traditional power system has devices which communicate among themselves like co-ordination in relays for protection and Supervisory Control and Data Acquisition (SCADA) for monitoring. The smart grid is very complex rendering these traditional communication technologies obsolete and therefore needs a more enhanced communication technology for real-time communication.

In the smart grid, there is going to be a two – way flow of information, this communication can be classified basically into two. Firstly, the communication from sensors and electrical appliances to smart meters which can be achieved with wireless communication such as ZigBee, Z-wave and secondly, the communication from smart meters to the utility's data centres which can be achieved with cellular mobile communication 3G, 4G/LTE and the current emerging 5G [12]. According to [12], the choice of communication must be based on certain communication requirements which are very paramount in the smart grid. These communication requirements include; security, system reliability, robustness, availability, scalability and Quality of Service (QoS).

2.2.2 Smart Management System

The smart grid has a lot of capabilities, and one of such capabilities is the ability to manage the power system with the relevant technologies. For example, in the traditional grid, what they have tried to do is to match the supply with the demand. And often it happens that the peak demand which is about 20% of the total demand is used within 5% of the total time [13]. This makes generation capacities which are meant to meet peak loads redundant most of the time.

However, in the smart grid, demand response is envisioned to solve this problem by rather matching the demand with the existing supply. This will be achieved through dynamic pricing of electricity using smart meters based on time of day to encourage users to use power during the off-peak period when the price is low. This will then help to smoothen the demand profile. The key management objectives of the smart grid are energy efficiency, demand profile improvement, emission control and utility and cost optimization [1].

2.2.3 Smart Protection System

Protection has been in existence since the inception of the power system operations with first protection devices being the electromechanical relays. As science and technology advanced, the quality of power generation, delivery and demand have also increased, we saw the protection system evolving into a more efficient one. As we are heading into a new mode of power delivery known as smart grid, the protection system also needs to be transformed to meet the requirement of the smart grid.

Two-way flow of information and power, integration of Distributed Generations (DGs) and Distributed Energy Resources (DERs), high-reliability requirement and the smart grid capabilities envisioned such as self-healing, resilience and stability make the traditional protection system inadequate for the smart grid operations.

Some of the reasons for the need of a smart protection system include: first, the integration of DGs into the distribution networks of the smart grid has changed them from Passive Distribution Networks (PDN) as known in traditional grids to Active Distribution Networks (ADN). The development of these ADNs faces new challenges including protection and control in relays. With the integration of DGs the magnitude and the direction of the fault current changes, therefore, protection schemes based on local information is becoming irrelevant. Research is shifting towards

the use of wide-area information where the fault is calculated based on the entire regional power system perspective [14].

Also, the protection schemes of the smart distribution grid become more complex especially if it involves Distributed Generations (DGs). This must be considered and dealt with to ensure reliability and security of the power system. This normally is due to the power from DG units which cause the power system to lose its radial configuration and eventually the co-ordination between the protective devices [15].

The smart protection system for smart grids can be achieved by taking advantage of the smart infrastructure available, which are the information, communication, and energy infrastructures. Technological advancement brought about an improvement in the measurement devices as we now have smart meters, and Phasor Measurement Units (PMUs). These provide accurate measurement and ranges of information that can be used to enhance protection in the smart grid.

2.3 Power System Protection

The power system is very complex, and it is subject to various natural disasters as well as variations in loads of customers, and that is where protection comes into play to detect any anomaly and respond to it as well as restoring the power system to its normal operating state. The important element of the protection system in power system protection engineering is the relay which applies principles or schemes to detect anomalies.

The first protective relays developed were the electromechanical relays. As science and technology advanced, these relays were changed from electro-mechanical to semi-conductors [16]. Semi-conductor relays were later replaced with integrated circuits and then microprocessor relays which are being used presently. Figure 2.3 shows the different types of relays. The advances in the technology of the relays only change their performance in terms of security, reliability, speed, dependability, selectivity etc.

2.3.1 Power System Protection Principles

Principles, as the meaning implies are the fundamental truths and foundations on which things are built, the same way, in power system protection, there are certain principles which serve as a foundation for building any protection scheme. These principles have been developed in the last

century and are still in use today, despite the advancement in technology, these principles remain valid and they include: overcurrent, directional, distance and differential protection.

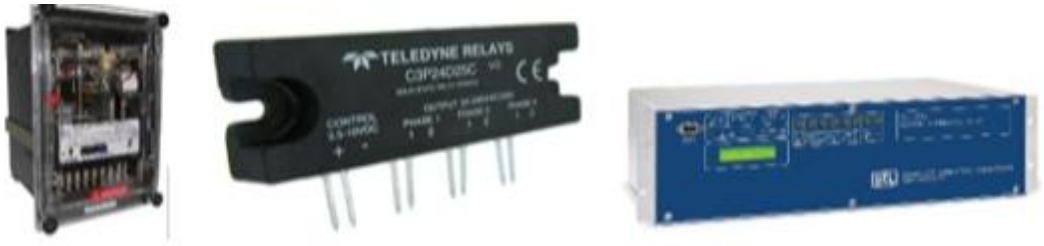

(a) (b) (c)

Figure 2.3: Different types relays (a) Electro-Mechanical (b) Semi-Conductor (c) Micro-Processor

a) Overcurrent Protection

Overcurrent protection in power systems was developed on the idea that the power system and its equipment have a certain current threshold value that can be allowed to flow, any current exceeding this value is dangerous to the health of the power system and could be caused by a fault or overloading and hence, must be disallowed to flow. The two causes of overcurrent in the power system which are overload and fault must be clearly distinguished by the protection schemes. There can be a temporary overload in the power system such as switching on of motor or a large load which may cause high current to flow. The overcurrent protection schemes in these cases are designed to sustain such occurrences.

There are two types of overcurrent protection; these are directional and non-directional overcurrent protection. Directional overcurrent protection at first was mostly used for protecting transmission lines but currently, due to the integration of DGs into the distribution systems, they became necessary also in the distribution systems protection schemes. The non-directional overcurrent protection is mostly used for conventional or traditional radial distribution grids.

The non-directional overcurrent protection basically monitors the current with a pre-set or threshold current value and then initiates definite minimum time (DMT) or inverse definite minimum time (IDMT) type of protection. As mentioned earlier, overcurrent due to loads must be distinguished from overcurrent due to faults. The non-directional protection achieves this by monitoring the current overtime typically between 4 – 40 ms so that an overcurrent that prolongs

is classified as a fault and then the relay initiates a trip in the circuit breakers to isolates the fault [17].

The directional overcurrent protection judges the current phasor against a reference voltage phasor measured at their measurement locations to determine the direction of a fault, hence the directional overcurrent protection depends on both current and voltage measurements. Looking at the diagram in Figure 2.4, a fault between the source and the relay is seen as a reverse fault whiles a fault that occurs between the relay and the grid is seen as a forward fault. In the diagram, I_{pre} is the pre-fault current, I_{rev} is the reverse current seen by the relay and I_{fwd} is the forward current seen by the relay.

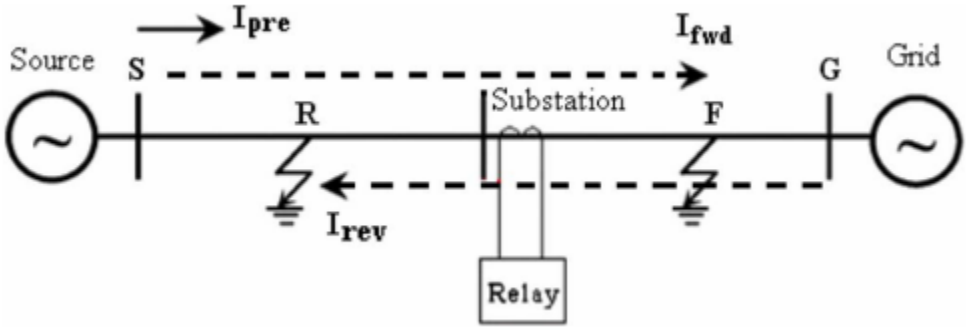

Figure 2.4. Overcurrent Relay. Reverse fault (R) and forward fault (F) [17]

In recent years, researchers have mainly focused on directional overcurrent protection because of the integration of DGs into the power grid, which make power flow bi-directional. Hence knowing the direction of the fault is imperative to relay operations in the protection schemes. The work in [17] was geared towards using current only to determine the direction of the fault to save the cost that comes with having to measure both current and voltage.

Papers [18] and [19] were concerned with developing an adaptive directional overcurrent protection scheme that can solve the protection issue that arises from the incorporation of Distributed Generations (DGs) and Active Network Management (ANM) in the distribution system.

In [18], the focus was on using an optimum protection setting for the overcurrent relay operations that can be applied to the network whether they are grid-connected or in islanded mode (unlike the

work by others where precalculated settings were used). In the case of precalculated settings, there can be several relay settings which are adjusted to the correct settings based on the network operation mode. Reference [18] stated that considering the effect of DGs and ANM on the distribution system and the number of possible network conditions that can be formed, it becomes unfeasible to have a precalculated group settings for all the network conditions hence they have proposed their approach.

b) Differential Protection

Differential protection is mainly used to protect power system equipment, transmission lines and feeders. It is based on Kirchhoff's current rule which compares the entering current with the outgoing currents and if there is a difference above a preset value then it means there is an internal fault i.e. it is mainly used for protecting the lines and equipment against internal faults. In Figure 2.5, in a case that there is an absence of an internal fault but an external fault or no fault at all, the current $I_1 = I_2$, but in the case that there is an internal fault on the protected line as shown in Figure 2.6, then $I_1 \neq I_2$. The relays will recognize this as an internal fault and trip the circuit breakers [20].

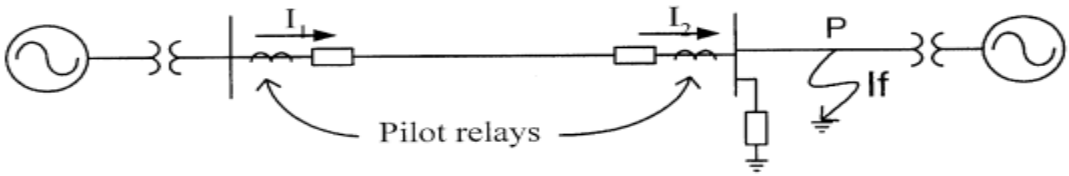

Figure 2.5. External fault in Differential protection [20].

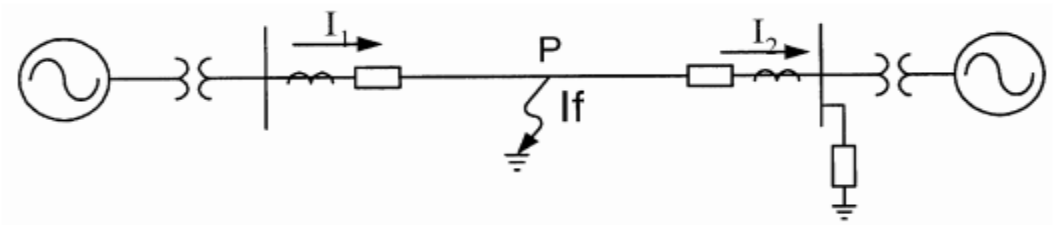

Figure 2.6. Internal fault in Differential protection [20]

The principles of differential protection have been utilized in power transformer, busbar, and transmission line protection schemes. In [21] differential protection based on fuzzy logic and

Clarke's transform was proposed which sought to deal with the issue that arises with some of the power transformer operating conditions which affect the normal differential protection behavior.

Sanjay *et al*. [22] proposed an adaptive differential protection scheme for transmission lines which was later extended to protect series compensated transmission lines. In their studies, they performed analysis on the following important protection characteristics; dependability versus security and speed versus accuracy. Reference [23] proposed an equivalent based travelling wave (ETW) differential protection for transmission lines, their choice of travelling wave was because it is immune to distributed capacitance current and current transformer (CT) saturation. In their scheme, the capability of travelling wave was built upon by solving other problems as low sensitivity and low reliability that may arise due to communication traffic because of sampling frequency.

c) Distance Protection

Distance protection is mainly used for transmission line protection, the distance relay uses the impedance measured on the line to determine the distance of the fault from the relay. Distance relay operates in zones, where the zones of protection cover up to a certain distance on the transmission lines. The zones of protection of a distance relay are divided into three zones; zone 1 protection which is the main protection covers up to 80% of the protected line and zone 2 protection goes a little further than the zone 1 protection, it usually covers up to 120% of the protected transmission line. The zone 3 protection which is backup protection for the transmission line next to the one protected by the relay, covers the whole length of the protected line and up to 80% of the next transmission line [24]. The illustration of the zones of protection can be seen in Figure 2.7.

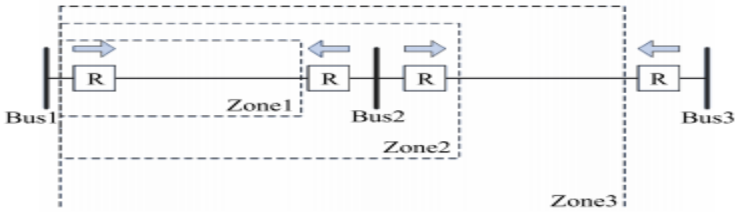

Figure 2.7. Distance protection of a distance relay; zone 1, zone 2 and zone 3

For correct operation of the zones, the zones of the relay are operated with different time delays. Zone 1 which is the primary protection is usually operated with no time delay at all. When a fault is detected by this zone, it is operated instantaneously. While zone 2 and zone 3, which are backup protections in the situation where the primary protection fails to operate, are given time delays of say 0.3s and 1s respectively.

2.4 Wide Area Measurement System (WAMS)

Before the development of Wide Area Measurement Systems (WAMS), the power system was being monitored as some are today, by Supervisory Control and Data Acquisition (SCADA) systems and Energy Management Systems (EMS). The issue with these systems which led to the development of WAMS is that they give only local area view of the power system and hence they are unable to provide solutions during a cascaded outage. But WAMS is developed to effectively handle the events of cascaded outage through optimized stabilizing actions because of its entire network coverage [25].

WAMS gives real-time information of the power system state, which has helped improve methods used for power system studies and analysis. Data obtained from WAMS is used for many applications some of which include real-time monitoring and control, transient stability analysis, voltage stability studies, state estimation, post-mortem analyses, power system restoration, adaptive protection, and power system planning [26], [27].

The hierarchical structure of Wide Area Measurement System consists of Phasor Measurement Units (PMUs) installed at different parts of the power system to measure and communicate voltage, current and frequency measurements, a Phasor Data concentrator (PDC) to collate PMU measurements received and a control centre where various applications and control algorithms are executed. Figure 2.8 shows the hierarchy structure of WAMS.

2.4.1 Optimal Placement of PMUs for full observability in WAMS applications

The phasor measurement unit is a key technology in WAMS and its applications. It obtains GPS time-synchronized measurement needed from various parts of the power system and then communicates the data to a PDC which verifies and correlates the data by their time-tag to a higher level PDCs or to a control centre. PMUs are expensive and as power delivery is to be optimized with cost, researchers are looking into how to optimize PMU placement in the power system to get full observability. Figure 2.9 shows a generic placement of PMU in a power system.

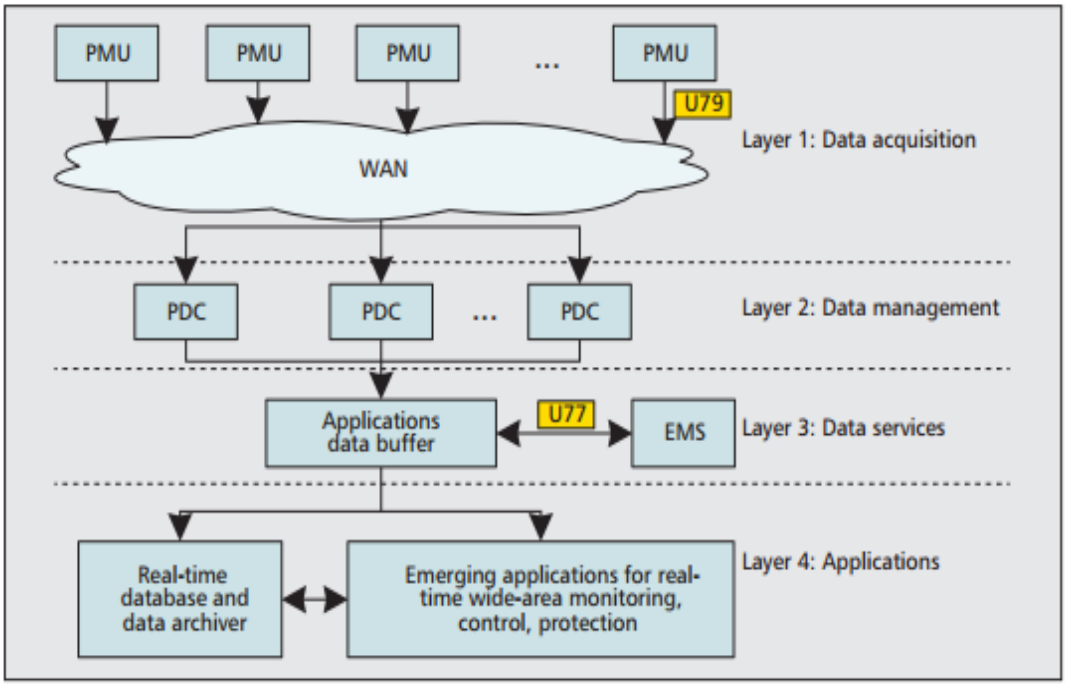

Figure 2.8: The Hierarchical and Generic Architecture of WAMS [28]

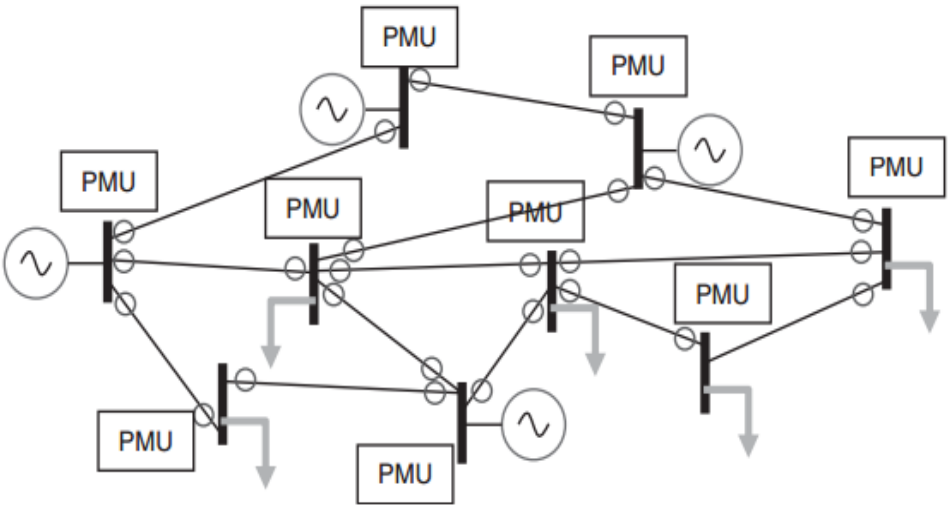

Figure 2.9: A Generic PMU placement in a Power System

Research on optimal placement of PMUs have several objectives. Work by [29] was based on determining the minimum number of PMUs needed to make a given power system fully observable using a binary search algorithm, where observability means all the states of the power system can

be uniquely determined. In [30]-[32] their objectives were to minimize the number of PMUs for a power system and minimize measurement redundancy. Lu *et al.* [33] proposed an optimal PMU placement in the power system for a reliable zero injections observation.

2.5 Wide Area Protection System (WAPS)

A cascading disturbance is a challenge for the utility industry due to the current complexities of the power system. The means to mitigate a disturbance that is fast spreading in the power system which will lead to a large area blackout has become an area of interest for researchers in recent years after the 2003 Northeast American blackout. Wide Area Monitoring, Protection and Control (WAMPAC) as a power system monitoring, protection and control paradigm has gained the attention both in the industry and academia. Out of this WAMPAC, we see emerging research topics such as Wide Area Measurement System (WAMS), Wide Area Control (WAC), Wide Area Protection (WAP) and Wide Area Protection and Control (WAPC).

In this research, the focus is on the wide area protection, which is the use of wide-area information to implement a protection scheme that will be used to control the power system protective relays operation to mitigate system disturbances and limit the impact of faults. Figure 2.10 and Figure 2.11 show the idea and the architecture of wide area protection, respectively. The architecture of WAPS in Figure 2.11 shows that, measurements data are taken from the power system by the PMUs and communicated to the wide area protection center through the local protection center. Trip decisions are made at the wide area protection center and sent to the breakers through the local protection center. The wide-area information is mainly synchronized phasor measurements obtained from PMUs installed at various buses across the power system. In this section, various works by other researchers on the Wide Area Protection System (WAPS), how the scheme is implemented, and their test systems used are presented.

a) Wide Area Backup Protection Schemes

Backup protection in power systems is a very important aspect of the power system operation and its value can be assessed when we investigate the causes and nature of power system major disturbances. Conventional backup protection schemes are self-contained and depend on local information which make it difficult for the protection to distinguish between internal faults and heavy loading, which causes mis-operation when the system is highly stressed [35],[36].

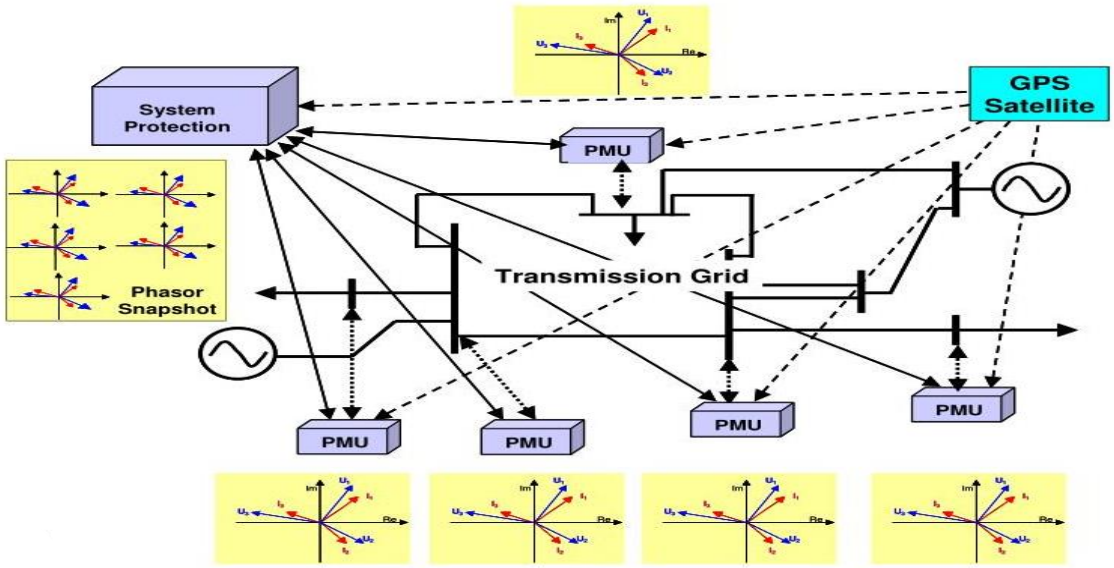

Figure 2.10: Wide Area Protection of the Power System; the idea [34]

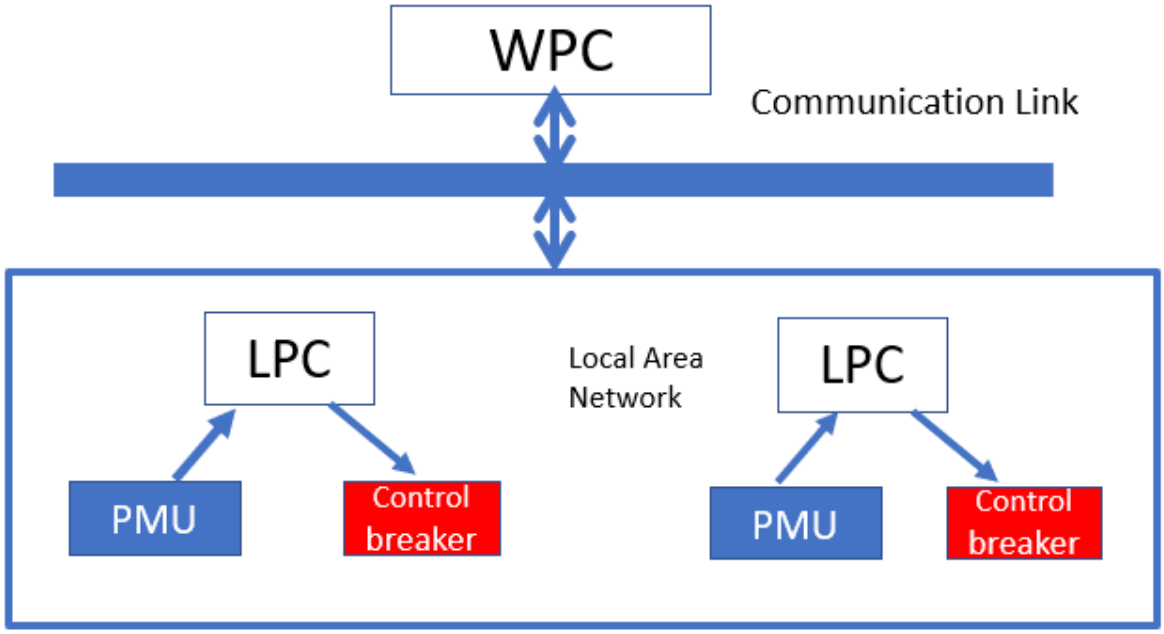

Figure 2.11: Wide Area Protection of the Power System; the system architecture

The advancement in communication technology and measuring devices leading to the development of the Wide Measurement System (WAMS) is bringing a solution to the problems

associated with conventional backup protection. Below are some of the works by researchers on using wide-area information instead of local information to develop algorithms and schemes for backup protection in the power system.

Eissa *et al.* in [2] proposed a wide area backup protection scheme for transmission grids known as wide-area differential protection (WADP) because it employs the principle of differential protection. The scheme uses phasor measurement units to obtain positive sequence voltages and current of the buses and compares these values to locate the bus nearest to the fault, then the absolute difference of the positive sequence current angles is calculated for all the lines connected to the bus to determine the fault line and location. This system was tested in MATLAB/SIMULINK using a 500kV Egyptian network. The time of fault detection is estimated to be 5 msec for all fault conditions and the relay is evaluated to be more suitable as a back-up relay and not a primary relay based on the communication speed for data transferring.

In [35], the authors proposed a wide area backup protection system using synchro-phasor with data requirement analysis. In the scheme only positive sequence measurements were employed, the scheme was implemented and tested on an IEEE 57-bus test system, the paper indicated that, with fast communication media, the algorithm could have practical merits.

In [36], a wide area backup protection using fault steady-state component for the development of fault detection algorithm was proposed. The algorithm works by forming protection correlation regions (PCRs) during normal operation of the power system. When a fault occurs, the algorithm locates the PCR where the fault occurred and then a fault correlation factor is calculated by which the faulted branch is located. The developed algorithm was tested with simulation on a 39-bus 10-generator New England test system and the results show that, the method can detect the faulted branch with limited measurement points.

Zhiqin He *et al.* [37], proposed a wide area backup protection scheme based on fault component voltage distribution. The scheme is composed of two parts: Fault area detection (FAD) and Fault Element Identification (FEI). After the faulted area is detected, only the substation that has the fault sends data to the regional wide area backup protection system, the scheme was verified using a simulation of the IEEE 10-generator 39-bus test system using PSCAD/EMTDC. The paper indicated that, the proposed method has the advantage of easy setting and low requirement for synchronized wide-area data.

Kalantar *et al.* [38] proposed an adaptive wide-area backup protection for transmission lines using phasor measurements. The scheme divides the power system into backup protection zones (BPZs) based on the placement of the phasor measurement units as well as the network topology. When a fault occurs in a zone, the entering positive and zero sequence voltages increases, and this is used to determine the faulted zone, after which the linear least square method is employed to find the faulted line in the zone, the scheme can adapt to the power system conditions. The system was tested using IEEE 9-bus and 118-bus test system. Simulation results verify successful identification of the faulted BPZ as well as the faulted line within the faulted BPZ with limited measurement points.

In [39], Javad Zare *et al*. wanted to address the communication delay constraint associated with the wide area backup Protection. The scheme was focused on regionalizing the power system using integer linear programming (ILP) by optimizing; the number and location of measuring devices (MD), the number and region of protection, the location of protection rooms and communication links between the MDs of the power system. So that the algorithm can be implemented in each region to reduce the computation burden. The system was tested using IEEE 57-bus test system. The paper concluded that; 'execution of the proposed ILP model on different test systems reveals that with regionalization of the systems, WABP schemes can reliably be used in practice'.

Manas Kuma *et al.* [40] proposed a wide area backup protection scheme for a series compensated transmission lines using phasor measurement units. The scheme employs the phase angle of the positive-sequence integrated angle (PAPSII) which is continuously monitored for each line at the PDC. This system was tested with real-time simulation using RTDS real-time digital simulator. The test results indicate that the proposed scheme can overcome the limitations of existing backup protection schemes and can provide a reliable protection.

CHAPTER THREE: SMART GRID OPERATION, PROTECTION, COMMUNICATION AND HIL SIMULATION

All over the world, utility companies, industry experts, power system operators and owners are all talking about the smart power system. The need to transition from the traditional ways of generating, managing, and controlling the electrical power system to smart methods has not been so emphasized as it is in recent years. Power system equipment manufacturing companies have moved their focus to produce products that will serve the purpose of the smart power system. This chapter explores in more details, the structure, functionalities, and principles of the smart power system.

3.1 Different Sources of Power Generation in the Smart Grid

Power system operation is faced with the challenge of running a true supply-on-demand system that is reliable [41]. In trying to run a system like this, what emerged was a supply that is controllable being matched with a demand that is uncontrollable and difficult to predict. In the smart grid, the power generation is not only from one large source such as a hydro-plant or thermal plant but with the addition of small generations known as DGs which are mostly in the form of renewables. With the inclusion of smart meters and other information structures, the demand can be matched with the supply without much difficulty.

The various sources of power generation in the smart power system as mentioned earlier include all forms of power sources, renewables and non-renewables, because, in the smart power system, reliability is a key issue. Power must always be available when needed, storage systems are also going to serve as power sources at certain times and loads at other times. Other sources of power generation which are classified as renewables that are being integrated into the smart power system are solar energy, wind energy, biomass energy, wave energy, tidal energy, hydropower energy and biogas energy.

3.2 Renewable Energy Integrations

As part of the vision of the smart grid is to have little or no adverse effect on the environment, renewable energy sources have become the best alternative to fossil fuel generating plants in realizing this vision. Fossil fuels as a means of generating power emit a lot of carbon dioxide into the environment, which is dangerous, therefore, one of the smart grid goals is to move to 100% renewable power generations [42].

Integration of renewable energy sources into the smart grid poses numerous challenges, which are currently under extensive research. These challenges are due to the intermittent and fluctuant nature of renewables generations because they are weather-driven. Hence their integration requires new operational procedures other than the conventional one. In the smart grid, some of the advanced control techniques that are being proposed and used for effective integration of the (RERs) include demand response, demand-side management (DSM), efficient use of transmission system and intelligent energy storage.

3.2.1 Variations in the Renewable Energy Generations

The operation of the traditional power system is such that the generation is controlled to supply the estimated uncontrolled network load. That is, the supply is made to follow the variations in the load and not otherwise, except during peak periods when there is insufficient generation and then load shedding programmes are used to match the load with the available generation. The dependence of the supply on renewable energy resources such as solar and wind which are not dispatchable makes the load following policy in the power system operation not feasible.

These RERs have minute-level, hourly-level, daily-level and yearly-level variations which must be factored into the generation plans to accurately predict the available power at any point in time. Solar energy, for instance, can change drastically with a passing cloud and wind energy also has a different generation pattern every day with rapid daily changes [43].

In every region where a renewable project is carried out, there are different variation patterns depending on the climate of that region. The variations change with the seasons of the year; for example, a solar energy generation project carried out in a year is expected to have higher generation during summer and low generation during winter. Also, on a typical day during summer where the solar power plant is expected to output more power, there is a huge variation pattern depending on the time of day. This information needs to be available to the power system operators from the meteorological department of that region. Figure 3.1 shows a typical daily solar power generation profile.

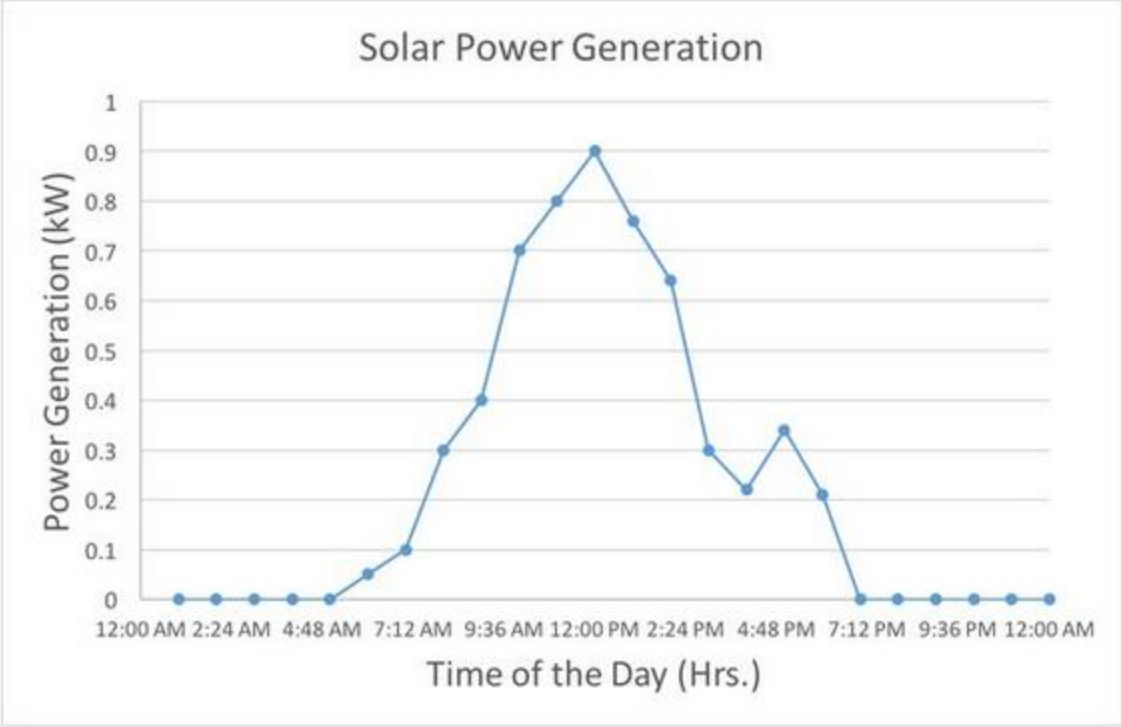

Figure 3.1: Solar Power generation profile on a typical day [44]

3.2.2 Demand Side Management to Solve Generation Fluctuations

To solve the fluctuation issues that arise with power generation from renewable sources, demand-side management (DSM) was proposed so that the load follows the available generation instead of the generation following the load [45]. The effects and benefits of DSM are enabling the use of a large share of solar photovoltaic systems. That is, it provides the means to balance the demand and supply in power systems with a greater share of renewable generators, including heat and power plants. It can also reduce the cost of power generation by eliminating expensive gas-fired, power plants which are only used a few times of the year to meet peak loads. Further, DSM improves the investment made in the transmission and distribution systems.

DSM can be achieved by the installation of smart meters at the customer side bringing another benefit of accurate billing and having detailed customer information. The issue is with the technology that can be used to achieve the objective of the load profile smoothening hence getting rid of high peak demands. There are various programmes implemented towards DSM which

include: demand response, residential and commercial load management, energy conservation and energy efficiency programmes [46].

Residential load management is geared towards reducing the overall power consumption in a household or shifting the demand to off-peak periods. Reducing the overall energy consumption can be achieved through energy conservation awareness, use of energy efficient appliances and by constructing a more energy-efficient building. Different approaches such as direct load control (DLC) and smart pricing have been proposed towards shifting the load to off-peak periods. Critical peak pricing (CPP), time of use pricing (ToUP) and real-time pricing (RTP) are the popular options available for smart pricing which encourages the consumers to voluntarily manage their loads [47]-[49].

3.2.3 Energy Storage Systems in Smart Grids

The electricity generated from renewable sources is not dispatchable and the methods used to forecast their production is bound by uncertainty. In some countries, the electricity produced from renewable sources contributes to around 20% of their total energy demand. The power system is such that it requires a continuous balance between supply and demand. This balance is achieved in the traditional system using automatic controls that are supervised by human operators.

Energy storage systems have been proposed as one of the solutions to address some of the challenges of smart grid operation, the energy storage system has the potential to improve variability and the accuracy of demand and supply prediction.

Energy storage systems have been used in the traditional grid to perform three major roles: increase efficiency and reduce the cost of electricity, improve the stability and reliability of the power grid and enhance the power quality of the grid. In the smart grid, the major roles that energy storage systems have to play in order to achieve the smart grid vision is to provide flexibility for power systems with greater level of intermittent renewable energy integration and also to strengthen the grid resilience to power outages due to extreme events such as severe weather conditions and attacks on the cyber-physical infrastructure [50].

Energy storage systems can increase efficiency and reduce electricity cost by what is termed as energy shifting. This can be achieved by storing the excess of energy which is generated during the time of day when the load is minimum (off-peak periods) and releasing it when the load

demand is maximum (peak periods). This kind of application requires storage systems which will be in service for several hours since the application involves constant charging and discharging.

Whenever there is a mismatch between the supply and demand in the power grid, voltage and frequency are destabilized. The energy storage system in the power grid is used in this case as a means to provide spinning and non-spinning reserve for voltage control and frequency regulation in the events of a sudden large generation, loss of generation or load outages. A rapid response storage system is required for this kind of application to cater for the small-timescale fluctuations of both demand and supply and it may be required to operate for a short or long period [51].

Power quality problems include harmonics distortion of voltages and currents, voltage sags and swells, supply interruptions, transient and flickers. The concern for the quality of power supply has become very important due to the recent increase in the use of non-linear loads; computers and electronic devices. An energy storage system can provide sufficient energy to get rid of the short-term power quality issues [52], [53].

3.3 Smart Grid Protection

There are many important areas that need to be researched and implemented in order to bring to realization, the smart grid vision. One of these important research areas is new trends for power system protection. Under this aspect of the smart grid, we have wide area protection, adaptive protection and protection with self-healing capabilities. The flow of fault current in the smart grid is from different directions as shown in Figure 3.2 because of the incorporation of several DG units into the smart grid. Hence, a protection technique that can detect, locate and identify faults in this scenario is required. The existing protection schemes and techniques were designed for the traditional grid which has power generation at one point and hence fault currents flowing from only one direction.

Further, the robustness and resilience of the power grid are paramount due to the many events that put the power grid at risk. The protection system plays a major role in maintaining this resiliency and robustness. A protection technique that will provide self-healing capability to the smart grid is under intensive research in the industry and academia, since reliability is one of the problems the smart grid is envisioned to solve.

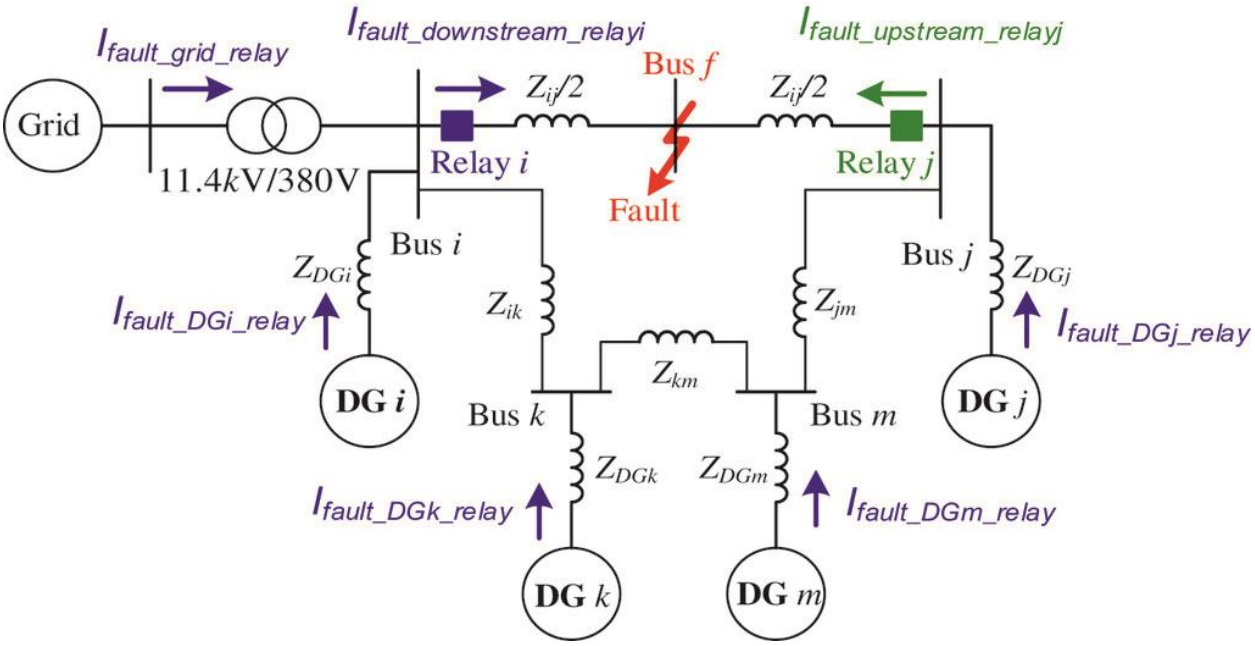

Figure 3.2: Fault current from different directions in the Power grid due to the DG units [54]

3.4 Communications in Smart Grid

The definition of the smart grid or the smart power system mentioned earlier in the introduction states that; '*the smart grid is the convergence of the advancement in power system with communication technology to provide efficient, reliable and safe power supply'*. This definition shows that communication technology is an important aspect of the smart grid. The smart grid has two-way communication as opposed to the one-way communication in the conventional grid. The two-way communication will provide a real-time interactive channel between the consumers and the power utility companies. This real-time communication will help users get information about their power consumptions and flexibly adjust the time of use of their appliances based on electricity pricing. The power companies, in turn, can also retrieve user's power usage information, manage the connections of distributed energy resources, and regulate the load on the grid by controlling the users' appliances.

To achieve this communication requirement in the smart grid, there are different communication technologies available to the power utility companies. The right form of communication technology must be selected for the right application in order to achieve the desired results. The two major forms (mediums) of communication available are wired and wireless. Wireless

communication has its own advantages such as high rate of success, fast communication, easy installation, and maintenance but has the problem of being vulnerable to interference, communication quality and the distance of communication is greatly affected by walls. This means that wireless communication is useful for some power system applications and not useful for other applications [55]. The major issue with the wired communication is that they are capital intensive.

The data transmission rate of the communication technologies is one of the major factors of consideration when selecting the type of communication technology for a particular power system application. For example, wide area measurement systems which involve collecting PMU data from several points of the power system will have large volumes of data to be communicated to a centralized centre, hence, this kind of application needs a communication technology with a very high data transmission rate.

3.4.1 Different Communication Technologies for the Smart Power System

There are various forms of applications in the smart grid environment which require incorporating advanced information technologies and intelligent communication networks. These applications include substation automation, automatic meter reading, advanced metering infrastructure etc. This section discussed the various communication technologies available for smart grid applications and compares them in terms of their data rate and distance coverage.

The choice of a communication network architecture design for a particular smart grid application must meet specific requirements such as reliability, latency, security, bandwidth as these are crucial for a reliable, affordable and sustainable power grid. Table 3.1 presents a comparison of both wired and wireless communication technologies.

3.4.2 The Smart Power System Communication Network Architecture, Data Rate and Coverage Range Requirements.

The communication architecture of the smart grid can be represented using a hierarchical structure. The layered architectures are applicable at various points of the power system. They comprise of wide area network (WAN), neighborhood area network (NAN)/field area network (FAN) and home/local area network at the customer premises. Figure 3.3 shows the communication architecture in smart grid, data rate and coverage range requirement.

3.4.3 Communication Network Requirement for different Smart Grid Applications

There are various smart grid applications that need network communication technologies. The communication requirements in terms of data rate, security, bandwidth, latency, and reliability vary and are specific for each type of application.

An application such as home automation will require a communication technology with short coverage distance and low data rate, in this case, network communication technologies such as Zigbee, WLAN, Z-wave and PLC are applicable. For an application in a wide area network such as synchrophasors, data communication will require a network that supports a higher data rate and can provide a long coverage distance; for this type of application, fibre optic communication technology will be suitable. Table 3.2 shows the various applications in smart grid, their communication requirements and the choice of communication technology that may be applicable.

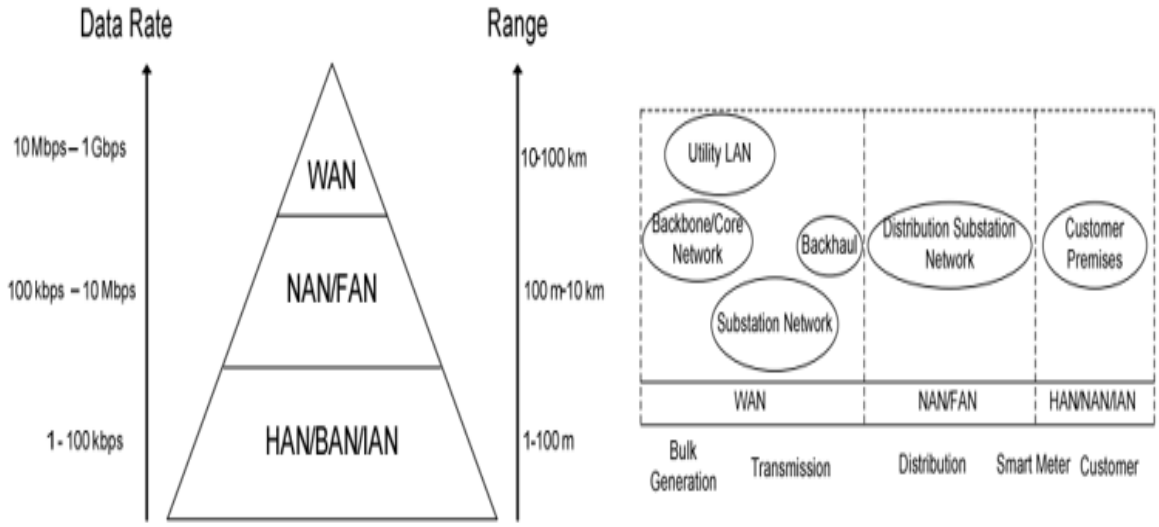

Figure 3.3: Smart grid communication architecture, data rate and coverage range requirements [56]

Table 3.1: Comparison of different communication technologies [56]

Technology	**Standard/Protocol**	**Data Rate**	**Coverage Range**
Wired Communication Technologies			
Fiber Optic	PON	155Mbps – 2.5Gbps	Up to 60 km
	WDM	40 Gbps	Up to 100 km
	SONET/SDH	10Gbps	Up to 100 km
SDL	ADSL	1-8 Mbps	Up to 5 km
	HDSL	2 Mbps	Up to 3.6 km
	VDSL	15-100 Mbps	Up to 1.5 km
Coaxial Cable	DOCSIS	172 Mbps	Up to 28 km
PLC	Home Plug	14 – 200 Mbps	Up to 20 m
	Narrowband	10 – 500 kbps	Up to 3 km
Wireless Communication Technologies			
Zigbee	Zigbee	250 kbps	Up to 100 m
	Zigbee Pro	250 kbps	Up to 1600 m
WLAN	802.11x	2 – 600 Mbps	Up to 100 m
Z-wave	Z-wave	40 kbps	Up to 30 m
Cellular	2G	14.4 kbps	Up to 50 km
	2.5G	144 kbps	
	3G	2 Mbps	
	3.5G	14 Mbps	
	4G	100 Mbps	
	5G	10 Gbps	
Satellite	Satellite internet	1 Mbps	100 – 6,000 km

Table 3.2: Smart grid applications and network communication technologies that will meet their requirements [56]

Network	**Application**	**Data rate**	**Latency**	**Security/ Reliability**	**Coverage range**	**Communication technologies**	
						wired	**wireless**
HAN/BAN/ IAN	Home Automation	<100kbps	<minutes	High	Up to 100m	PLC	Zigbee, WLAN, Z-wave
NAN/FAN	On meter demand reading	>100kbps	<sec	High	Up to 10km	DSL, coaxial cable, PLC	WiMAX, Cellular
	Multi-interval meter reading	>100kbps	<several hours			DSL, coaxial cable, PLC	WiMAX, Cellular
	Load management	> 50 kbps	<5 sec			DSL, coaxial cable,	WiMAX, Cellular
	Distribution automation	>18 kbps	< 1 sec			DSL, coaxial cable,	WiMAX, Cellular
WAN	Synchrophasor	>2 Mbps	<20 ms	Very High	100 km or more	Fiber optic	WiMAX, Cellular
	Backhaul/core/ metro networks	>10 Mbps	<50 ms			Fibre optic	WiMAX, Cellular, satellite

3.5 Hardware-in-the-loop (HIL) Simulation

To better understand the performance of a power system control hardware, the hardware must be tested within the real power system. This testing of how the control hardware will interact with the power system cannot be tested on the actual power system as by doing so, customers loads will be interrupted. To build a real power system for the sole purpose of testing control hardware algorithms will be very expensive, hence by replacing the actual power system with the real-time simulated one, these problems can be solved [57].

Real-Time Digital Simulator (RTDS), OPAL-RT Real-Time Simulator, Simulink real-time using speedgoat target hardware etc. provide platforms for simulating the power system in real-time. Hardware-in-the-loop (HIL) simulation is widely used in the automotive, aerospace and defense, and industrial automation and machinery industries to test embedded designs. HIL is currently being adopted in medicine, communication, and several industries. The most common HIL simulation examples include [58]:

1. Aerospace and defense: Flight simulators and flight dynamic control, where it is too expensive to test the control algorithm on the actual aircraft.
2. Automotive: Vehicle dynamics and controls, where it is impractical to test functionality on the road in the initial phases.
3. Industrial automation: Controller plant-testing, when stopping the production or assembly line to test control algorithms involves a huge amount of resources and business loss.
4. Power System Protection and Control: Testing of protection and control algorithms, where testing on the actual power system is dangerous and will also interrupt customer loads.

3.5.1 Importance of Real-Time and HIL Simulations.

The idea of real-time simulation became very important because we want to test the performance of our control algorithms using the real physical hardware that will be used in real life. There are different reasons why it is important to do real-time simulations. One of these reasons is that it helps engineers to reduce cost in fixing errors in any control algorithms as the errors are detected at the design stage. The cost involved in fixing an error at the design stage is almost zero, but when the control hardware is deployed, it costs so much to fix the same error. Hence by doing real-time and HIL simulations using the real hardware that will be deployed, it helps to identify any error that will occur and then fix it before deployment.

The real-time simulation also helps us to perform tests on systems in the laboratory which previously would not be possible to do as those tests can only be done on the field. Tests performed on the field are difficult, expensive and hazardous. The real-time simulation allows us to perform verifications of our design all along with the project, detect errors at early stages and gives room for infinite test capabilities.

Figure 3.4 shows the cost of fixing an error at the different stages of the manufacturing and deployment of any control hardware. Figure 3.5 shows the old and new approaches to error discovery. In the old approach, errors are only discovered during tests performed on the field, whereas in the new approach, with the aid of real-time and HIL simulations, errors can be discovered even at the design stage.

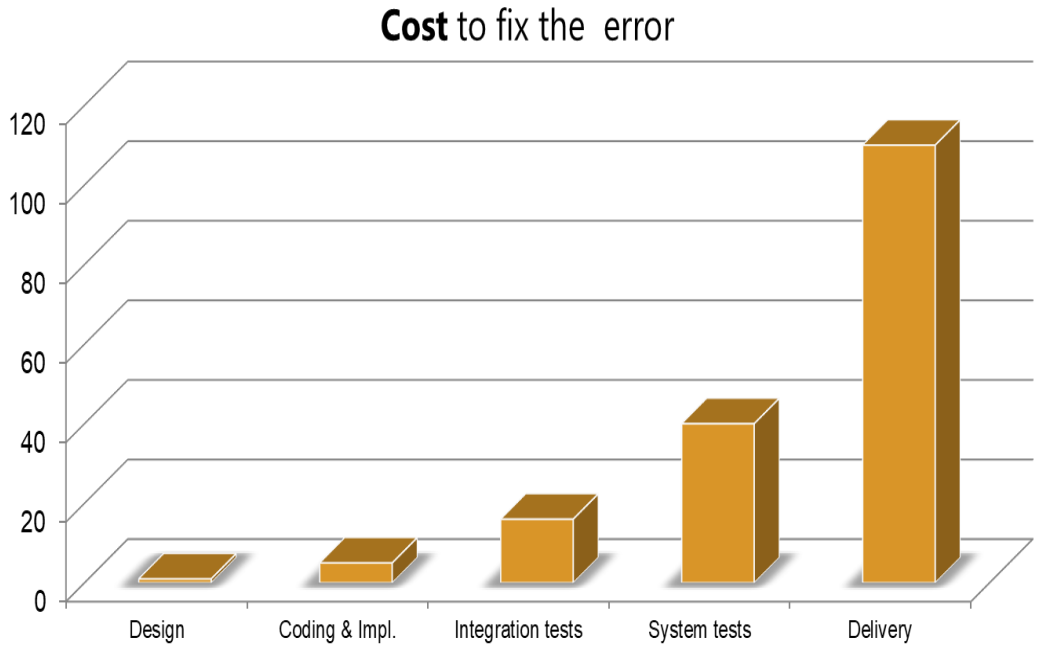

Figure 3.4: Cost of fixing error at different stages of development of systems [59]

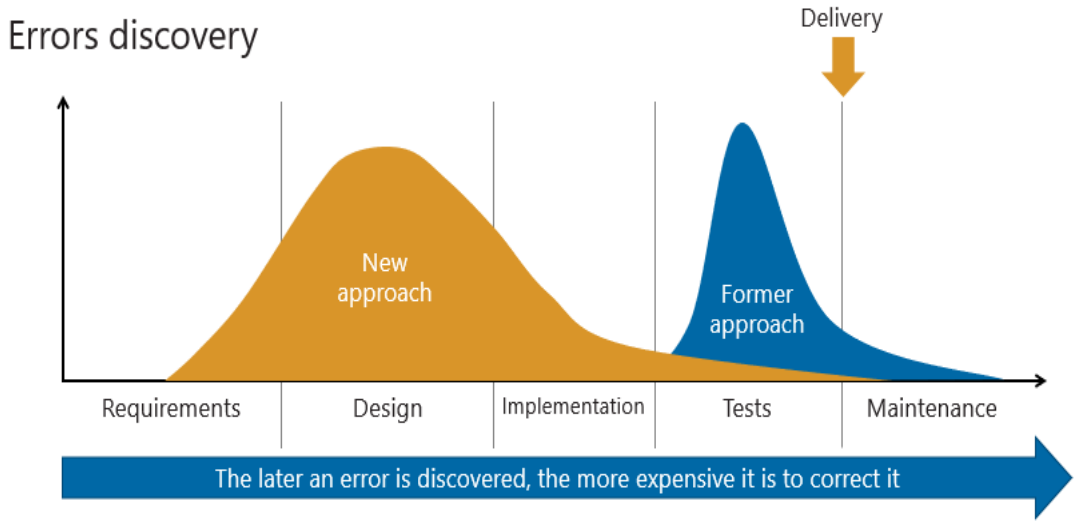

Figure 3.5: Old and New approach for error discovery in systems development [59]

3.5.2 Real-Time Simulation and Offline Simulation

Simulation is the representation of the operation or features of a system through the use of the other. One cannot talk about hardware-in-the-loop-simulation without talking about real-time simulation. In simulation, there are different types of simulation solvers used. Discrete time with constant time-step is the simulation type suitable for real-time simulation. In this type of simulation, time moves forward in steps of equal duration. To solve mathematical functions and equations at a given time-step, each variable or system state is solved successively as a function of variables and states at the end of the preceding time-step. During discrete simulation at a fixed time-step, the amount of real-time needed to compute all equations and functions consisting a system during a given time-step may be shorter or longer than the duration of the simulation time-step. Figure 3.6 (a) and Figure 3.6 (b) show these scenarios. In (a), the computing time is shorter than the fixed time-step; this type of simulation is also referred to as accelerated simulation whereas in (b), the computing time is longer; these two types of simulation are known as offline simulation. In both cases, the time when the results become available is not relevant, the objective mainly with offline simulation is to obtain results as fast as possible.

However, during real-time simulation, the accuracy of the computations does not only depend on the precise dynamic representation of the system but also on the length of time used to produce

the results. Figure 3.6 (c) shows a scenario for real-time simulation. For a real-time simulation to be valid, the simulation must accurately produce the internal variables and outputs of the simulation within the same length of time that the real-world (physical) systems would. The real-time needed to compute the solution at a given time step must be shorter than the actual clock duration of the simulation time-step. This enables the real-time simulator to perform all operations necessary to make a real-time simulation relevant, including driving inputs and outputs (I/O). Figure 3.7 shows the simulation time-step requirements by application to achieve real-time simulation [60].

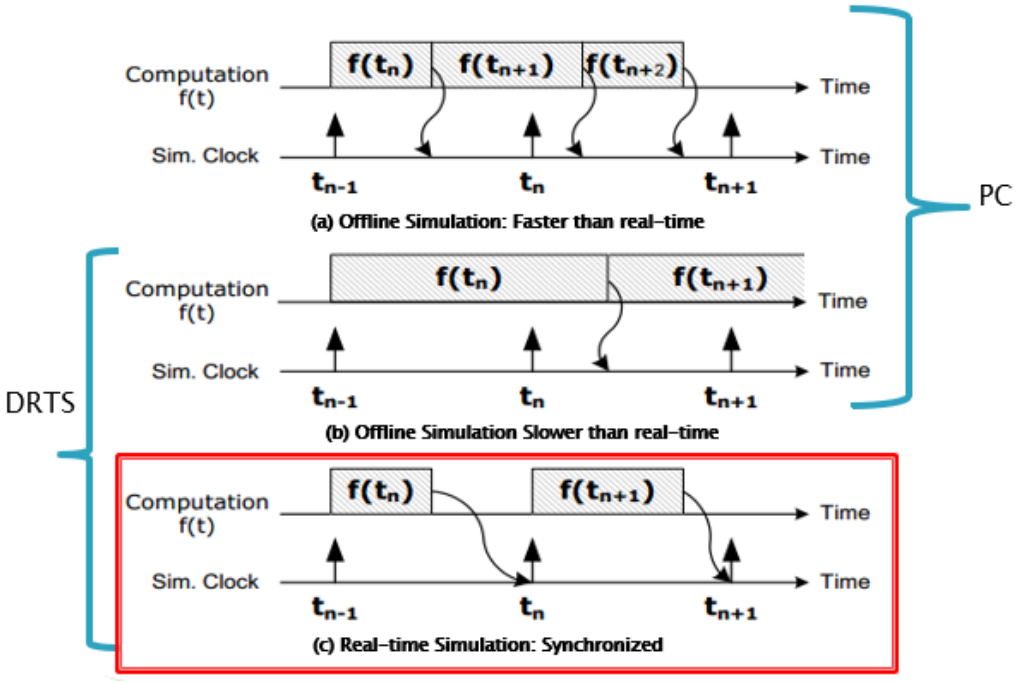

Figure 3.6: Real-Time Simulation requirements [60]

3.5.3 Hardware-in-the-loop (HIL) Simulation Configurations for Power System Studies

The concept of HIL simulations can be applied in different ways to test different systems. The basic application of HIL in power system engineering includes: Controller Hardware-in-the-Loop (CHIL) and Power hardware-in-the-Loop (PHIL).

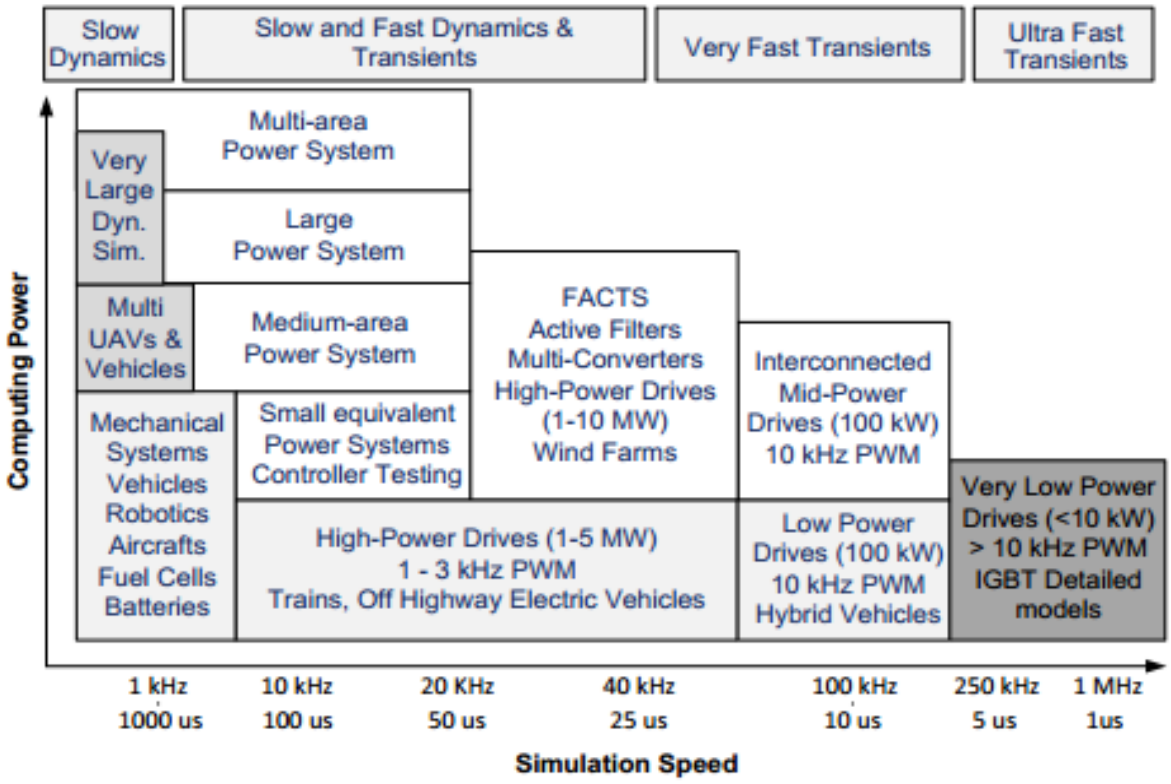

Figure 3.7: Simulation Time-Step by Application for Real-Time Simulation [60]

A. Controller Hardware-in-the-Loop (CHIL)

Controller hardware-in-the-Loop simulation allows many control hardware such as controllers for inverters, capacitor banks and smart thermostat to be evaluated with simulated inputs. The hardware under test is generally an embedded controller with inputs and outputs of small-signal levels [61].

A power system simulation running on a digital real-time simulator (DRTS) is configured with the actual grid conditions to provide realistic input data to the controller hardware. The output signals from the controller hardware are fed back as inputs to the power system simulation running in real-time. The power system simulation is updated based on the signal received from the controller hardware which also updates the signal sent to the controller hardware. Analog to Digital converters (ADC) and Digital to Analog Converters (DAC) are needed for the exchange of data between the power system simulation running on the DRTS and the controller hardware [62].

B. Power Hardware-in-the-Loop (PHIL)

This hardware-in-the-Loop simulation is an extension of CHIL which incorporates hardware with inputs and outputs of higher voltages, it allows power hardware with its embedded control to be interfaced with the executed power system running on the DRTS. The power hardware and its embedded control can then be tested under realistic but simulated conditions. The power hardware needs an operational power; AC or DC or both that is consistent with the conditions in the power system simulation [61]-[64]. Figure 3.8 shows a diagrammatic illustration of PHIL and CHIL.

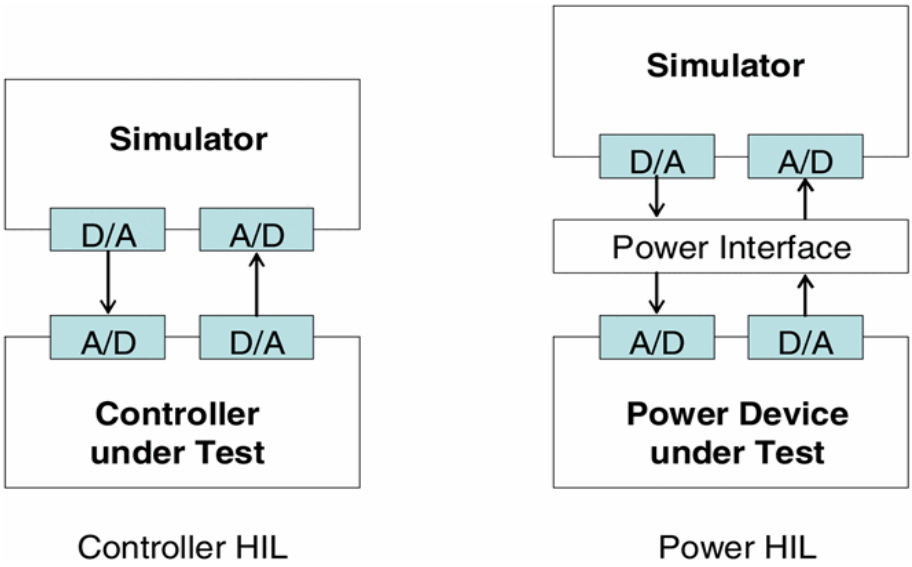

Figure 3.8: Illustration Comparison of CHIL and PHIL simulations [64]

3.5.4 Hardware-in-the-Loop (HIL) Simulation of Power System Relay

In this research, the focus is to test and evaluate the performance of different wide area protection algorithms, hence the hardware under test for consideration here is the power system relay specifically **SEL-351A relay**. A power system relay requires higher voltage (Power) signals of 300 Vac continuous and 1 Amp or 5 Amps continuous from the power system simulation that is executed on the DRTS, hence using these signals for the HIL test is considered a power hardware-in-the-loop simulation (PHIL). The DRTS that is used for the real-time simulation of the power system in this research is the OPAL-RT real-time simulator. The output and input signals of the simulator have a dynamic range of 32V peak-peak and 60V peak-peak maximum respectively and a few milliamps (mA) for analog signals. The digital output has a user-defined range of 5 to 30 V

with a maximum output current of ± 50 mA per channel and a flexible input of 4 to 30 V with an input current of 3.6 mA. This requires a power interface (amplifier) to make the interaction possible when doing HIL.

However, SEL relays provide a low-level test interface with a maximum input voltage of 9 V peak-peak which allows for testing of the relays using low-level voltage and current signals. This makes controller hardware-in-the-loop simulation and relay testing using the Opal-RT and RTDS real-time simulator possible without amplifiers. Many researches in literature including [65]-[67], have made use of the low-level test interface provided by SEL relays for power system protection testing through HIL. The laboratory used for this research does not have amplifiers hence the HIL testing in this work made use of the low-level test interface of the SEL relays. Figure 3.9 depicts the interactions between MATLAB/Simulink, Opal-RT simulator, amplifier and the SEL-351 relay during PHIL simulations.

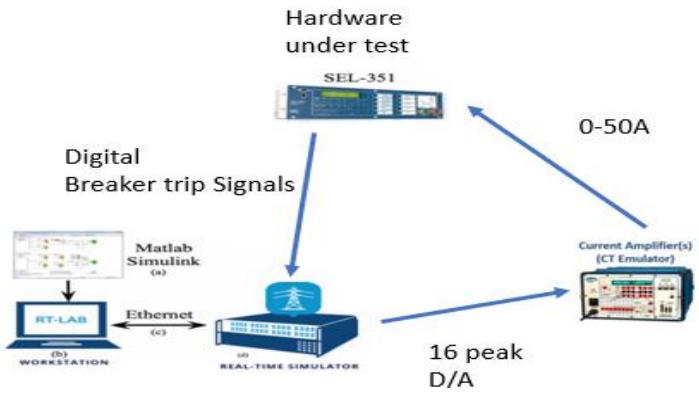

Figure 3.9: PHIL Simulation of power system relays

CHAPTER FOUR: MATLAB IMPLEMENTATION OF WIDE AREA PROTECTION ON A POWER SYSTEM

In this chapter, the simulation of some selected wide-area protection schemes on the IEEE 9-bus power system in MATLAB/Simulink is discussed. The performances of the protection algorithms during the MATLAB/Simulink simulation are also presented.

4.1 Software Simulations

In order to test the behavior of the power system when a fault occurs especially its effect on voltage, current and frequency, the simulation of the power system was started with a single bus and the number of buses were increased progressively. These simulations were carried out and the knowledge gained was transferred to the actual test system under study-the IEEE 9-bus system. Some of the results of these simulation are shown in Appendix D.

4.2 Wide Area Protection algorithm simulations on IEEE 9-bus system

The IEEE 9-bus 3-generator power system was chosen as the test system for evaluating the various selected algorithms for wide area protection (WAP). The diagram of the IEEE 9-bus power system is shown in Figure 4.1.

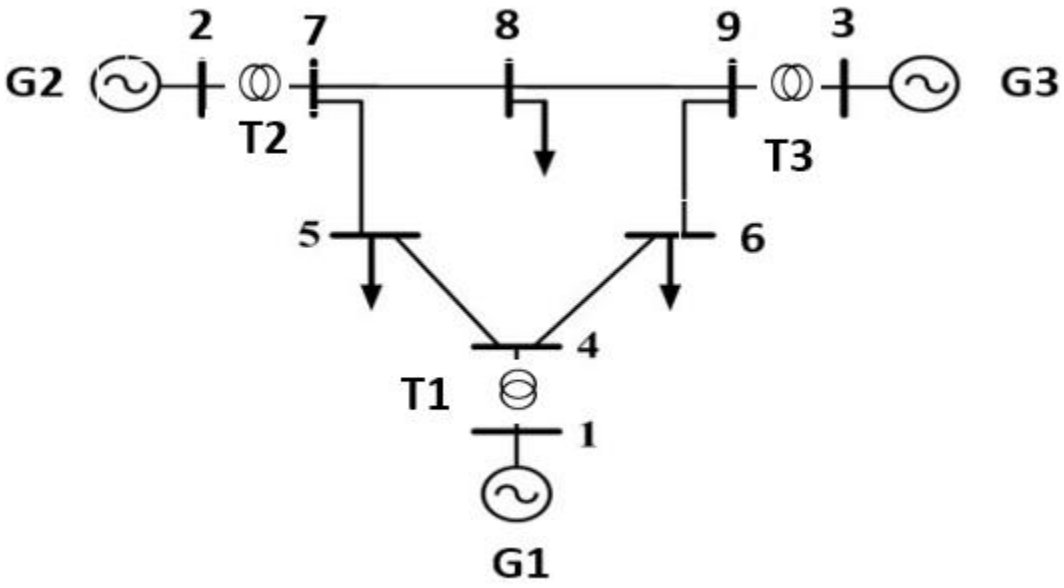

Figure 4.1: IEEE 9-bus 3-generator power system

4.3 Selected WAP Techniques

The three algorithms selected from the literature for implementation and comparison include:

- **WAP Technique A:** A novel backup wide-area protection technique for power system transmission grids using phasor measurement unit (PSVM for faulted zone detection) [2].
- **WAP Technique B:** A new decentralized approach to wide-area backup protection of transmission lines (GIM for faulted zone detection) [70].
- **WAP Technique C:** An adaptive PMU-based wide area backup protection for power transmission lines (Sum of positive and zero sequence currents for faulted zone detection) [38].

4.3.1 Similarities Existing Between the Chosen Algorithms

In order to compare two or more algorithms accurately, they must have certain things in common which will be the basis for drawing conclusions on their effectiveness. These algorithms have been carefully selected to ensure their performance evaluations are comparable. The following are the common features of the algorithms:

1. The use of Phasor Measurement Units data
2. Formation of zones of protection
3. Determination of faulted zones
4. Determination of faulted lines in a faulted zone
5. Used for Transmission line protection

4.3.2 Differences that Exists Between the Chosen Algorithms

Despite the similarities among the algorithms, significant differences exist among them. For instance, the data used by one algorithm for determining the zone that has a fault is different from the data used by the other. These differences help to measure their performance and effectiveness in terms of accuracy and speed. Table 4.1 shows the differences that exist among the algorithms.

4.4 WAP Technique A [2].

The technique uses the formation of protection zones based on the PMUs placement in the power system and the network topology. When a fault is detected in a particular protection zone, then the information of the various connected lines in that zone is sent to the protection centre to detect the particular line on which the fault occurs.

Table 4.1: Differences that exist between the chosen algorithms

Algorithm / **Factor**	Positive sequence voltage magnitude (PSVM) for faulted zone detection **(A)**	Gain in momentum (GIM) for faulted zone detection **(B)**	Sum of positive and zero sequence currents (SPZSC) for faulted zone detection **(C)**
Determination of Faulted Zone	Uses the positive sequence voltage magnitude	Uses Gain in momentum of the generators	Uses the sum of zero or positive sequence currents entering the PMU bus
Determination of Faulted Bus	The PMU bus in the faulted zone is the faulted bus of consideration	Uses Positive sequence voltage magnitude	The PMU bus that has the sum of currents exceeding the threshold is the bus of consideration
Determination of Faulted line	Uses the absolute difference of the positive sequence current angles	Uses the flow of reactive power on the line connected to the faulted bus	Uses a linear least square method

The data that are measured by a PMU include positive sequence magnitude and angle of voltages and currents, voltage and current phasors and frequency. In this algorithm, the data used for fault detection are positive sequence voltage magnitudes V_n and positive sequence current angles $< I_\Phi$

A. Formation of Backup Protection Zones

The protection zones are formed based on the PMU placement in the power system and the network topology. As shown in Figure 4.3, buses 4, 7 and 9 are PMU buses hence the three zones in the power system are defined based on the coverage area of each of the three PMUs.

B. Faulted Zone Identification

The algorithm compares the positive sequence voltage magnitude (PSVM) of PMU buses in each zone of protection. The zone with the minimum positive sequence voltage magnitude below a set threshold has the fault. Mathematically the statement can be expressed as:

$$Min\{|V_1|,\ |V_2|, \dots |V_m|, \dots\ |V_n|\} < V_{th} \tag{4.1}$$

where V_n is the positive sequence voltage magnitude measured by PMUs in zone "1", "2" … "m" to "n" and V_{th} is the threshold for PSVM.

C. Faulted Line Identification

When the faulted zone is detected, then the absolute angle of the positive sequence current angle is used to detect the line with the fault. If a zone labelled "m" is detected as the zone with the fault, then the absolute angle of all lines connecting to the PMU bus will be compared and the maximum one is the line with fault.

$$Max\{|\Delta\Phi_{m1}|,\ |\Delta\Phi_{m2}|, \dots\ |\Delta\Phi_{m3}|, \dots |\Delta\Phi_{mn}|\} \tag{4.2}$$

where $|\Delta\Phi_{mn}| = |\Phi_{mn} - \Phi_{nm}|$ (4.3)

D. Summary of Fault detection algorithm

The faulted zone is detected by monitoring the positive sequence voltage of the various protection zones. The zone with the minimum positive sequence voltage that is below a certain set threshold (that is obtained from the simulation of the power system) has the fault. After that, the absolute magnitude of the current angle difference of the various connected lines to the PMU bus in that zone is calculated, and the line with the maximum value has the fault. The flowchart for this wide area protection technique is shown in Figure 4.2.

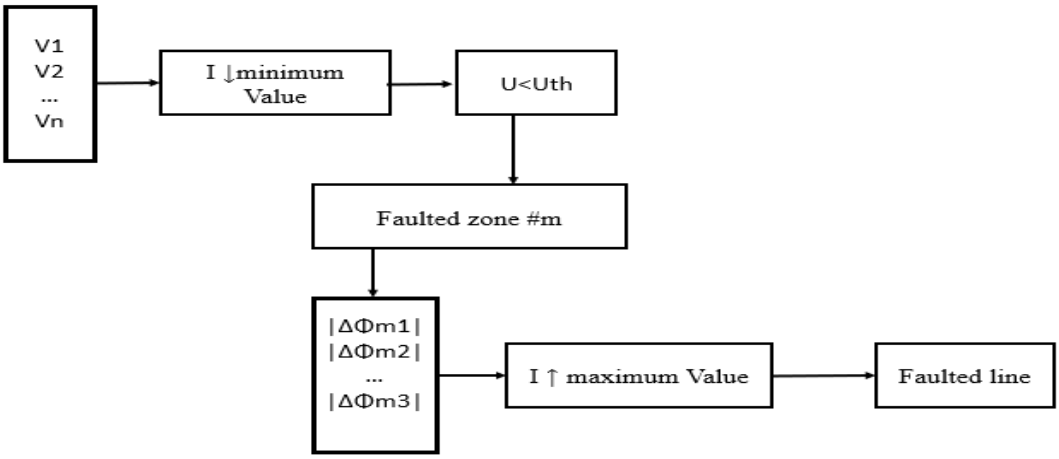

Figure 4.2: The flow chart for the WAP Technique A

Before implementing the algorithm, no-fault, single phase to ground fault and three phase fault were simulated to determine the threshold for the Positive Sequence Voltage Magnitude (PSVM) for identifying the faulted zone in the IEEE 3-generator 9-bus system and the following results in Table 4.2 were obtained. The faults locations were changed, however, the maximum PSVM is taken as the threshold. The diagram in Figure 4.3 shows the IEEE 9-bus power system with the different zones of protection and the PMU buses based on this WAP algorithm. From the table, when there is no fault, the PSVM of the PMU buses ranges from 0.85 to 0.87. A zone with the fault has the PSVM of its PMU bus smaller than the other PMU buses and this is indicated in red in the table.

Table 4.2: Positive sequence voltages in per unit obtained from PMUs for faulted zone identification

	PMU 1		PMU 2		PMU 3	
No Fault	0.85		0.86		0.87	
Fault Type	(L-L-L)	(L-G)	(L-L-L)	(L-G)	(L-L-L)	(L-G)
Zone 1	8.03e-6	0.6094	0.2801	0.6954	0.2641	0.6974
Zone 2	0.2922	0.6965	7.37e-6	0.6267	0.2163	0.6904
Zone 3	0.3117	0.7066	0.256	0.7001	7.163e-6	0.6401

4.4.1 MATLAB/Simulink Results of the WAP Technique A Implementation

The IEEE 9-bus 3-geneartor power system was simulated in MATLAB/Simulink and the algorithm implemented to detect various faults; this was done to test the accuracy of the algorithm. The voltage and current recordings (waveforms) of all the PMU buses following a three-phase (L-L-L-G) fault simulated in zone 3 at bus 3 are shown in Figure 4.4 and Figure 4.5 respectively. The highest fault current as well as a significant reduction in the fault voltage were recorded at the PMU located at bus 9 because the fault is in zone 3. These characteristics are important for determining the faulted zone in the power system.

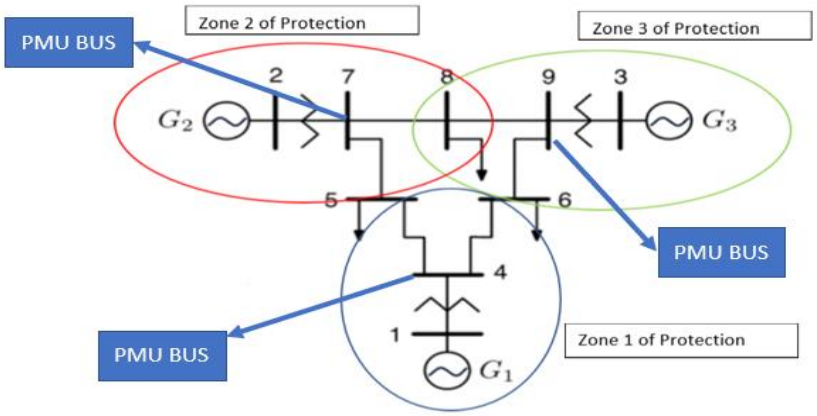

Figure 4.3: IEEE 9-bus power system with the different zones of protection and PMU buses for WAP technique A

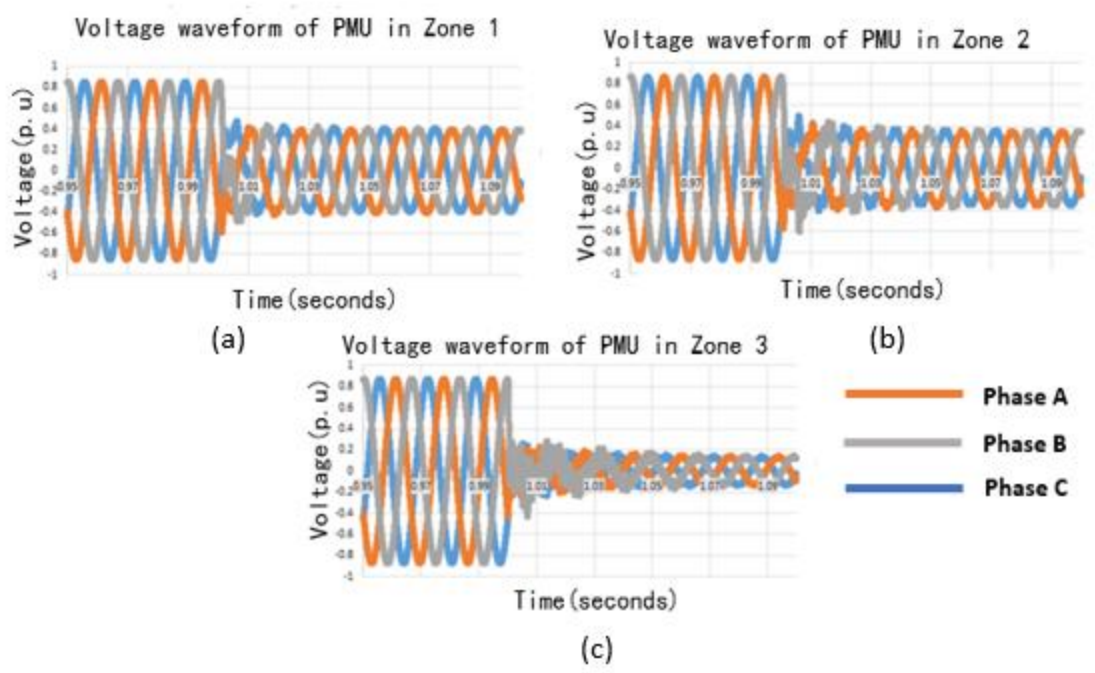

Figure 4.4: Voltages of PMU buses in zones 1 (a), 2 (b) and 3 (c) for a fault in zone 3.

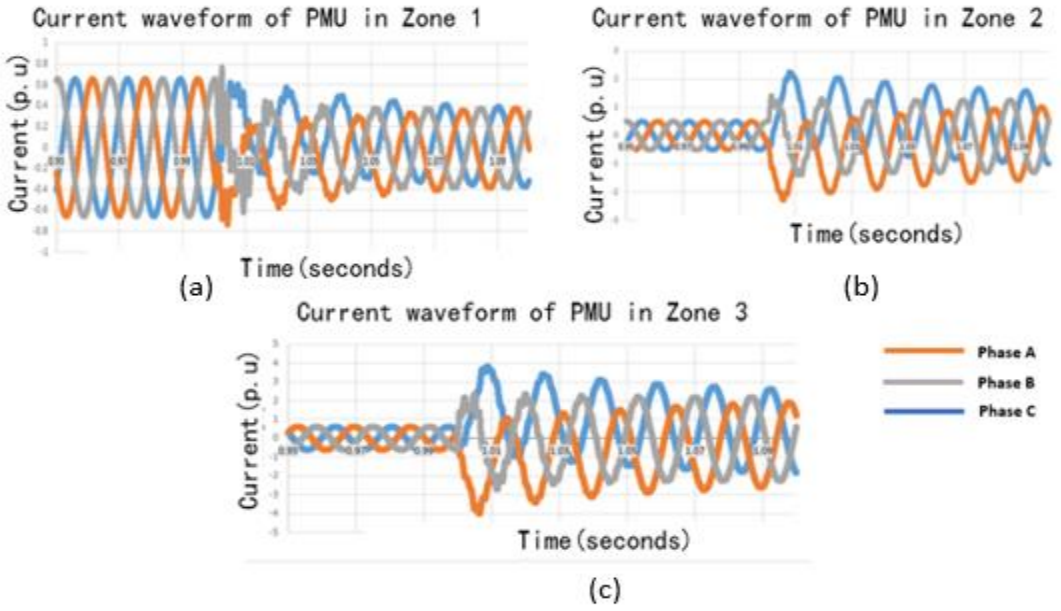

Figure 4.5: Currents of PMU buses; in zones 1 (a), 2 (b) and 3(c) for a fault in zone 3.

4.4.2 Evaluation of WAP Technique A in MATLAB/Simulink

The algorithm was evaluated in terms of the speed it takes to detect and clear all types of faults as well as the accuracy in detecting all faults on the various lines of the IEEE 9-bus system. Different types of faults were simulated on each line and the algorithm was used to detect the zone and the line on which the fault occurred. The fault detection accuracy is given by the following equation:

$$\text{Zone detection accuracy} = \frac{\text{Number of zones accurately detected}}{\text{Total number of faults tested}} \times 100\% \quad (4.4)$$

$$\text{Line detection accuracy} = \frac{\text{Number of lines accurately detected}}{\text{Total number of faults tested}} \times 100\% \quad (4.5)$$

To determine the fault clearing time of the algorithm, the voltage and current waveforms of the bus closest to the circuit breaker was recorded. For WAP technique A, the fault clearing time varies depending on the type of fault, the range of the fault clearing time is between 15 ms to 35 ms.

From Figure 4.6 and Figure 4.7, the time period from when the waveforms begin to distort to when the waveforms recovered or stabilized is the fault clearing time. The current and voltage waveforms show that a two-phase fault (L-L) was cleared in ***0.03 seconds*** and a three-phase to ground fault (L-L-L-G) was cleared in ***0.015 seconds*** during the MATLAB/Simulink simulation. Table 4.3 shows the time it took the algorithm to clear the different types of faults tested during simulations, the time taken to clear the faults is higher for single-phase to ground fault and lower for three-phase to ground faults. The accuracy of the algorithm in detecting all faults was tested, Figure 4.8 shows a block diagram of how a faulted line is detected. Some of the faulted lines detected and the actual lines on which the faults occurred are indicated in Table 4.4. The accuracy is determined by the ability of the algorithm to correctly determine the actual faulted zone and line in all the tested fault cases.

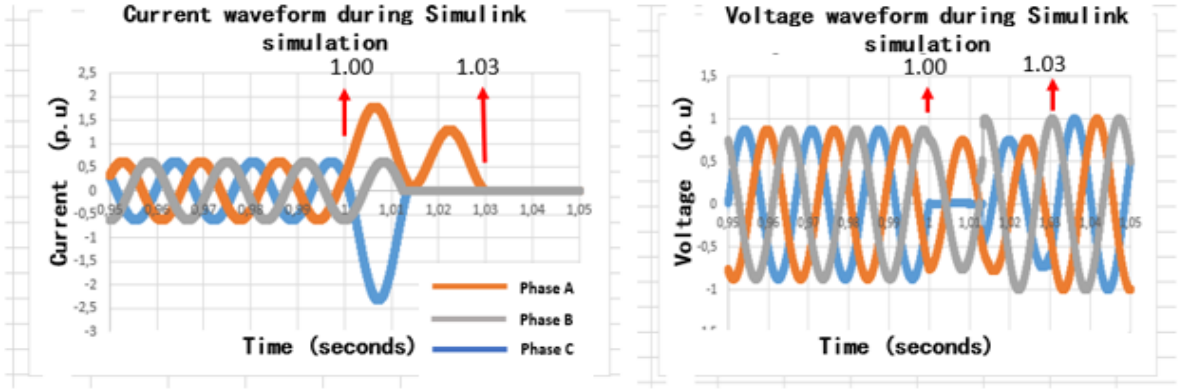

Figure 4.6: Current and voltage waveforms before, during and after a fault (L-L) in Simulink

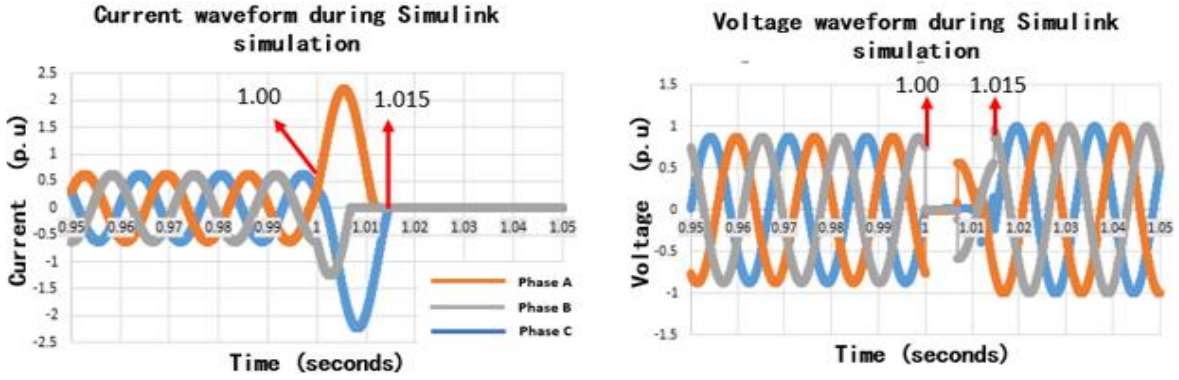

Figure 4.7: Current and voltage waveforms before, during and after a three-phase to ground fault (L-L-L-G) in Simulink

Table 4.3: Fault clearing times of WAP Technique A

	Fault Clearing Time(seconds)			
Fault Type	**L-G**	**L-L**	**L-L-G**	**L-L-L-G**
Zone 1	0.035	0.03	0.025	0.02
Zone 2	0.035	0.03	0.026	0.02
Zone 3	0.035	0.029	0.025	0.015

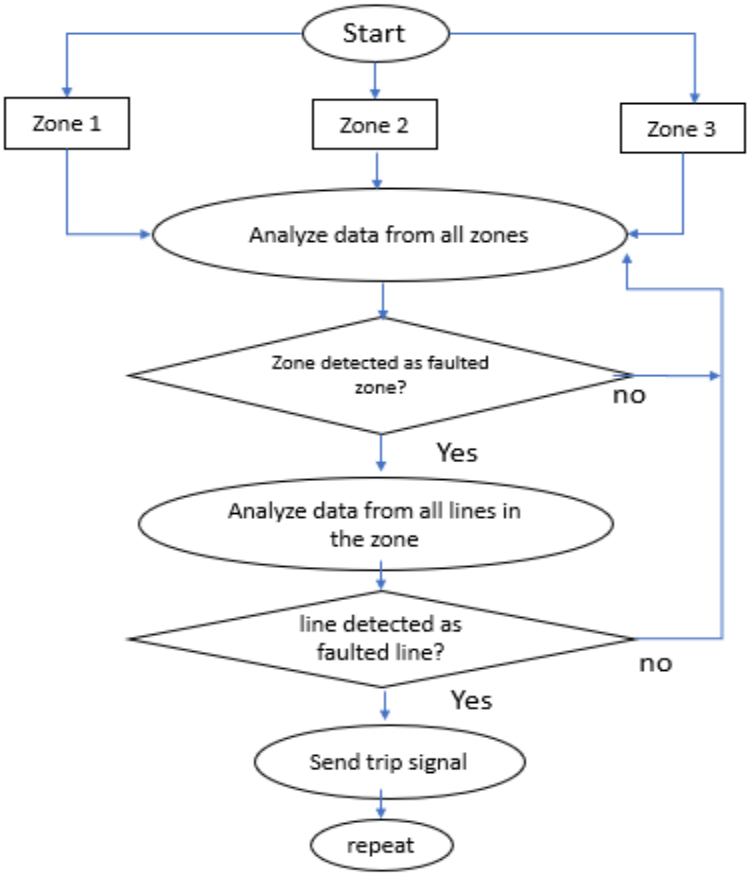

Figure 4.8: Block diagram used to test the accuracy of the Algorithm

4.5 WAP Technique B [70]

This scheme also uses the decentralized approach by forming a vulnerable protection zone (VPZ) based on the placement of the generator in the power system. The Gain in Momentum (GIM) of the generators are used to locate the vulnerable protection zone and then the positive sequence voltage magnitude (PSVM) of each bus in the VPZ is used to detect the bus closest to the fault, after which the reactive power flow information is used to determine the faulted line.

Table 4.4: WAP Technique A accuracy in detecting faults

Faulted line	Faulted Zone	Type of fault	Zone detected	Line detected
4 - 1	1	L-L-L-G	1	4-1
		L-L-G		4-1
		L-L		4-1
		L-G		4-1
4 - 5	1	L-L-L-G	1	4-5
		L-L-G		4-5
		L-L		4-6
		L-G		4-5
4 - 6	1	L-L-L-G	1	4-6
		L-L-G		4-6
		L-L		4-5
		L-G		4-6
2 – 7	2	L-L-L-G	2	2-7
		L-L-G		2-7
		L-L		2-7
		L-G		2-7
7 – 8	2	L-L-L-G	2	7-5
		L-L-G		7-8
		L-L		7-8
		L-G		7-5
7 – 5	2	L-L-L-G	2	7-5
		L-L-G		7-5
		L-L		7-5
		L-G		7-5
3 – 9	3	L-L-L-G	3	3-9
		L-L-G		3-9
		L-L		3-9
		L-G		3-9
9 - 8	3	L-L-L-G	3	9-8
		L-L-G		9-8
		L-L		9-6
		L-G		9-8
9 – 6	3	L-L-L-G	3	9-6
		L-L-G		9-6
		L-L		9-8
		L-G		9-6

A. Formation of Backup Protection Zones

The protections zones (PZs) of the power system are formed in corresponding to the generator buses in the power system, this is because the algorithm uses the Gain in Momentum of the generators to detect a vulnerable protection zone. The protection zones are as illustrated in Figure 4.3 similar to WAP technique A.

B. Faulted Zone Identification

The gain in momentum of each generator bus is closely monitored with a certain threshold obtained from the simulation of the power system. Whenever a fault occurs in a zone, the GIM index of that generator bus rises above the set threshold, and this is used to detect the faulted zone after which the positive sequence voltages of that zone is used to detect the bus closest to the fault.

The dynamics of a generator following a fault is governed by:

$$M\frac{d^2\delta}{dt^2} = P_m - P_e = P_a \tag{4.6}$$

where M is the inertia constant, δ is the rotor angle, P_m and P_e are the mechanical and electrical power respectively, and P_a is the accelerating power. During the dynamic behavior, the speed of the generator can be calculated in terms of the rotor angle as follows:

$$\omega = \frac{d\delta}{dt} \tag{4.7}$$

The GIM is defined as:

$$GIM_i = M_i \times (\Delta\omega)_i \tag{4.8}$$

where

GIM_i is the gain in moment of each machine "i"

M_i moment of inertia of each machine "i"

$(\Delta\omega)_i$ gain in speed of each machine "i" in the first 0.1 s following fault

The faulted zone is identified when

$$GIM > K_1 \tag{4.9}$$

Where $K_1$is the threshold selected for *GIM*

C. Faulted Line Identification

The faulted line is identified in this algorithm by using the positive sequence voltage magnitude to determine the faulted bus and the reactive power flow information of the various lines connected to the faulted bus to determine the faulted line.

When the GIM of a given BPZ exceeds the threshold, then the Local Protection Centre (LPC) in that zone is notified to monitor the PSVM of that zone in order to identify the bus closest to the fault as follows

$$V_i^1 \leq (K_m V_{in} = K_1) \tag{4.10}$$

where

V_i^1 is the PSVM of the ith bus of the VPZ

V_{in} is the rated voltage magnitude

K_m is a constant coefficient

Following a fault inception on a transmission line, reactive power is fed to the fault point, hence the reactive power flowing on the faulted line rises above a given threshold. Figure 4.9 shows the flowchart for the algorithm.

$$\Delta Q_{ij} \geq K_2 \tag{4.11}$$

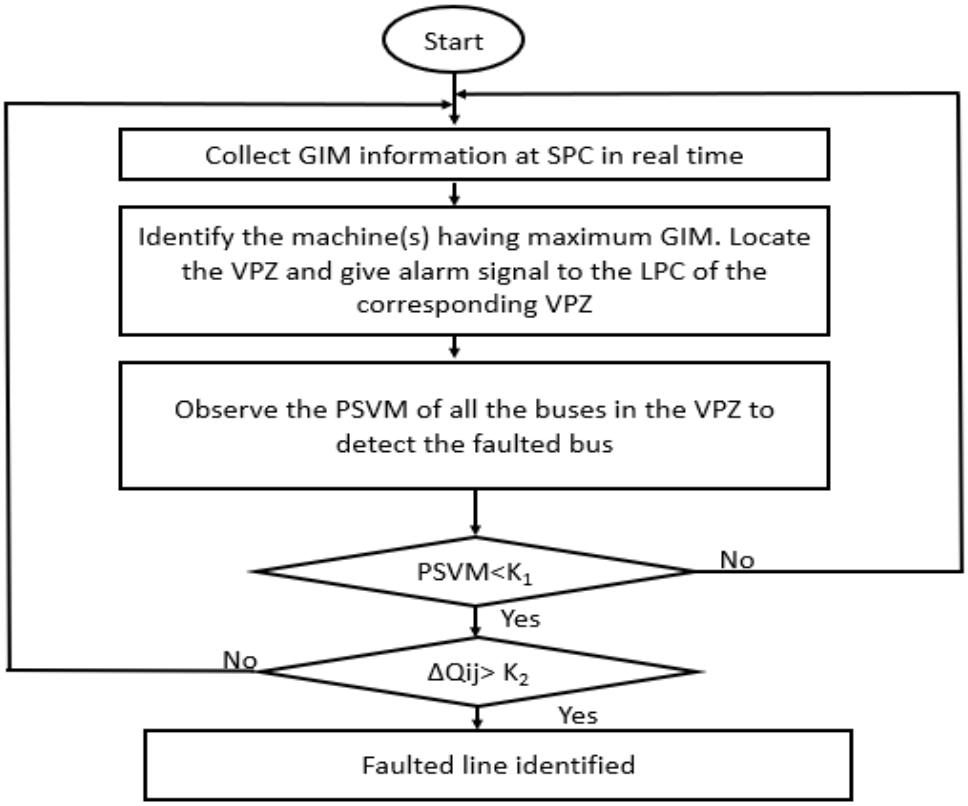

Figure 4.9: Flow Chart for WAP technique B

4.5.1 Results of WAP Technique B implementation in MATLAB/Simulink

The wide area protection technique is implemented on the IEEE 9-bus system. The power system was simulated using MATLAB Simulink without any fault and the GIM of the three generators were plotted as shown in Figure 4.10. Furthermore, a three-phase fault was simulated in all the zones of the IEEE 9-bus system and the corresponding GIM of all generators were plotted as shown in Figure 4.11. The change in GIM of the generators in the first 0.1 seconds following a fault are the criteria used in determining the faulted zone using this WAP technique. As depicted in Figure 4.11, there is a significant change in the GIM of the generators in the zone where the fault occurs whiles the GIM of the other generators remains unchanged. In Figure 4.12, the GIM of generator three after a fault was closely analyzed and the behavior show that, it is possible to use that as a fault detection criterion. The response time of the wide area protection technique to detect and clear faults, as well as the accuracy in detecting all types of faults, were analyzed as was done in the previous section for technique A.

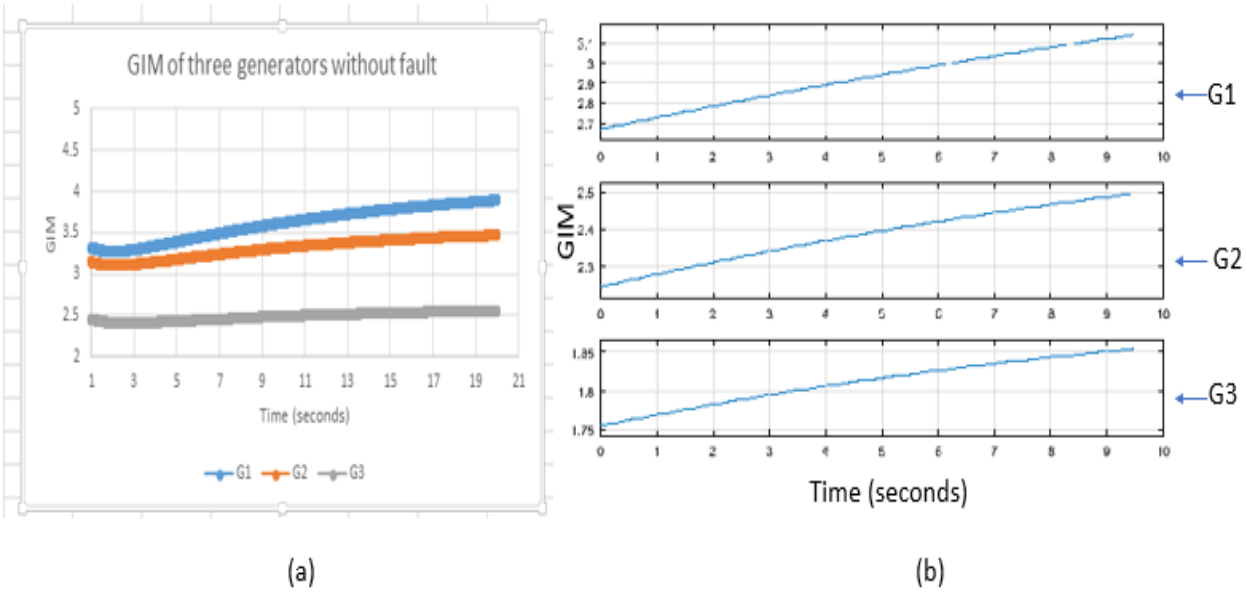

Figure 4.10: GIM of the generators without fault, (a) on the same graph and (b) separately

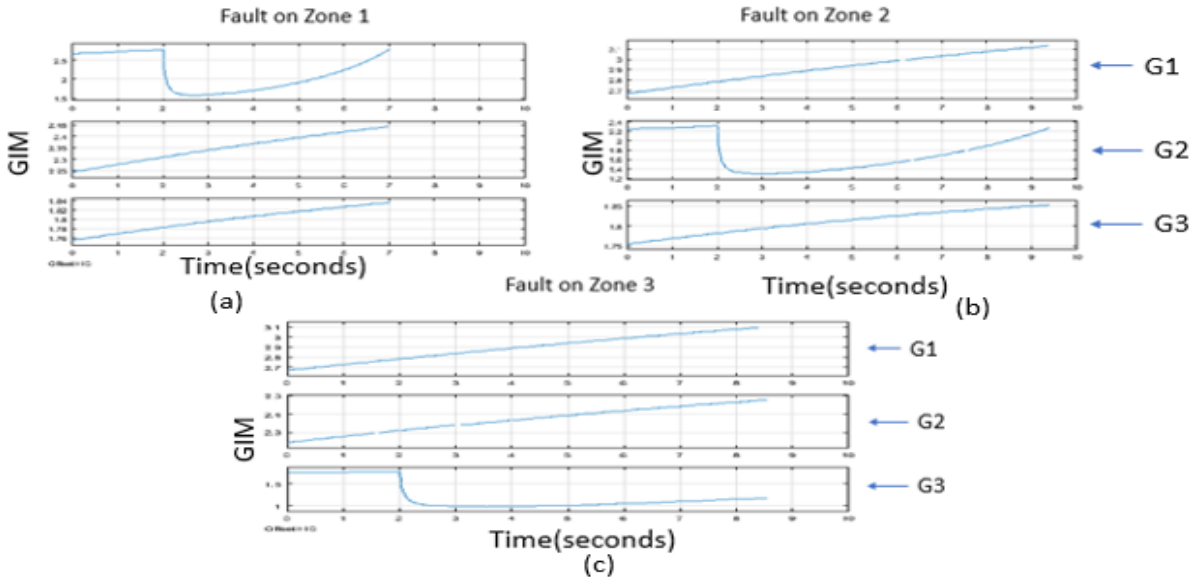

Figure 4.11: GIM of the generators after a three-phase fault is simulated in the respective zones 1 (a), 2 (b) and 3 (c).

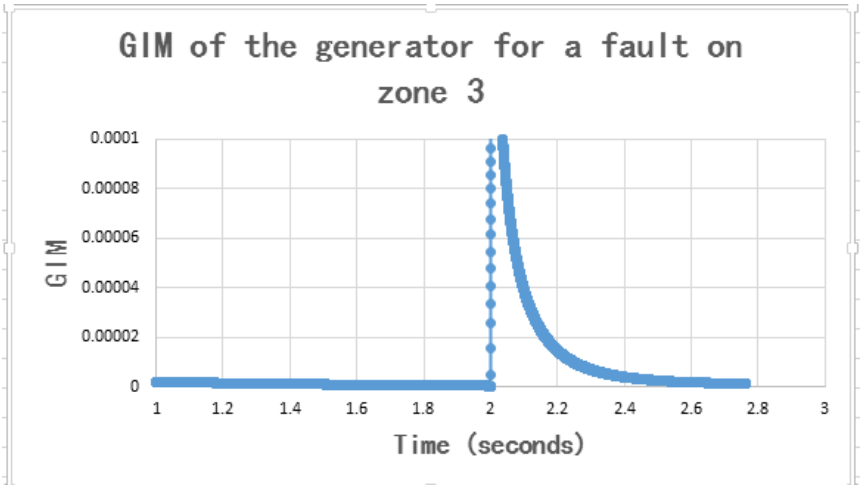

Figure 4.12: Close analysis of GIM of generator three after fault occurrence on that zone

4.5.2 Evaluation of WAP Technique B in MATLAB/Simulink

The performance of the algorithm was evaluated in terms of its accuracy and fault clearing time in MATLAB/Simulink similar to WAP algorithm A. Figure 4.13 and Figure 4.14 show the current and voltage waveforms before, during and after a two phase (L-L) and a three phase (L-L-L-G) faults were simulated and cleared with the algorithm within 0.15 and 0.04 seconds respectively. The fault clearing time range of this algorithm is between 0.04 to 0.15 seconds. Table 4.5 shows the different faults clearing times recorded in the zones and Table 4.6 shows the faulted zones and lines detected by the algorithm and the actual lines and zones on which the fault occurred.

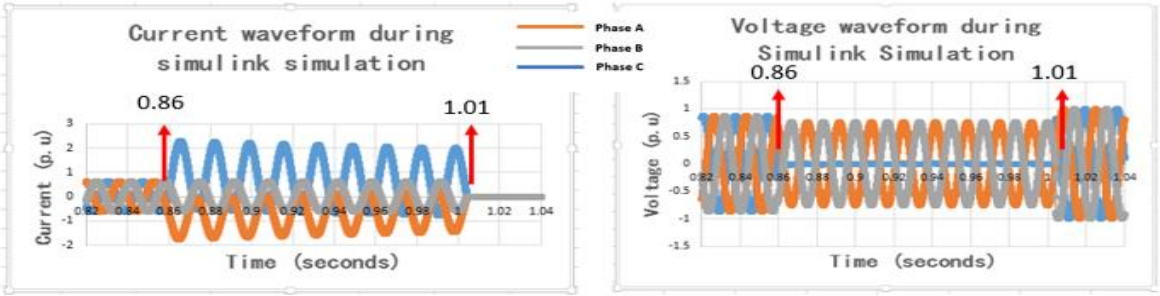

Figure 4.13: Current and voltage waveforms before, during and after a two (L-L) fault in Simulink

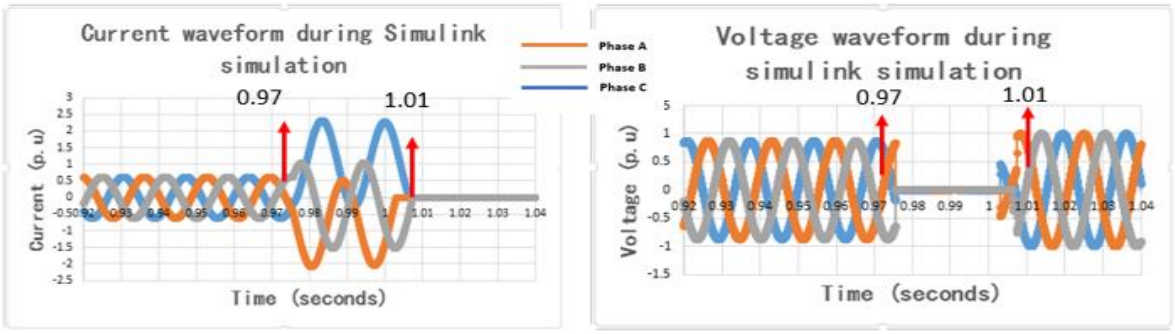

Figure 4.14: Current and voltage waveforms before, during and after a three phase (L-L-L-G) fault in Simulink

Table 4.5: Fault clearing times of WAP Technique B

	Fault Clearing Time (seconds)			
Fault Type	**L-G**	**L-L**	**L-L-G**	**L-L-L-G**
Zone 1	0.04	0.04	0.02	0.02
Zone 2	0.04	0.04	0.022	0.02
Zone 3	0.04	0.04	0.025	0.015

Table 4.6: WAP Technique B accuracy in detecting faults

Faulted line	Faulted Zone	Type of fault	Zone detected	Line detected
4 - 1	1	L-L-L-G	1	4-1
		L-L-G		4-1
		L-L		4-1
		L-G		4-1
4 - 5	1	L-L-L-G	1	4-5
		L-L-G		4-5
		L-L		4-5
		L-G		4-5
4 - 6	1	L-L-L-G	1	4-6
		L-L-G		4-6
		L-L		4-6
		L-G		4-5
2 – 7	2	L-L-L-G	2	2-7
		L-L-G		2-7
		L-L		2-7
		L-G		2-7
7 – 8	2	L-L-L-G	2	7-5
		L-L-G		7-5
		L-L		7-5
		L-G		7-5
7 – 5	2	L-L-L-G	2	7-5
		L-L-G		7-5
		L-L		7-5
		L-G		7-5
3 – 9	3	L-L-L-G	3	3-9
		L-L-G		3-9
		L-L		3-9
		L-G		3-9
9 - 8	3	L-L-L-G	3	9-8
		L-L-G		9-8
		L-L		9-8
		L-G		9-8
9 – 6	3	L-L-L-G	3	9-6
		L-L-G		9-6
		L-L		9-8
		L-G		9-6

4.6 WAP Technique C [38]

This algorithm also utilizes the formation of backup protection zones after which the faulted line within the faulted zone is detected.

A. Formation of Backup Protection Zones (BPZ)

The backup protection zones are formed based on the PMU placement and the network topology. A backup protection zone within the network topology consists of the lines and buses that are surrounded by a PMU equipped bus. The protection zones for this WAP technique is shown in Figure 4.15.

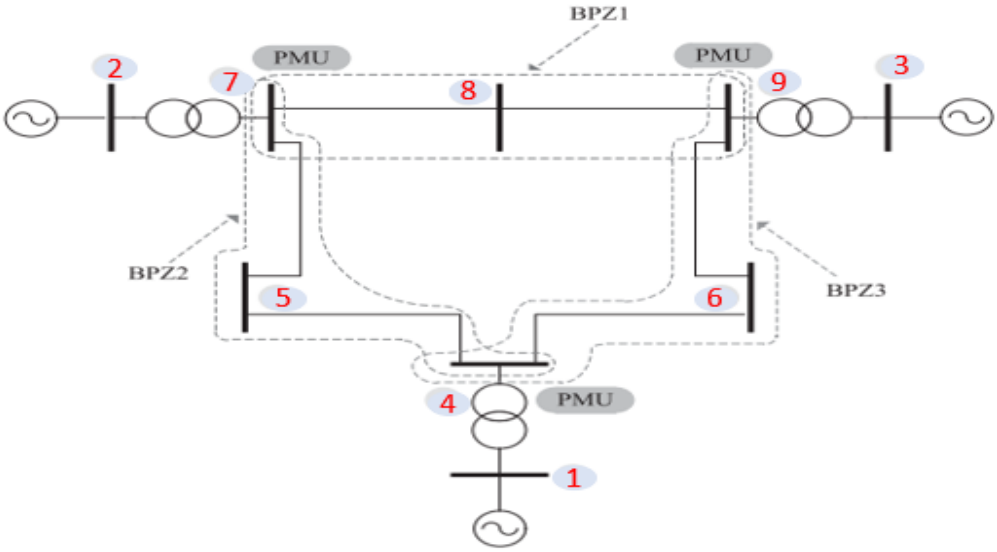

Figure 4.15: IEE 9-bus power system with the zones of protection based on WAP technique C

B. Faulted Zone Identification Algorithm

Each BPZ is surrounded by PMUs as shown in Figure 4.15, therefore all the currents that enter a BPZ is measured by the corresponding PMUs. The sum of zero or positive sequence currents entering a zone is noted at pre-fault conditions. When a fault occurs, these currents rise above the threshold, hence the *mth* zone with an increase in the zero or positive sequence currents entering the zone has the fault.

$$I_{ent,BPZ_m}^{(s)} > I_{th,BPZ_m}^{(s)} \quad (4.12)$$

where

$$I_{ent,BPZ_m}^{(s)} = \left\lfloor \sum_{l \in L_m} I_l^{(s)} \right\rfloor \quad (4.13)$$

The thresholds for determining the pre-fault conditions of the *mth* BPZ are defined in an adaptive manner as follows:

$$I_{th,BPZ_m}^{(0)} = \max\left\{(d_{0,BPZ_m}).(I_{ent,BPZ_m}^{(0)}), I_{\min,BPZ_m}\right\} \quad (4.14)$$

$$I_{th,BPZ_m}^{(1)} = \max\left\{(d_{1,BPZ_m}).(I_{ent,BPZ_m}^{(1)}), I_{\min,BPZ_m}\right\} \quad (4.15)$$

where the superscripts (0) and (1) represent the zero and positive sequence measurements respectively. $I_{\min,BPZ_m}$ is a constant that determines the minimum value of $I_{th,BPZ_m}^{(s)}$ and is determined through the power system transient studies, it takes a value between 0 to 1 p.u. For any BPZs having no load, the $I_{th,BPZ_m}^{(s)}$ will be equal to $I_{\min,BPZ_m}$. At any point in time, $I_{ent,BPZ_m}^{(1)}$ is the average of $I_{ent,BPZ_m}^{(1)}$ in the last minute. d_{0,BPZ_m} and d_{1,BPZ_m} are constant coefficients determining $I_{th,BPZ_m}^{(0)}$ and $I_{th,BPZ_m}^{(1)}$ respectively. By updating $I_{ent,BPZ_m}^{(1)}$, the threshold of the BPZs is adapted constantly according to the power system conditions. To implement this fault zone identification algorithm in a smart transmission grid, all generator buses must be equipped with PMUs.

C. Faulted Line Identification

Each BPZ is surrounded by PMUs and the internal buses have no PMU. A faulted BPZ containing n_p PMU buses and n_{np} non-PMU buses is shown in Figure 4.16. The faulted BPZ is considered as a sub-network which is connected to the remaining network by surrounding PMU buses. $I_{ent,i}$ is the total current entering the faulted BPZ through the ith PMU bus. f_1 and f_2 are two end buses of the faulted line; f is a fictitious bus at the fault point; x is per-unit distance between fault point f and bus f_1 and I_f is the fault current injected into the fault point. In Figure 4.16, boundary PMU buses are connected to some non-PMU buses via transmission lines. Currents entering from

PMU buses to these lines are $I_1, I_2, ...I_{nL}$. $V_1, V_2, ..., V_{np}$ are the voltages of the n_p boundary PMU buses.

Only voltage and current phasors measured by boundary PMU buses are available and used for the faulted line identification in the faulted BPZ. The voltages measured by these PMU buses can be expressed as;

$$V_i = Z_{if} I_f + \sum_{r=1}^{np} Z_{ir} I_{ent,r} \forall i = 1, 2, ..., np \qquad (4.16)$$

where $Z_{i,j}$ is the $i-j$ element of the matrix Z.

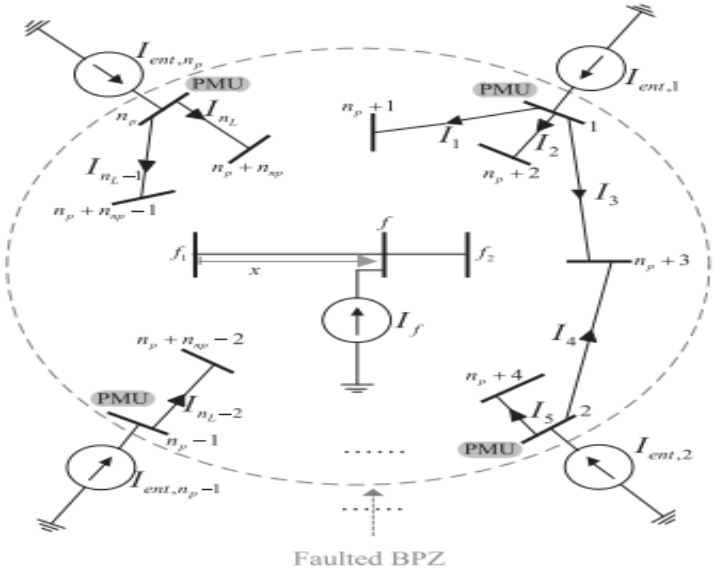

Figure 4.16: Analysis of faulted line in a BPZ

Z is the bus impedance matrix of the faulted BPZ including fictitious bus f. The elements of Z can be calculated by utilizing the elements of Z^0; the pre-fault bus impedance matrix of the faulted BPZ, which does not include the fictitious bus f hence the dimension is $nb \times nb$. The elements of this matrix are as follows:

$$Z^0 = \begin{bmatrix} Z^0_{11} & \cdots & Z^0_{1f1} & \cdots & Z^0_{1f2} & \cdots & Z^0_{1nb} \\ \vdots & & \vdots & & \vdots & & \vdots \\ Z^0_{f11} & \cdots & Z^0_{f1f1} & \cdots & Z^0_{f1f2} & \cdots & Z^0_{f1nb} \\ \vdots & & \vdots & & \vdots & & \vdots \\ Z^0_{f21} & \cdots & Z^0_{f2f1} & \cdots & Z^0_{f2f2} & \cdots & Z^0_{f2nb} \\ \vdots & & \vdots & & \vdots & & \vdots \\ Z^0_{nb1} & \cdots & Z^0_{nbf1} & \cdots & Z^0_{nbf2} & \cdots & Z^0_{nbnb} \end{bmatrix} \quad (4.17)$$

Z_{ir} is determined by utilizing the elements of Z^0 as:

$$Z_{ir} = Z^0_{ir} \quad \forall i, r = 1, \ldots, nb \quad (4.18)$$

And by neglecting the shunt capacitance of the faulted line Z_{if} can be calculated as:

$$Z_{if} = Z^0_{if1} + (Z^0_{if2} - Z^0_{if1}) \times \forall i = 1, \ldots, nb \quad (4.19)$$

The currents of transmission lines which are connected to the PMU buses are measured by PMUs. According to the KCL, these currents can be expressed as follows:

$$I_l = \frac{V_{l1} - V_{l2}}{z_l} + \frac{y_l}{2} V_{l1} \quad \forall l = 1, \ldots, nL \quad (4.20)$$

where l is the line that connects PMU bus l_1 to the non-PMU bus l_2. By substituting (4.16) into (4.20) we obtain:

$$I_l = C_{lf} I_f + \sum_{r=1}^{n_p} C_{lr} I_{ent,r} \quad \forall r = 1, \ldots, nL \quad (4.21)$$

where C_{lr} and C_{lf} are constants, calculated by the BPZ parameters.

Equation (4.16) and (4.21) can be written in matrix form as:

$$Hu = m \quad (4.22)$$

where matrix H consists of two sub-matrices H_V and H_I as

$$H = \begin{bmatrix} H_V \\ H_I \end{bmatrix} \tag{4.23}$$

The dimensions of H_V and H_I are $n_P \times 2$ and $n_L \times 2$, respectively. These are constant matrices which are determined by BPZ parameters.

In (4.22) vector m consists of two sub-vectors m_V and m_I as follows:

$$m = \begin{bmatrix} m_V \\ m_I \end{bmatrix} \tag{4.24}$$

The dimensions of m_V and m_I are $n_P \times 1$ and $n_L \times 1$, respectively. These are determined on the basis of the voltages and currents measured by PMUs and BPZ parameters.

And u is the 2×1 unknown vector whose elements are as follows:

$$u = \begin{bmatrix} u_1 \\ u_2 \end{bmatrix} = \begin{bmatrix} I_f \\ xI_f \end{bmatrix} \tag{4.25}$$

If a fault occurs on one of the lines connected to a PMU bus, (4.20) and (4.21) are not valid for that line. Therefore in equation (4.22), the related row is deleted and the dimension of matrix H_1 and vector m_1 will become $(n_L - 1)\times 2$ and $(n_L - 1)\times 1$, respectively.

In (4.22), matrix H and vector m are known and only vector u is unknown, on the other hand, this equation is linear. Hence, u can readily be estimated by the linear least square's method and afterwards u_1, u_2 are specified as:

$$u_1 = \frac{1}{g}\left[\left(h_2^* \cdot h_2\right)\left(h_1^* \cdot m\right) - \left(h_1^* \cdot h_2\right)\left(h_2^* \cdot m\right)\right] \tag{4.26}$$

$$u_2 = \frac{1}{g}\left[\left(h_1^* \cdot h_1\right)\left(h_2^* \cdot m\right) - \left(h_1 \cdot h_2^*\right)\left(h_1^* \cdot m\right)\right] \tag{4.27}$$

where the dot and asterisk denote inner product and complex conjugate, respectively. h_1 and h_2 are first and second columns of matrix *H*, respectively. Also, g is determined as follows:

$$g = \left[\left(h_1^* \cdot h_1 \right) \left(h_2^* \cdot h_2 \right) - \left(h_1^* \cdot h_2 \right) \left(h_1 \cdot h_2^* \right) \right] \tag{4.28}$$

Therefore, the estimation of the fault location, i.e. χ is acquired as:

$$x = \frac{\left(h_1^* \cdot h_1 \right) \left(h_2^* \cdot m \right) - \left(h_1 \cdot h_2^* \right) \left(h_1^* \cdot m \right)}{\left(h_2^* \cdot h_2 \right) \left(h_1^* \cdot m \right) - \left(h_1^* \cdot h_2 \right) \left(h_2^* \cdot m \right)} \tag{4.29}$$

The purpose of the algorithm is the determination of the faulted line in the faulted BPZ, which means the main unknown is the faulted line. For each line that belong to the faulted BPZ, this algorithm first supposes that the fault has occurred on that line, and next estimates the fault location χ by equation (4.29). The faulted line is the line who's estimated χ is between 0 and 1. If more than one line satisfy this condition, then, for each of these suspected lines the relative residual error estimation is calculated as:

$$J(u) = \frac{\sqrt{\Delta u . \Delta u^*}}{\sqrt{m . m^*}} \tag{4.30}$$

where

$$\Delta u = H \begin{bmatrix} u_1 \\ u_2 \end{bmatrix} - m \tag{4.31}$$

The line, who's estimated u best matches the measured values, is selected as the faulted line. Which means, the line which has the least residual error is selected as the faulted line.

4.6.1 Results of WAP Technique C Implementation in MATLAB/Simulink

This WAP technique was implemented on the IEEE 9-bus power system shown in Figure 4.3 with zones of protection and the PMU buses as indicated. The no-fault condition was simulated and the sum of zero and positive sequence voltages entering the zones were recorded as shown in Table 4.7. After that, selected fault conditions were simulated to analyze the behavior of the positive and zero sequence currents entering each protection zone, and these were also recorded in Table 4.7.

4.6.2 Evaluation of WAP Technique C in MATLAB/Simulink

The execution time of this WAP technique was investigated for all fault conditions to determine the speed of operation of the WAP technique. Figure 4.17 and Figure 4.18 show the waveforms

used to determine the fault clearing time. From the waveforms shown in Figure 4.17 and Figure 4.18, the fault clearing time of 20 ms is the same for both two-phase and three-phase faults. The fault clearing time for this algorithm is the same for all the investigated fault conditions. Table 4.8 shows the various fault clearing times and Table 4.9 shows the zones and lines detected and the actual zones and lines on which the faults were simulated. How the three algorithms compare is discussed in chapter 7.

Table 4.7: Positive and zero sequence currents entering each protection zone

Faulted Case		**Positive and zero sequence current entering each zone**					
		Zone 1		**Zone 2**		**Zone 3**	
		positive	**zero**	**positive**	**zero**	**positive**	**zero**
No Fault	No Fault	1.133	9.4e-14	1.167	1.8e-13	1.109	1.6e-13
L-L-L-G	Zone 1	3.139	6.3e-14	2.95	1.2e-13	1.662	8.4e-14
L-L		1.916	5.5e-5	1.884	4.7e-5	1.209	2.4e-5
L-G		1.515	0.8782	1.527	0.7525	1.109	0.3841
L-L-L-G	Zone 2	1.170	4.32e-14	2.571	1.5e-13	1.329	6.1e-14
L-L		0.960	1.9e-5	1.648	4.5e-5	1.003	2.15e-5
L-G		0.9872	0.31	1.4	0.7563	0.9899	0.3544
L-L-L-G	Zone 3	1.515	1.2e-13	1.133	1.1e-13	3.106	9.5e-14
L-L		1.19	2.13e-5	0.8919	2.3e-5	1.875	5.5e-5
L-G		1.125	0.3186	0.9539	0.3557	1.461	0.8242

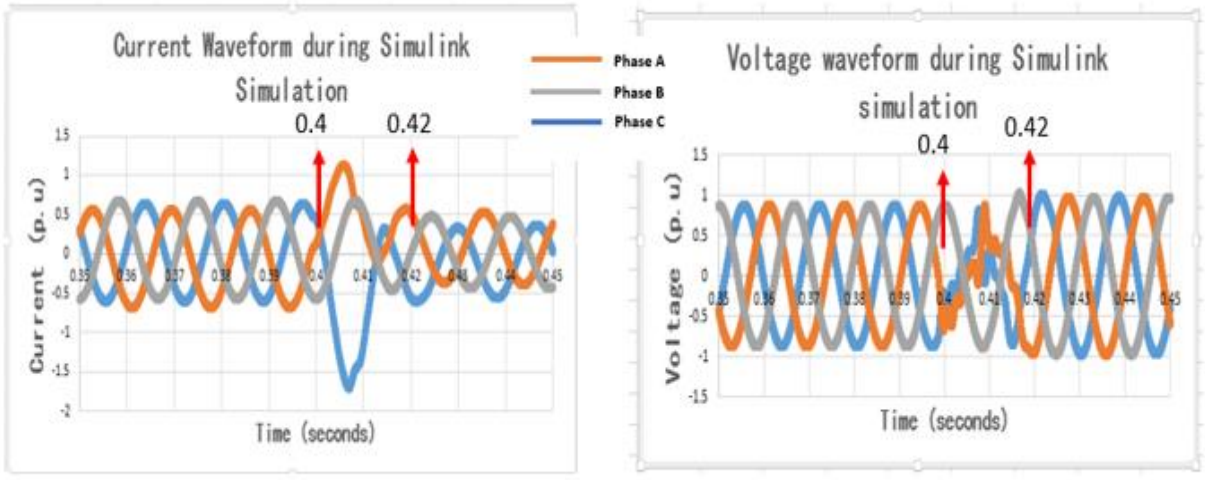

Figure 4.17: Two-phase fault clearing time of the WAP Technique C during Simulink Simulation

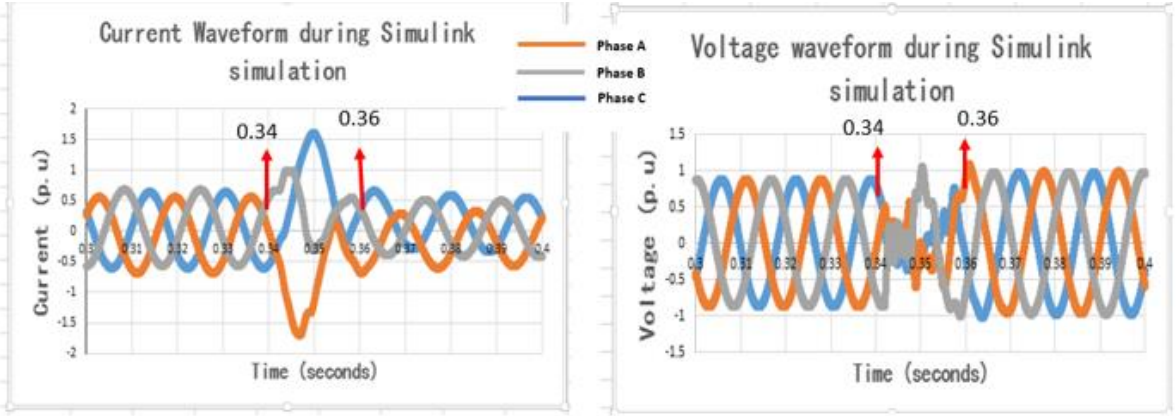

Figure 4.18: Three-phase fault clearing time of the WAP Technique C during Simulink Simulation

Table 4.8: Fault clearing times of WAP Technique C

	Fault Clearing Time (seconds)			
Fault Type	**L-G**	**L-L**	**L-L-G**	**L-L-L-G**
Zone 1	0.02	0.02	0.02	0.02
Zone 2	0.02	0.02	0.02	0.02
Zone 3	0.02	0.02	0.02	0.02

Table 4.9: WAP Technique C accuracy in detecting faults

Faulted line	Faulted Zone	Type of fault	Zone detected	Line detected
4 - 1	1	L-L-L-G	1	4-1
		L-L-G		4-1
		L-L		4-1
		L-G		4-1
4 - 5	1	L-L-L-G	1	4-5
		L-L-G		4-5
		L-L		4-5
		L-G		4-5
4 - 6	1	L-L-L-G	1	4-6
		L-L-G		4-6
		L-L		4-5
		L-G		4-6
2 – 7	2	L-L-L-G	2	2-7
		L-L-G		2-7
		L-L		2-7
		L-G		2-7
7 – 8	2	L-L-L-G	2	7-8
		L-L-G		7-8
		L-L		7-8
		L-G		7-5
7 – 5	2	L-L-L-G	2	7-5
		L-L-G		7-5
		L-L		7-5
		L-G		7-5
3 – 9	3	L-L-L-G	3	3-9
		L-L-G		3-9
		L-L		3-9
		L-G		3-9
9 - 8	3	L-L-L-G	3	9-8
		L-L-G		9-8
		L-L		9-8
		L-G		9-8
9 – 6	3	L-L-L-G	3	9-6
		L-L-G		9-6
		L-L		9-6
		L-G		9-8

CHAPTER FIVE: REAL-TIME SIMULATION USING OPAL-RT DIGITAL SIMULATOR

In this chapter, simulating the models on the real-time target as well as the results of the real-time simulation of the wide area protection algorithms are presented and discussed.

5.1 Executing Real-Time Simulation on OPAL-RT Simulator.

The OPAL-RT allows MATLAB/Simulink to interface with the RT-LAB software where the simulation models created in Simulink can be modified into a compatible mode for execution on the OPAL-RT simulator. To run a simulation on the OPAL-RT, first, the system model that needs to be run in real-time must be created using Simulink and it must be running before converting it to a form that the simulator can read. When the model is in the right form, then it can be deployed onto the simulator through an ethernet cable where it is then executed in real-time. The output signals can then be taken from the real-time simulator with inputs and outputs connections (I/Os) and other communication protocols such as IEC61850, IEC104, C37.118. The signals can be measured using an oscilloscope or used to perform hardware-in-the-loop (HIL) simulation. Figure 5.1 shows a summary of real-time simulation using OPAL-RT simulator. **Appendix B** shows detailed explanation and figures of how the real-time simulation was carried out.

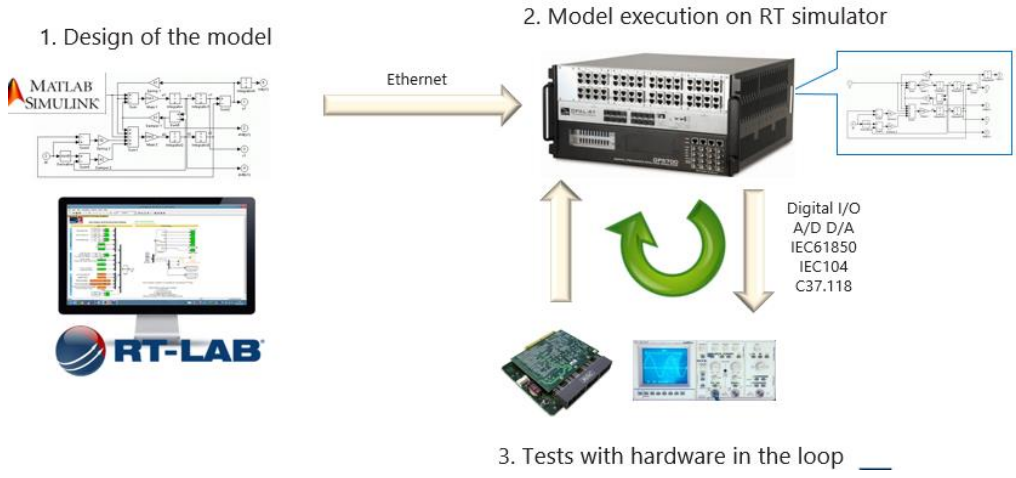

Figure 5.1: Real-time and Hardware-In-the-Loop (HIL) simulation using OPAL-RT [59]

5.2 Results of Real-time Simulation of the WAP Techniques

The performances of the algorithms were tested during a real-time simulation on Opal-RT as was done during Simulink simulation. The time taken to clear faults in real-time as well as the accuracy of detecting all types of faults were analyzed. Figure 5.2 shows the model that was executed in real-time. The RT-LAB software and OPAL-RT target use only subsystems at the top level of the model, so the model depicted in Figure 5.2 shows the computation subsystem which contains the IEEE 9-bus system and the algorithm that is being tested whereas the console contains the switches and scopes for faults simulation, visualizing and analyzing of signals.

During the real-time simulation, it is only the console that is accessible to the user on the user's PC whiles the computation subsystem is loaded onto the real-time target which is why any block for fault simulation and scopes for viewing signals must be placed in the console. Figure 5.3 shows the console after the model has been loaded onto the target. The RT-LAB stamp in yellow which says '*automatically generated by RT-LAB during compilation*' shows that the model is compiled and loaded successfully and ready for execution in real-time.

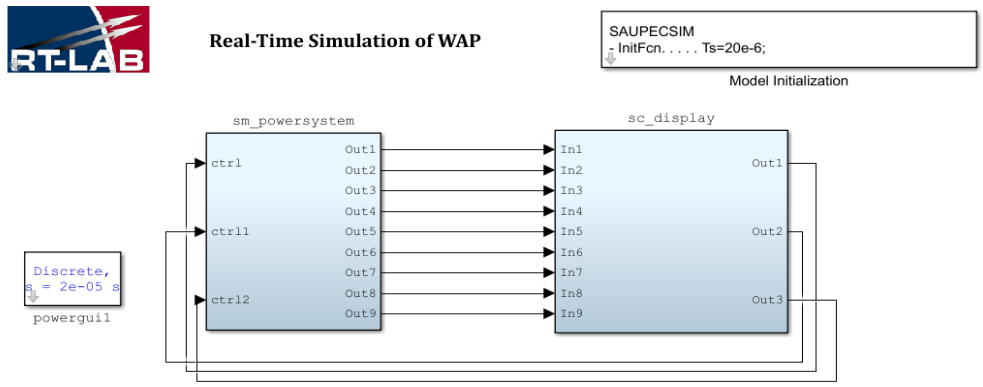

Figure 5.2: The Model for execution on the Opal-RT target

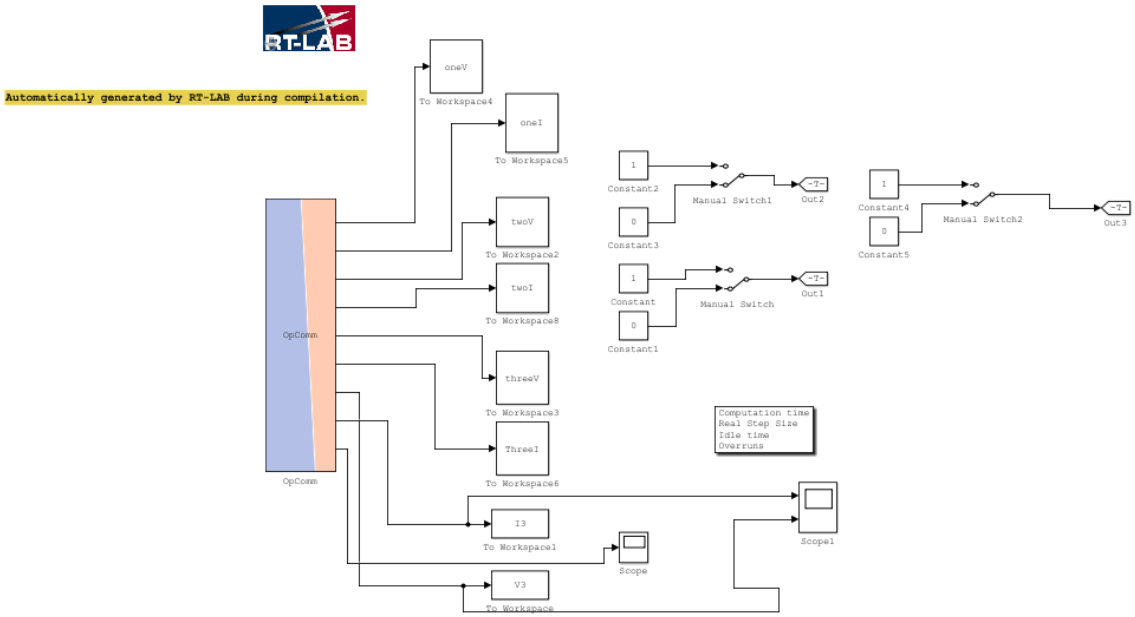

Figure 5.3: The Model Console after successful compilation and loading onto the target.

5.2.1 WAP Technique A Simulation in Real-Time on OPAL-RT.

A fault on zone 3 of the IEEE 9-bus system was simulated and the voltage and current waveforms of all the PMU buses were recorded as shown in Figure 5.4 and Figure 5.5. The time taken to clear all types of fault were analyzed during the real-time simulation as was done in MATLAB/Simulink. Figure 5.6 and Figure 5.7 show the current and voltage waveforms of a bus closest to the circuit breaker before, during and after a two-phase line-to-line and a three-phase line to ground fault in zone 3 were simulated and cleared with the algorithm. The waveforms show that the faults were cleared in 0.032 sec and 0.015 sec respectively.

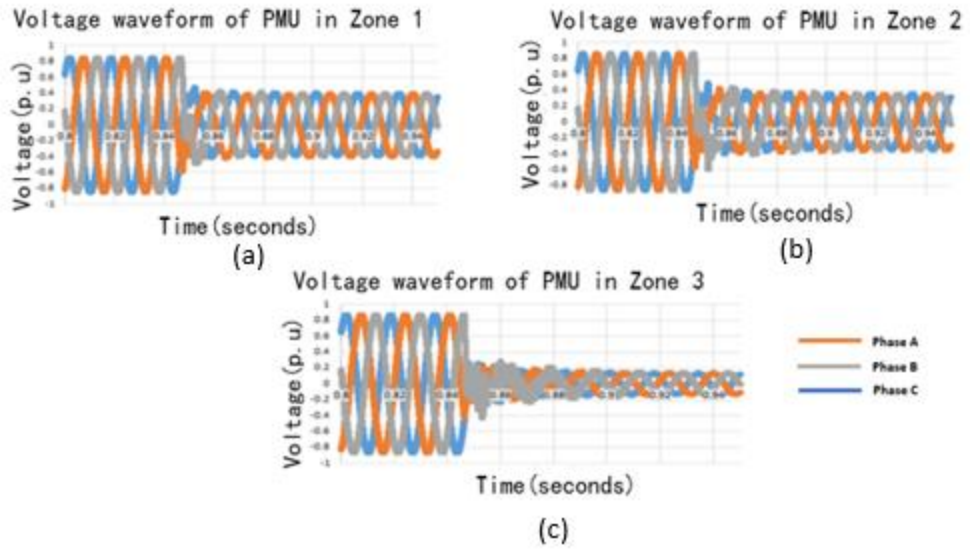

Figure 5.4: Voltages of PMU buses; before and after a fault on zone 3 during simulation in real-time, zone 1 (a), zone 2 (b) and zone 3 (c)

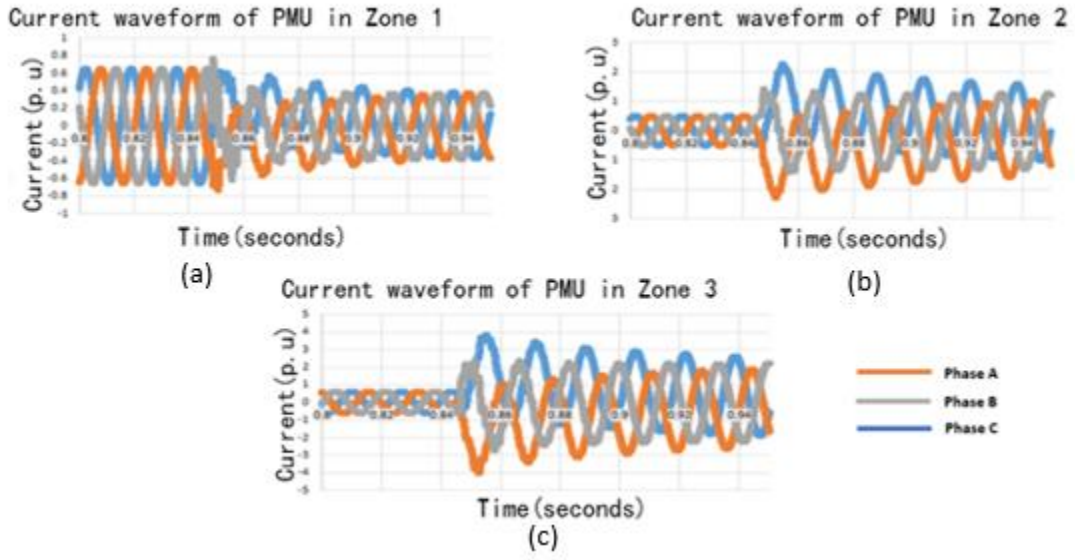

Figure 5.5: Currents of PMU buses; before and after a fault on zone 3 during simulation in real-time, zone 1 (a), zone 2 (b) and zone 3 (c)

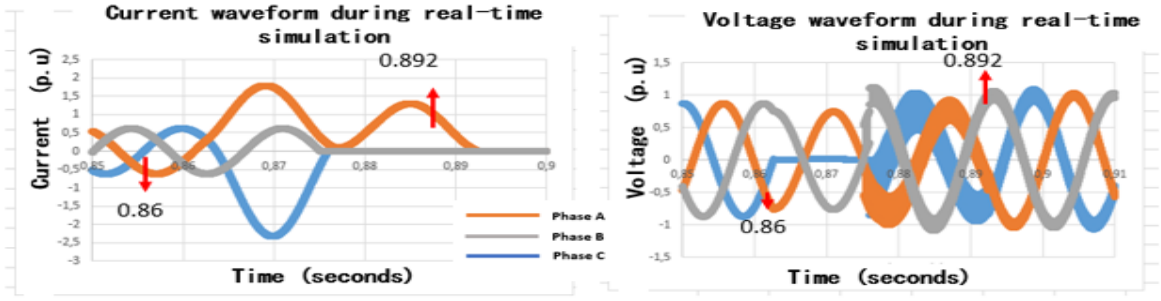

Figure 5.6: Current and voltage waveforms before, during and after a two-phase fault in real-time

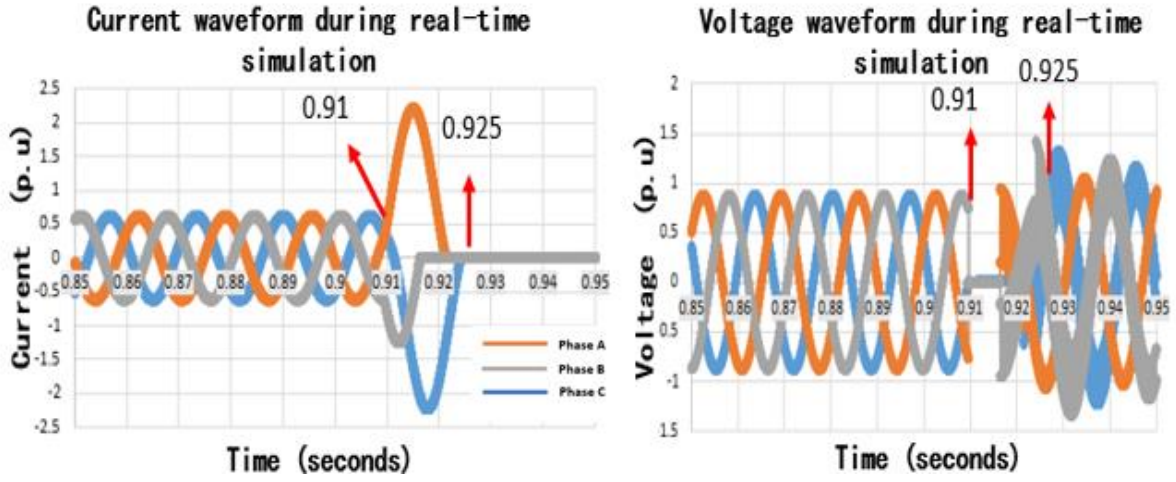

Figure 5.7: Current and voltage waveforms before, during and after a three-phase to ground fault in real-time

5.2.2 WAP Technique B Simulation in Real-Time on OPAL-RT

This Wide area protection technique was also executed in real-time on the Opal-RT target and the performance in terms of speed and accuracy were analyzed as was done during Simulink simulations. The Gain in the momentum of the generators without any fault and with a fault in the respective zones during real-time simulation are shown in Figure 5.8, also, the fault clearing times of the algorithm in real time are shown in Figure 5.9 and Figure 5.10. From Figure 5.8, it clearly shows that there is a significant change in the GIM of the generator in the zone at the time when

fault occurs. Figure 5.9 and Figure 5.10 show that the faults were cleared in 0.03 sec and 0.02 sec respectively.

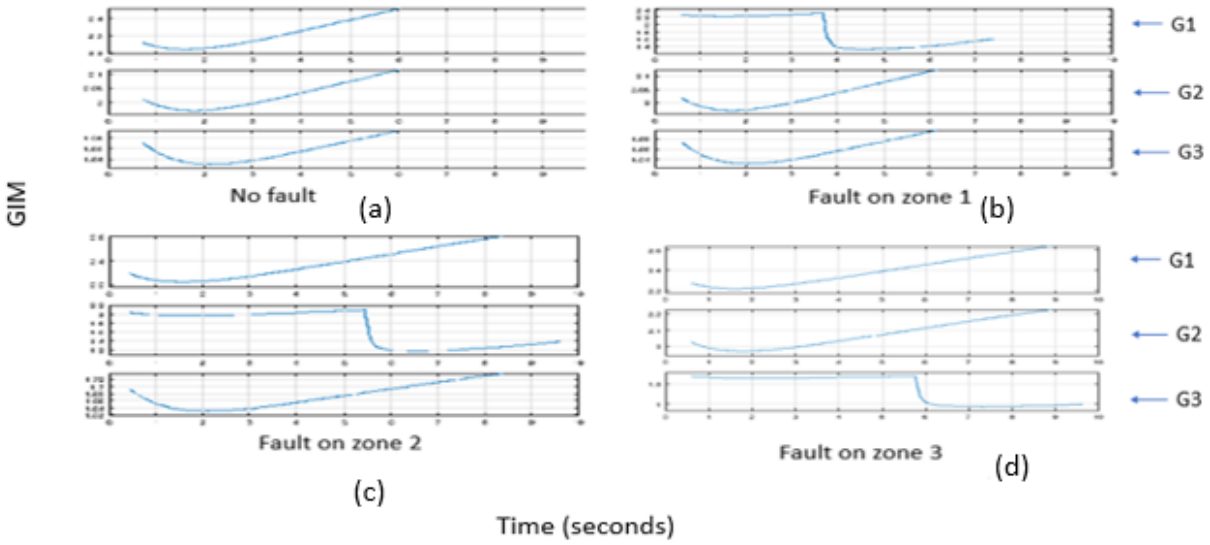

Figure 5.8: GIM of the generators in real-time without fault (a) and with a fault on respective zones 1(b), 2(c) and 3(d)

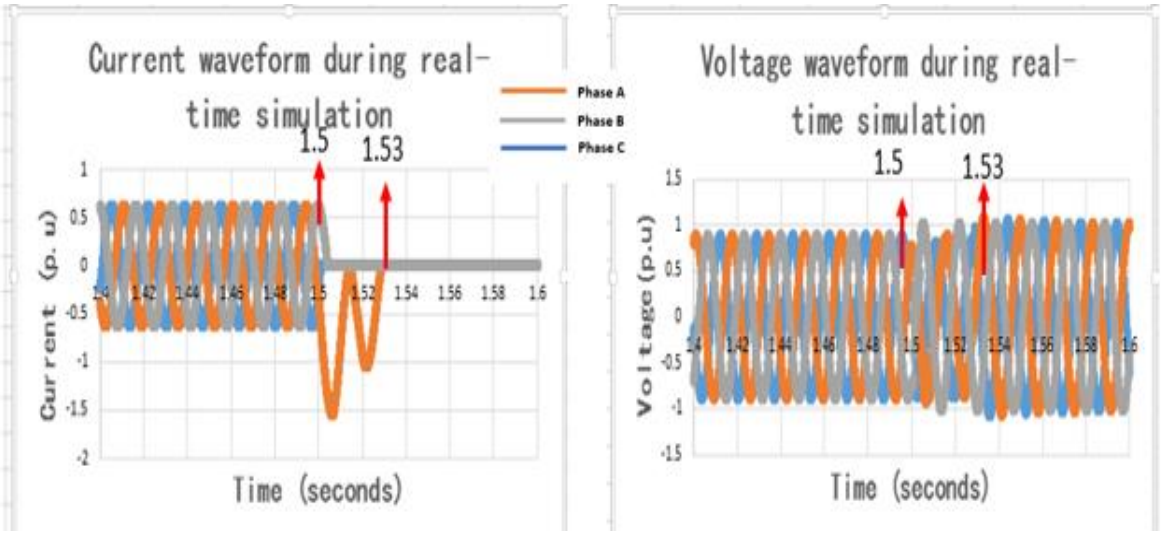

Figure 5.9: Single phase to ground fault clearing time of the WAP Technique B during real-time Simulation

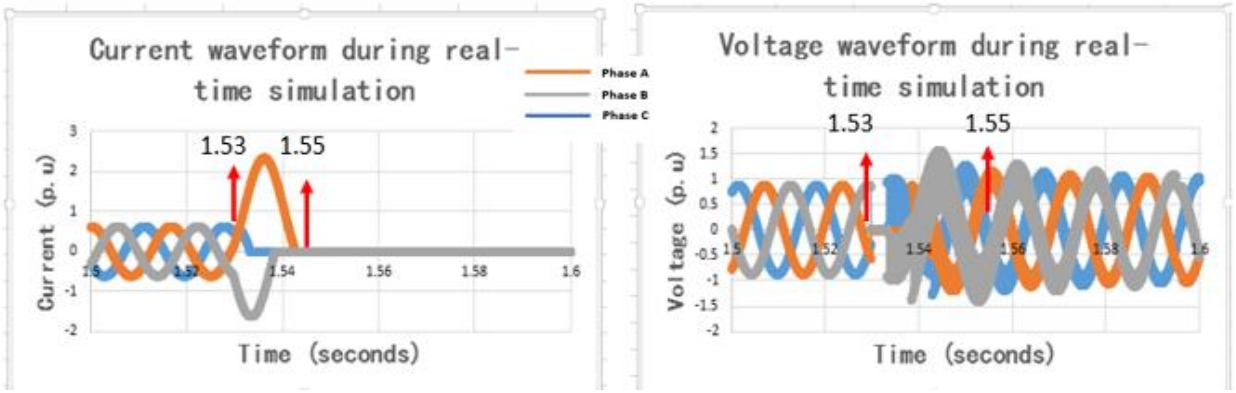

Figure 5.10: Two-phase fault clearing time of the WAP Technique B during real-time Simulation

5.2.3 WAP Technique C Simulation in Real-Time on OPAL-RT

This protection technique was also executed in real-time using the Opal-RT real-time simulator. The Figures 5.11 and 5.12 show the waveforms used to determine the fault clearing times of the wide area protection technique in real-time. How the three algorithms perform during MATLAB/Simulink and real-time is discussed in chapter 7.

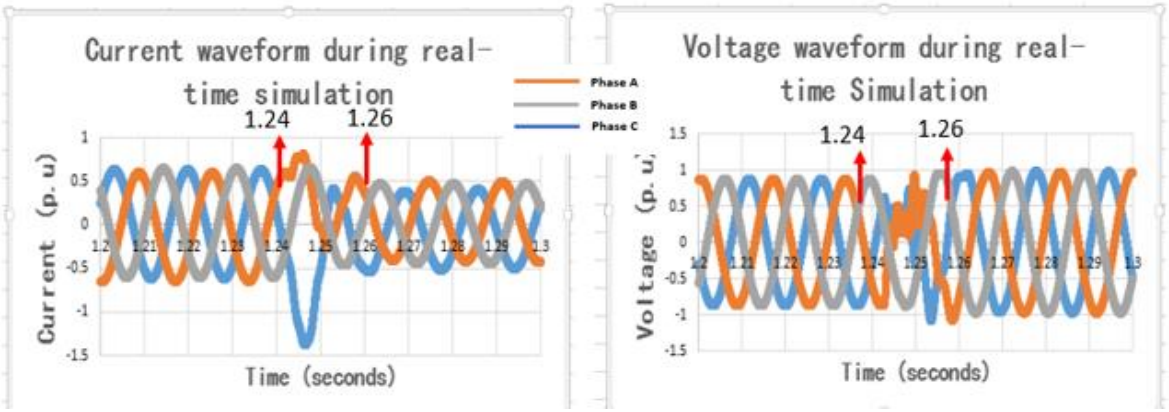

Figure 5.11: Two phase fault clearing time of the WAP Technique C during real-time Simulation

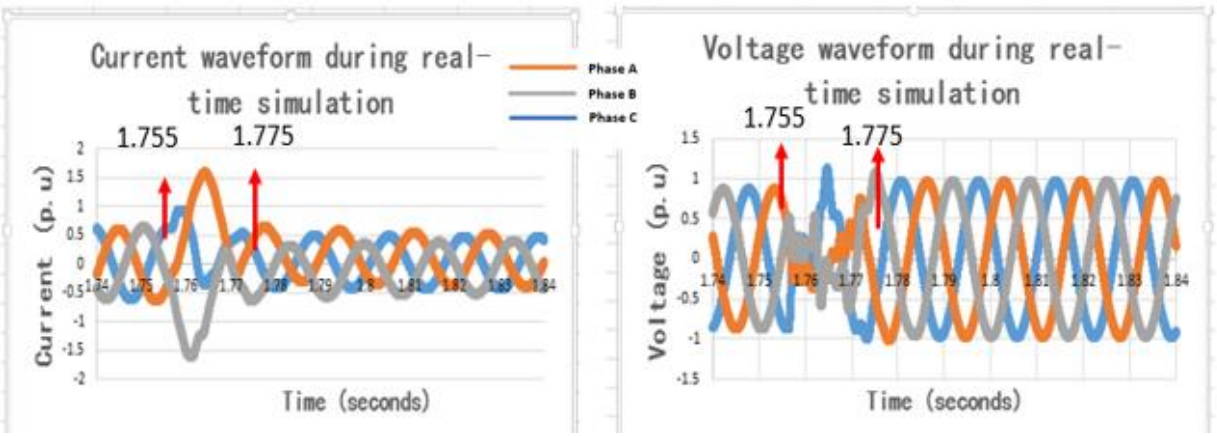

Figure 5.12: Three-phase fault clearing time of the WAP Technique C during real-time Simulation

CHAPTER SIX: HARDWARE-IN–THE–LOOP IMPLEMENTATION USING THE OPAR-RT DIGITAL SIMULATOR

In this chapter, the process of simulating the various wide area protection techniques and evaluating their performances in terms of fault clearing time through hardware-in-the-loop using OPAL-RT and SEL-351A relay is presented and discussed. Detailed explanations of how the HIL simulation was achieved and the relevant figures are shown in appendix C. The purpose of the HIL simulation in this project is to verify additional time delay introduced by communication delay in the algorithms' response times.

6.1 External Hardware, Inputs and Outputs (I/Os)

To perform hardware-in-the-loop (HIL) testing, the model running on the real-time target acts as the actual system and hence the analog and digital signals taken from the simulator is used to test the performance of the control hardware. In the case of this research, where the focus is on the protection of the power system, the control hardware here is the relay (SEL-351A) as shown in Figure 6.1; which also illustrates the tools and connections necessary to achieve HIL simulation using the OPAL-RT real-time target.

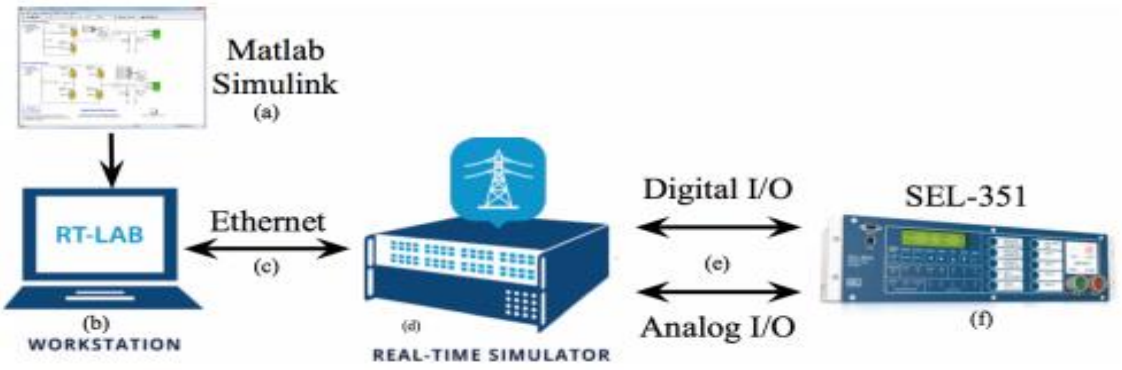

Figure 6.1: HIL simulation for protection studies using a relay [71]

The signal output of the real-time target has a maximum of ±16 V peak signal, any signal value exceeding that value is truncated as shown in Figure 6.3. Hence, to perform a HIL test using the protective relays which require a higher voltage and current signals than the output of the target, a

voltage and a current amplifier is required. The connection diagram for HIL simulation using amplifiers is shown in Figure 6.2.

However, as mentioned earlier in Chapter three, SEL relays provide a low-level test interface for testing the relays using low voltage signals up to a maximum of 9 V peak-to-peak. This made the interaction between the Opal-RT and the SEL-351A relay used in this research possible without the current and voltage amplifier. Figure 6.4 shows the low-level test interface of the SEL-35A relay.

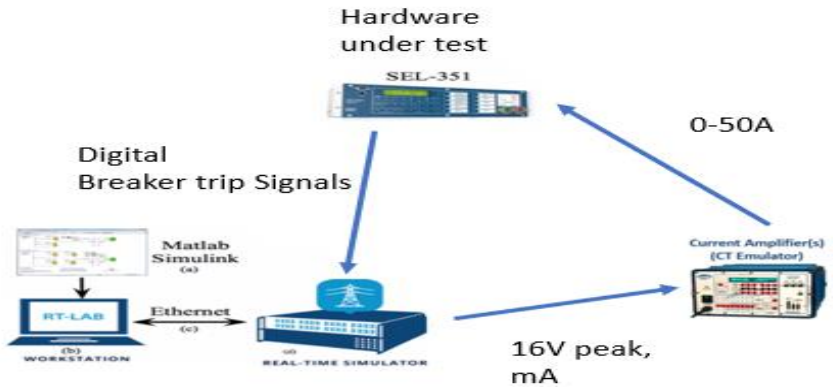

Figure 6.2: HIL simulation and testing of relays using current and voltage amplifiers

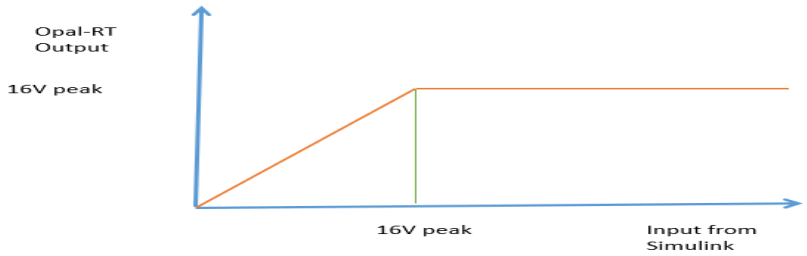

Figure 6.3: Simulink Input signal and Opal-RT output signal during real-time simulation

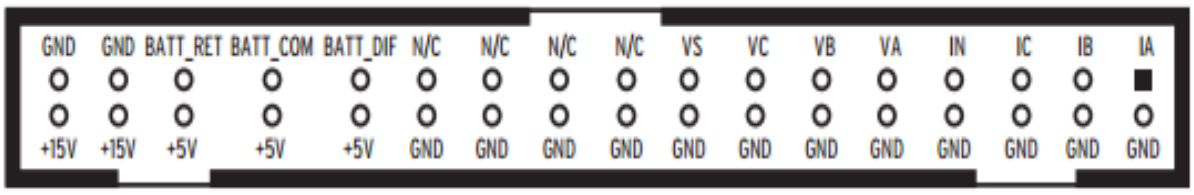

Figure 6.4: Low-level test interface of SEL-351A relay accessible after the removal of the front panel

6.2 The Control Hardware for HIL simulation; SEL-351A Relay

Performing a hardware-in-the-loop simulation requires external hardware often referred to as the hardware under test which will be inserted into the simulation loop. By inserting the hardware into the computer model, it enables the hardware device to go through realistic operation - just as it will in the actual field. SEL-351A relay is used in this research as the hardware under test. AcSELerator quickset software by SEL provides the platform for establishing a connection between the relay and a host PC to: read and change settings in the relay, read relay meter readings, retrieve relay events for reading by SEL synchroWAVe event software and a human-machine interface (HMI) to interact with the relay. The settings in the SEL relay include global, group, report, text, DNP and port settings. These settings allow the relay to be configured according to the particular application.

6.3 SEL- 351A relay in the simulation loop of the IEEE 9-bus system

The SEL-351A relay was placed in the computer simulation loop through the hardware-in-the-loop implementation to record fault events as well as a trip in the events of a fault. The idea of the wide area protection is to send trip signals from a centralized protection centre to the relay and circuit breakers in the event of a fault, in this case, the trip logic and trip decision are taken out of the relay. However, the current relays (SEL-351A) are based on local protection where they are equipped with protection elements such as phase overcurrent elements, phase time overcurrent elements etc. which are set with threshold values obtained from the power system simulation so that the relay can detect a fault when those threshold values are exceeded. The phase time overcurrent element in the relay was set to respond to overcurrent conditions during a fault on a particular zone. This element controls the trip logic which also controls the output contact (OUT101).

The relay generates sequential event recorder (SER) events whenever any of the elements listed in SER changed state. These SER events are readable and analyzable with the synchroWAVe event software which helps to know the elements that have triggered and the states of the various output contacts (OUT101 – OUT107) controlled by the states of the relay protection elements. The output contacts are responsible for opening and closing of the circuit breakers in the power system. In this research, whilst the local protection elements' states were monitored in the SER to know their response to any fault events simulated, the WAP algorithm is used to control the breakers in the

power system and the voltage and current waveforms are monitored to know when the breaker opened or closed. This was necessary because it is not possible to implement the WAP in the relay since the idea of a WAP technique is to have the control logic in a centralized centre known as wide area protection centre or local protection centre. This aided the comparison of the response of conventional protection and the wide area protection.

The relay which is the hardware under test was placed in the simulation loop and a two-phase line-to-line fault (a-b) was simulated on zone 3. The events recorded by the SEL-351A relay were read and analyzed with the synchroWAVe event software and the scope in MATLAB/Simulink as shown in Figure 6.5 and Figure 6.6 respectively.

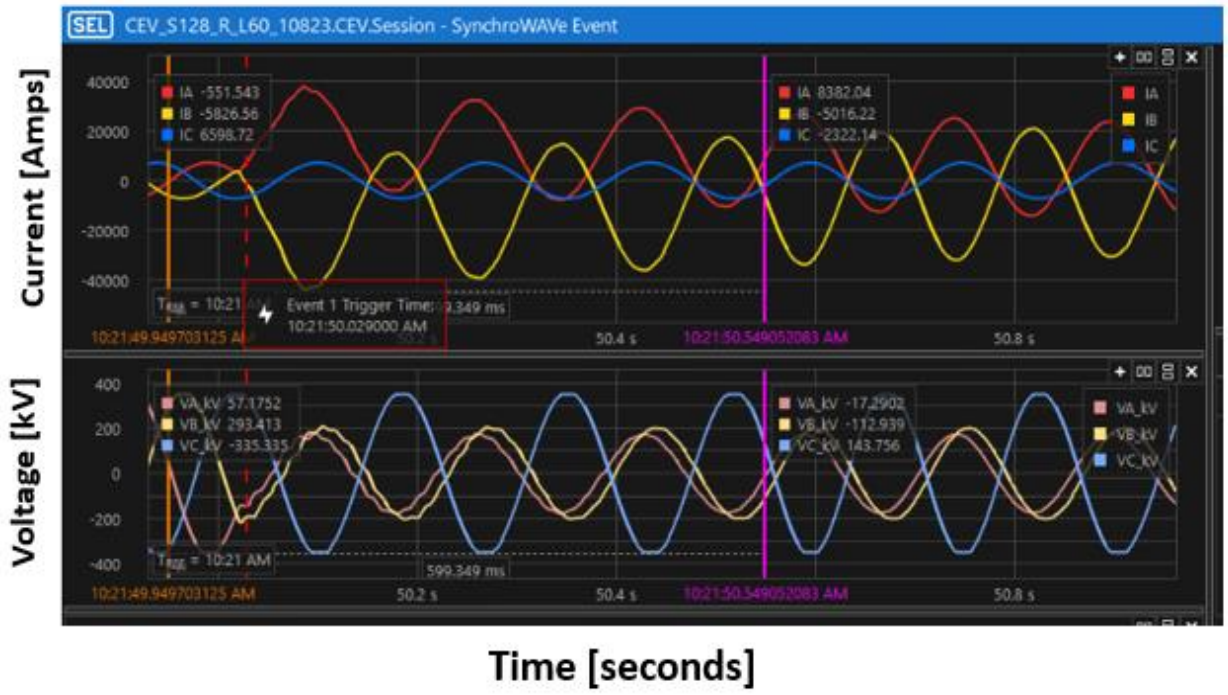

Figure 6.5: Current and voltage waveforms recorded by SEL-351A relay before and after an L-L (a-b) fault

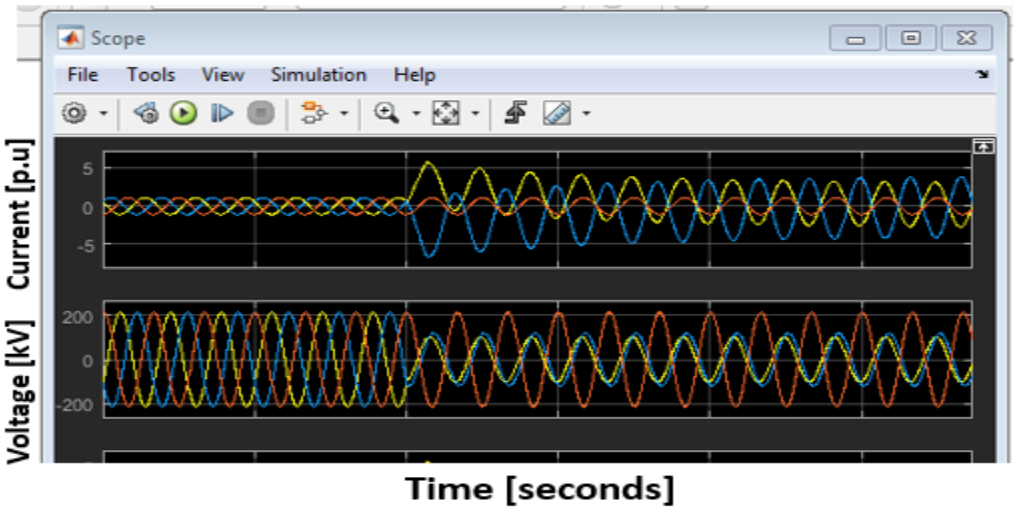

Figure 6.6: Current and voltage waveforms recorded with scope in Simulink before and after an L-L (a-b) fault

A three-phase to ground (L-L-L-G) fault was also simulated and the current and voltage waveforms were recorded with both SEL-351A relay and the scope in MATLAB/Simulink as shown in the Figure 6.7 and Figure 6.8 respectively. These were done to analyze and verify the readings and recordings of the SEL-351A relay used as the hardware under test in this research work.

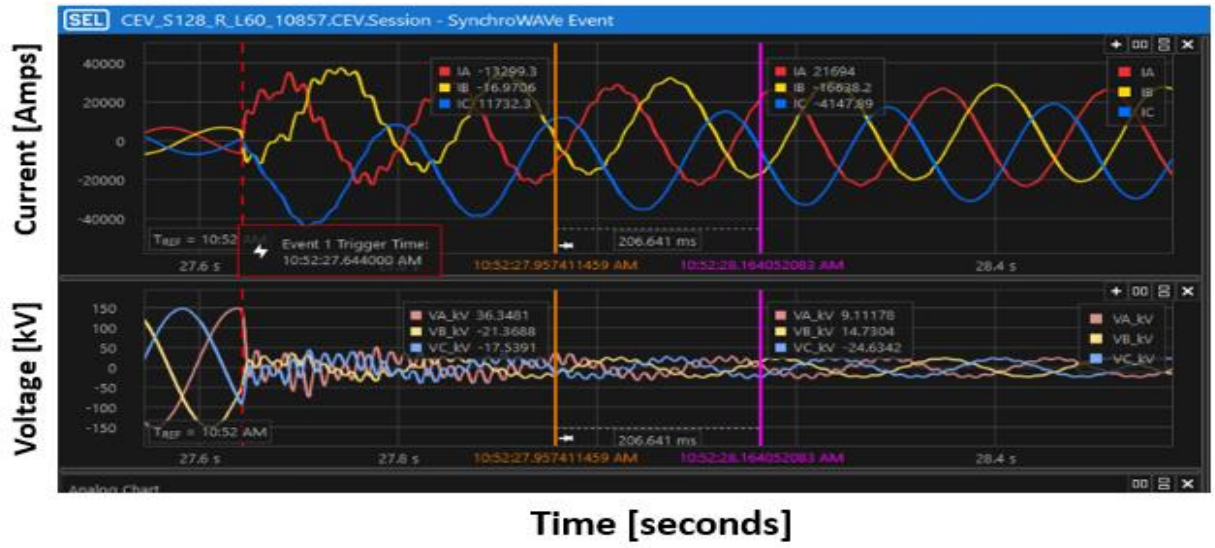

Figure 6.7: Current and voltage waveforms recorded by SEL-351A relay before and after an L-L-L-G (a-b-c-g) fault.

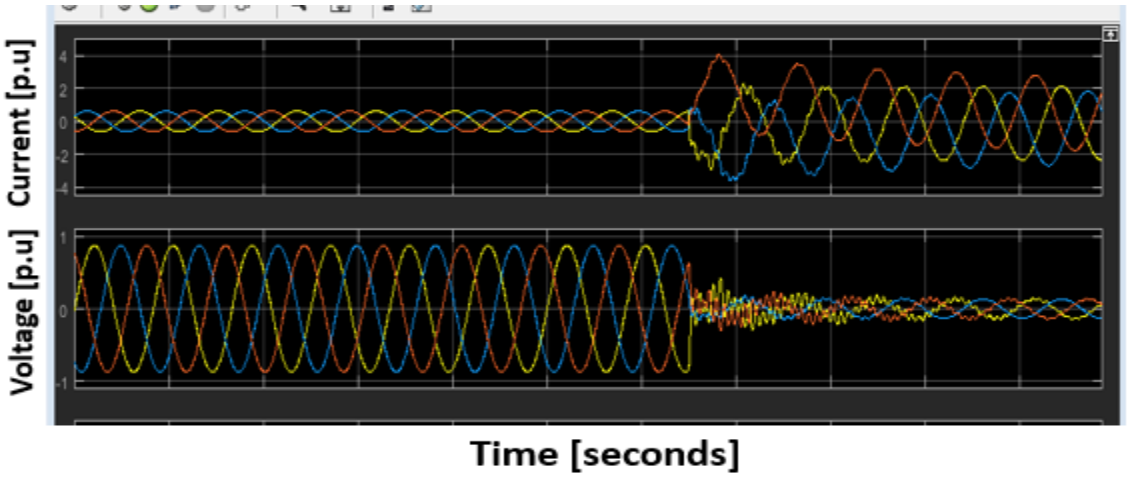

Figure 6.8: Current and voltage waveforms recorded by scope in Simulink before and after an L-L-L-G (a-b-c-g) fault.

6.4 Hardware-In-the-loop (HIL) Implementation of the WAP techniques.

The HIL simulation of the WAP protection techniques was used purposely in this research to verify the response time of the various protection techniques under investigation. Using only the waveforms recorded in MATLAB/Simulink and during real-time simulation is not enough to

conclude on the response time of the protection algorithms. Since the SEL-351A relay is the actual control hardware that will be used in the power system when these algorithms are implemented, testing its behavior in the events of a fault through the HIL simulation helps to validate how it will respond to those same faults conditions in real-life.

The phase time overcurrent elements were enabled (E51P) and set to respond to overcurrent conditions during fault simulations which in turn control the output contact OUT101 of the relay but not the circuit breakers in the power system. The circuit breaker in the power system simulation running in real-time on the Opal-RT is controlled by the WAP techniques. This setup helps to monitor the response time of both the conventional protection and the wide area protection.

6.4.1 WAP Techniques Response to Fault Conditions during HIL Simulations

The setup for the HIL simulations is shown in Figure 6.9. During the HIL simulations of various fault conditions on the IEEE 9-bus system, the WAP techniques were used to control the states of the circuit breakers in the power system running in real-time. The pre-fault, fault and post-fault events were recorded by the control hardware SEL-351A and these events were analyzed using synchroWAVe software by SEL. The response times of the WAP techniques were recorded as shown in Figure 6.10- Figure 6.12. How the three algorithms perform during MATLAB/Simulink and real-time and HIL are discussed in chapter 7.

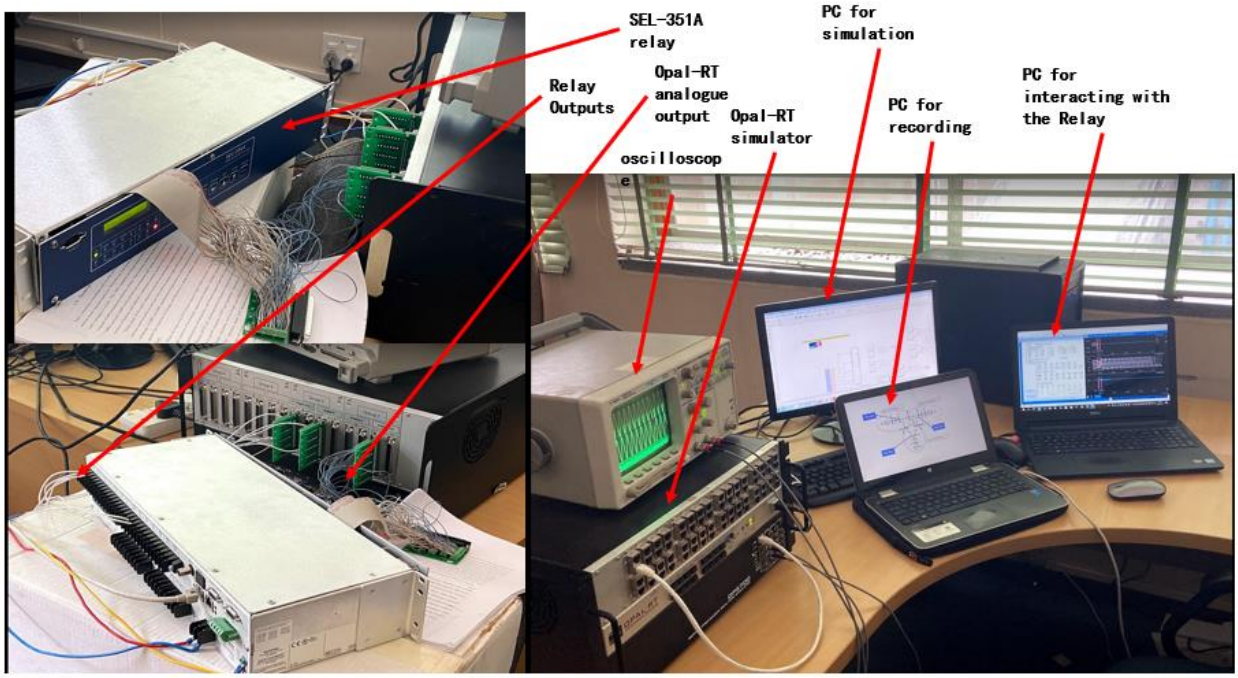

Figure 6.9: The setup for the Experiment

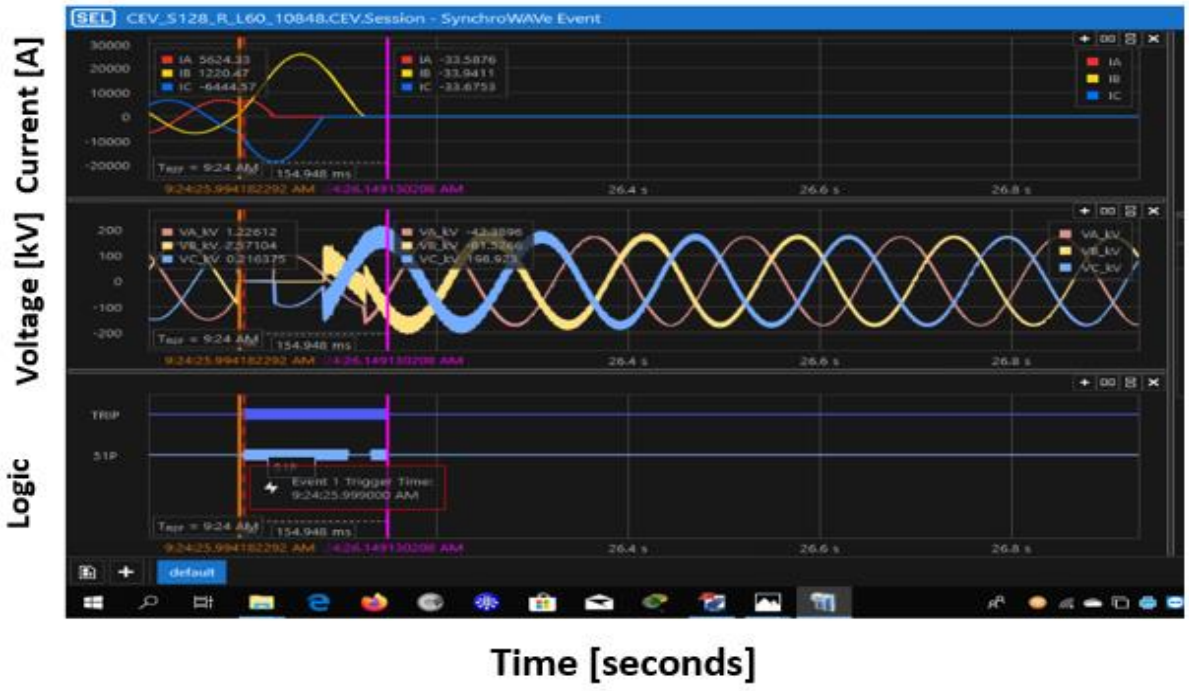

*Figure 6.10: Response time of **WAP technique A** recorded by SEL-351A*

*Figure 6.11: Response time of **WAP technique B** recorded by SEL-351A*

*Figure 6.12: Response time of **WAP technique C** recorded by SEL-351A*

CHAPTER SEVEN: RESULTS ANALYSIS AND DISCUSSION

7.1 Fault Detection Accuracy

The three wide area protection techniques have been implemented in MATLAB/Simulink, real-time simulation (i.e., software in the loop) using OPAL-RT and hardware-In-the-Loop simulation using SEL-351A relays. The performances of the WAP techniques were tested using IEEE 9-bus 3-generator test system with three PMU buses. The simulation results show that all the three algorithms can detect faults on the power system with 100% accuracy in determining the faulted zone but an accuracy less than 100% in determining the faulted line. Figure 7.1 shows the percentage accuracy in determining the faulted line for the three WAP techniques. As shown in the figure WAP technique A has 86% accuracy level, WAP technique B has 94% accuracy and WAP technique C has 92% accuracy. The sources of errors that may contributes to this level of inaccuracies are due to the network topology with adjacent lines presenting similar characteristics in a given faulted condition, making it difficult for the algorithm to detect the actual faulted line.

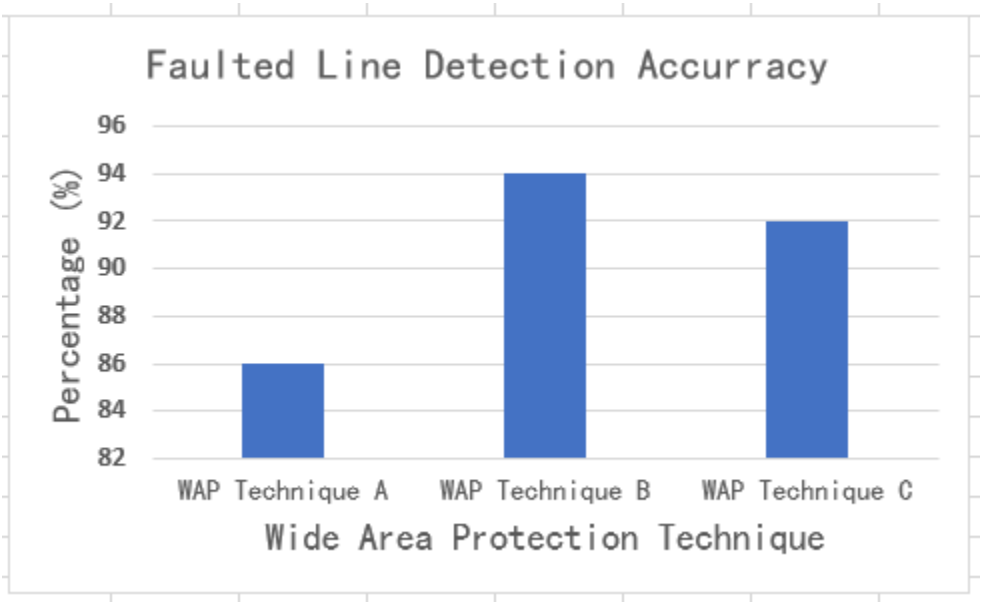

Figure: 7.1 Faulted line detection accuracy for the WAP techniques

7.2 Fault Response and Clearing Time

The speed of the protection techniques in clearing all faults conditions that occur on the power system was investigated and analyzed using current and voltage waveforms during Simulink, real-time and HIL simulation. The fault response times during Simulink and real-time were similar but

far different from the HIL due to the communication delay between the real-time target and the SEL-351A relay. Whereas nothing can be done to the fault clearing time of the algorithms without communication which is purely based on the method and the data used, depending on the communication medium, the actual response time can be reduced. Figures 7.2 – 7.4 show the response times of the WAP techniques in the three different simulation type used. The response time of the WAP technique A during Simulink and real – time ranges from 15 ms to 35 ms. WAP technique B fault clearing time ranges from 15ms to 40 ms. For WAP technique C, it has the same fault clearing time for all types of fault and this is estimated as 20 ms. These faults clearing time variations depend on the data used in detecting the faulted zone as well as the faulted line. The more data the algorithm depends on to detect and clear faults the slower the fault clearing time. Moreover, the algorithms take data from all the PMUs and use that to distinguish the faulted zone from the rest, the quicker the value recorded from the PMU in the faulted zone is distinguished from the others, the faster the fault clearing time.

This explains why the Technique A which uses the PSVM for faulted zone detection follows the expected trend of the fault clearing time for single phase to ground fault having the highest clearing time and three-phase to ground fault having the lowest fault clearing time. Also, Technique B which uses the GIM for faulted zone detection has similar fault clearing time for single-phase to ground faults and two-phase line to line faults. The fault clearing time is lower for two-phase line to ground faults and is lowest for three-phase to ground faults in all the zones. This is due the variations in GIM of the generators after each fault occurs in the zone. Furthermore, technique C uses the sum of positive and zero sequence currents entering a BPZ to detect the faulted zone. It was observed that this value (the sum of positive and zero sequence currents) of the PMU in the faulted zone varies significantly from the values at the other PMUs when any fault occurs and this explains why algorithm C has the same fault clearing time for all fault conditions as well as having averagely the lowest fault clearing time.

With an added communication delay during the HIL simulation, the maximum fault clearing time of the techniques recorded were 404 ms, 256 ms and 150 ms for technique A, B and C respectively and this variation is due to the different fault detection methods used in the three algorithms.

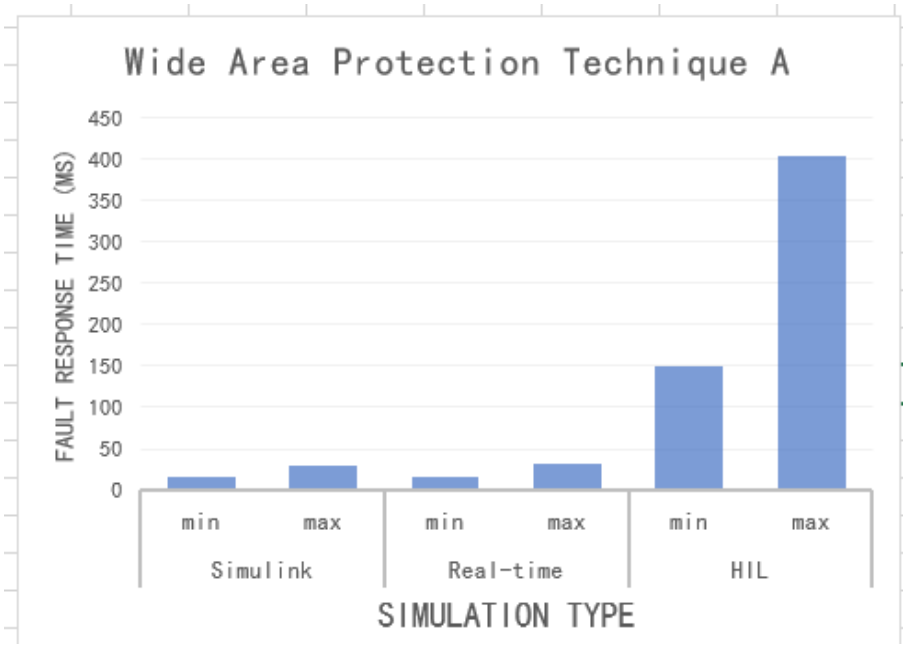

Figure:7.2 Fault clearing time of WAP technique A during the different simulation methods

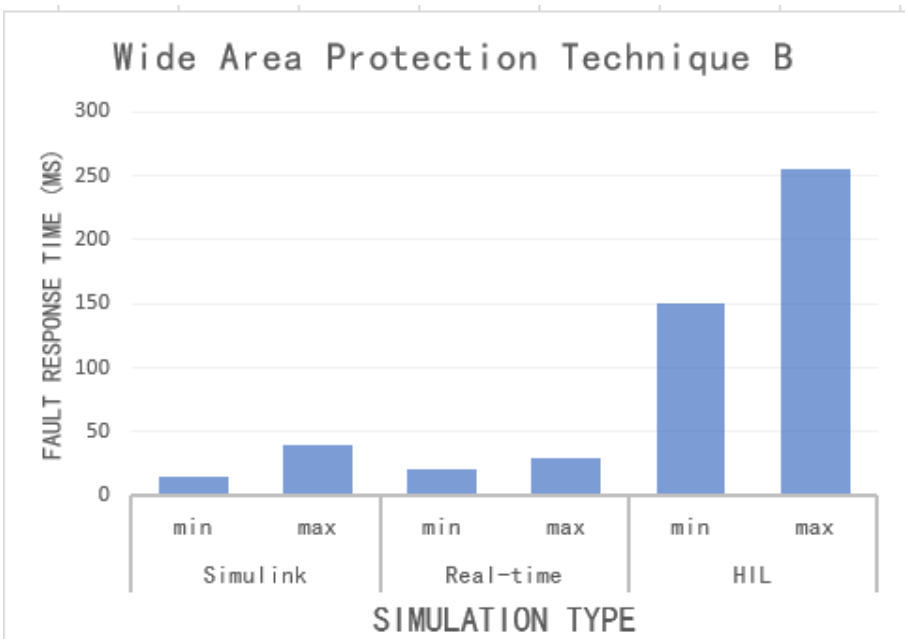

Figure:7.3 Fault clearing time of WAP technique B during the different simulation methods

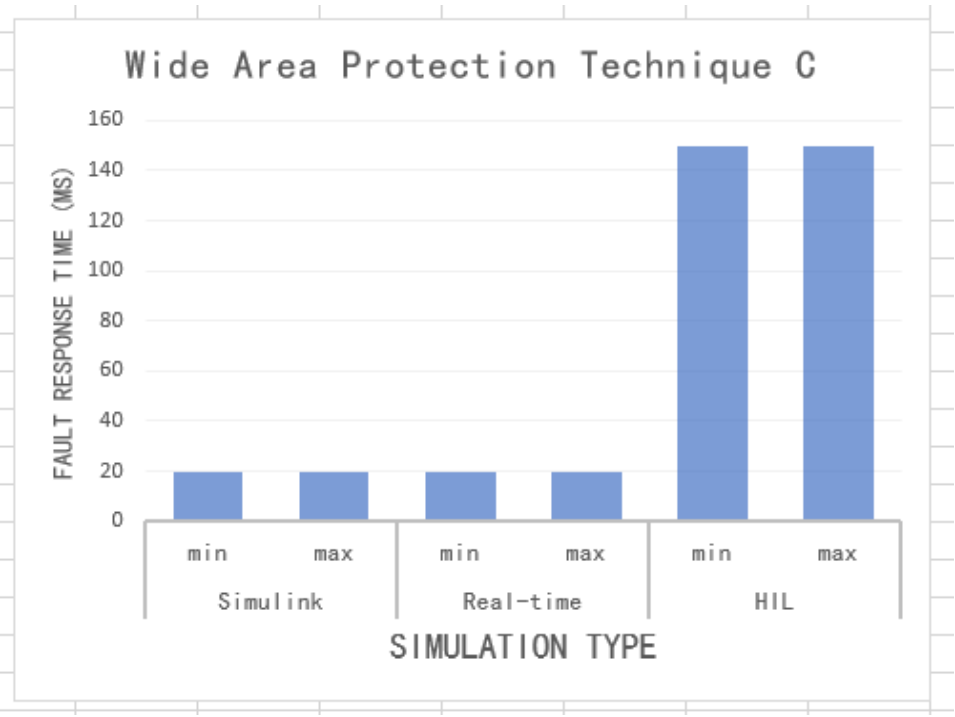

Figure:7.4 Fault clearing time of WAP technique C during the different simulation methods

CHAPTER EIGHT: CONCLUSION

Various techniques for wide area protection of the power grid have been proposed which are mainly for backup protection purposes. Three of these methods have been carefully selected based on the *data used for protection, method of protection, the purpose of protection, ease of implementation and scalability of the method.*

The investigations show that the wide area protection technique based on positive sequence voltage for faulted zone detection and positive sequence current for faulted line detection have 100% accuracy in detecting the faulted zone and 86% accuracy in determining the faulted line with maximum fault clearing time of 404 ms which includes the communication delay using ethernet communication with RJ45 cable. The wide area protection technique based on Gain in Momentum of the generators for faulted zone identification and the use of positive sequence voltage magnitude and flow of reactive power for faulted line identification has 100% accuracy in determining the vulnerable protection zones and 94% accuracy in determining the faulted line. This technique has a maximum fault clearing time including the communication delay which was tested using the HIL simulation to be 256 ms. And lastly, the third algorithm investigated based on the sum of currents entering the zone of protection for faulted zone identification and linear least square method for faulted line identification has 100% accuracy and 92% accuracy respectively and maximum fault clearing time of 150 ms which includes communication delay. From the performance data presented, it is evident that these algorithms will perform better when used as backup protection since the common timer settings for backup protection schemes range is from 1200 ms to 1800 ms.

With an advanced (fast) communication technology, the WAP algorithms fault clearing time could possibly be reduced such that it could be used for primary protection as stated in the research hypothesis. It is recommended that a hybrid of these algorithms be developed using the strengths of each algorithm to supplement the weakness of the other. For example, in the case of the WAP technique B which uses GIM of the generators to detect faulted zones, since some of generators in the new power systems do not have rotating parts e.g. solar power plants, this aspect of the technique can be replaced with the use of the sum of current entering each protection zone

proposed by WAP technique C to detect the faulted zone while retaining its (technique B) faulted line identification method which has a much higher accuracy.

Future work will be looking at developing a more robust technique which has a higher accuracy for both faulted zone and faulted line identification. More efficient communication mediums like optical fibre cable, 5G technology could be used to investigate the technique to see its suitability as a primary protection for the power system.

REFERENCES

[1] X. Fang, S. Misra, G. Xue and D. Yang, "Smart Grid - The New and Improved Power Grid: A Survey," *IEEE Communications Surveys & Tutorials*, vol. 14, *(4)*, pp. 944-980, 2012.

[2] M. M. Eissa, M. E. Masoud and M. M. M. Elanwar, "A Novel Back Up Wide Area Protection Technique for Power Transmission Grids Using Phasor Measurement Unit," *IEEE Transactions on Power Delivery*, vol. 25, *(1)*, pp. 270-278, 2010.

[3] Jason Griffey, "Chapter 1: Introduction," *Library Technology Reports*, vol. 54, *(1)*, pp. 5-10, 2018.

[4] M. Hashmi, S. Hänninen and K. Mäki, "Survey of smart grid concepts, architectures, and technological demonstrations worldwide," *2011 IEEE Pes Conference On Innovative Smart Grid Technologies Latin America (ISGT La)*, Medellin, 2011, pp. 1-7.

[5] S. J. Bossart and J. E. Bean, "Metrics and benefits analysis and challenges for Smart Grid field projects," *IEEE 2011 EnergyTech*, Cleveland, OH, 2011, pp. 1-5.

[6] J. N. Bharothu, M. Sridhar and R. S. Rao, "A literature survey report on Smart Grid technologies," *2014 International Conference on Smart Electric Grid (ISEG)*, Guntur, 2014, pp. 1-8.

[7] G. Xu, W. Yu, D. Griffith, N. Golmie and P. Moulema, "Toward Integrating Distributed Energy Resources and Storage Devices in Smart Grid," *IEEE Internet of Things Journal*, vol. 4, *(1)*, pp. 192-204, 2017.

[8] *The Smart Grid: What's "the grid" and how is it "smart?"*. Available: https://www.powerelectronicsnews.com/the-smart-grid-whats-the-grid-and-how-is-it-smart/.

[9] P. T. Manditereza and R. C. Bansal, "Introducing A New Type of Protection Zone for the Smart Grid Incorporating Distributed Generation," *2018 IEEE Innovative Smart Grid Technologies - Asia (ISGT Asia)*, Singapore, 2018, pp. 86-90.

[10] D. Recalde, A. Trpovski, S. Troitzsch, K. Zhang, S. Hanif and T. Hamacher, "A Review of Operation Methods and Simulation Requirements for Future Smart Distribution Grids," *2018 IEEE Innovative Smart Grid Technologies - Asia (ISGT Asia)*, Singapore, 2018, pp. 475-480.

[11] F. Li *et al*., "Smart Transmission Grid: Vision and Framework," *IEEE Transactions on Smart Grid*, vol. 1, *(2)*, pp. 168-177, 2010.

[12] V. C. Gungor *et al*., "Smart Grid Technologies: Communication Technologies and Standards," *IEEE Transactions on Industrial Informatics*, vol. 7, *(4)*, pp. 529-539, 2011.

[13] H. Farhangi, "The path of the smart grid," *IEEE Power and Energy Magazine*, vol. 8, *(1)*, pp. 18-28, 2010.

[14] F. Zhang, L. Mu and W. Guo, "An Integrated Wide-Area Protection Scheme for Active Distribution Networks Based on Fault Components Principle," *IEEE Transactions on Smart Grid*, vol. 10, *(1)*, pp. 392-402, 2019.

[15] Y. Ates, M. Uzunoglu, A. Karakas and A. R. Boynuegri, "The case study based protection analysis for smart distribution grids including distributed generation units," *12th IET International Conference on Developments in Power System Protection (DPSP 2014)*, Copenhagen, 2014, pp. 1-5.

[16] Z. Bo *X. N. Lin, Q. P. Wang, Y. H. Yi & F. Q. Zhou*, "Developments of power system protection and control," *Protection and Control of Modern Power Systems*, vol. 1, *(1)*, pp. 1-8, 2016.

[17] A. Ukil, B. Deck and V. H. Shah, "Current-Only Directional Overcurrent Relay," *IEEE Sensors Journal*, vol. 11, *(6)*, pp. 1403-1404, 2011.

[18] F. Coffele, C. Booth and A. Dyśko, "An Adaptive Overcurrent Protection Scheme for Distribution Networks," in *IEEE Transactions on Power Delivery*, vol. 30, no. 2, pp. 561-568, April 2015.

[19] P. Mahat, Z. Chen, B. Bak-Jensen and C. L. Bak, "A Simple Adaptive Overcurrent Protection of Distribution Systems With Distributed Generation," in *IEEE Transactions on Smart Grid*, vol. 2, no. 3, pp. 428-437, Sept. 2011.

[20] Chi-Kong Wong, Chi-Wai Lam, Kuok-Cheong Lei, Chu-San Lei and Ying-Duo Han, "Novel wavelet approach to current differential pilot relay protection," *IEEE Transactions on Power Delivery*, vol. 18, *(1)*, pp. 20-25, 2003.

[21] D. Barbosa, U. C. Netto, D. V. Coury and M. Oleskovicz, "Power Transformer Differential Protection Based on Clarke's Transform and Fuzzy Systems," *IEEE Transactions on Power Delivery*, vol. 26, *(2)*, pp. 1212-1220, 2011.

[22] S. Dambhare, S. A. Soman and M. C. Chandorkar, "Adaptive Current Differential Protection Schemes for Transmission-Line Protection," in *IEEE Transactions on Power Delivery*, vol. 24, no. 4, pp. 1832-1841, Oct. 2009.

[23] L. Tang, X. Dong, S. Luo, S. Shi and B. Wang, "A New Differential Protection of Transmission Line Based on Equivalent Travelling Wave," in *IEEE Transactions on Power Delivery*, vol. 32, no. 3, pp. 1359-1369, June 2017.

[24] K. El-Arroudi, G. Joos, D. T. McGillis and R. Brearley, "Comprehensive transmission distance protection settings using an intelligent-based analysis of events and consequences," *IEEE Transactions on Power Delivery*, vol. 20, *(3)*, pp. 1817-1824, 2005.

[25] H. Shafiei, A. Khonsari and M. Ould-Khaoua, "An effective countermeasure against traffic analysis attacks in wide area measurement systems," *Information Systems*, vol. 53, pp. 182-189, 2015.

[26] Yi Deng, Hua Lin, A. G. Phadke, S. Shukla, J. S. Thorp and L. Mili, "Communication network modeling and simulation for Wide Area Measurement applications," *2012 IEEE PES Innovative Smart Grid Technologies (ISGT)*, Washington, DC, 2012, pp. 1-6.

[27] R. Dubey, M. Popov and Muro, Jose de Jesus Chavez, "Cost Effective Wide Area Measurement Systems for Smart Power Network," *IEEE Power and Energy Technology Systems Journal*, vol. 5, *(3)*, pp. 85-93, 2018.

[28] Y. W. Law, M. Palaniswami, G. Kounga and A. Lo, "WAKE: Key management scheme for wide-area measurement systems in smart grid," in *IEEE Communications Magazine*, vol. 51, no. 1, pp. 34-41, January 2013.

[29] S. Chakrabarti and E. Kyriakides, "Optimal Placement of Phasor Measurement Units for Power System Observability," *IEEE Transactions on Power Systems*, vol. 23, *(3)*, pp. 1433-1440, 2008.

[30] S. Chakrabarti, E. Kyriakides and D. G. Eliades, "Placement of Synchronized Measurements for Power System Observability," *IEEE Transactions on Power Delivery*, vol. 24, *(1)*, pp. 12-19, 2009.

[31] S. M. Mazhari, H. Monsef, H. Lesani and A. Fereidunian, "A Multi-Objective PMU Placement Method Considering Measurement Redundancy and Observability Value Under Contingencies," *IEEE Transactions on Power Systems*, vol. 28, *(3)*, pp. 2136-2146, 2013.

[32] L. Huang, Y. Sun, J. Xu, W. Gao, J. Zhang and Z. Wu, "Optimal PMU Placement Considering Controlled Islanding of Power System," *IEEE Transactions on Power Systems*, vol. 29, *(2)*, pp. 742-755, 2014.

[33] C. Lu, Z. Wang, M. Ma, R. Shen and Y. Yu, "An Optimal PMU Placement with Reliable Zero Injection Observation," *IEEE Access*, vol. 6, pp. 54417-54426, 2018.

[34] *Set-up of Wide Area Protection Scheme with PMUs*. Available: https://www.slideserve.com/sereno/set-up-of-wide-area-protection-scheme-with-pmus.

[35] J. Zare, F. Aminifar and M. Sanaye-Pasand, "Synchrophasor-Based Wide-Area Backup Protection Scheme with Data Requirement Analysis," *IEEE Transactions on Power Delivery*, vol. 30, *(3)*, pp. 1410-1419, 2015.

[36] J. Ma, J. Li, J. S. Thorp, A. J. Arana, Q. Yang and A. G. Phadke, "A Fault Steady State Component-Based Wide Area Backup Protection Algorithm," *IEEE Transactions on Smart Grid*, vol. 2, *(3)*, pp. 468-475, 2011.

[37] Z. He, Z. Zhang, W. Chen, O. P. Malik and X. Yin, "Wide-Area Backup Protection Algorithm Based on Fault Component Voltage Distribution," *IEEE Transactions on Power Delivery*, vol. 26, *(4)*, pp. 2752-2760, 2011.

[38] M. K. Neyestanaki and A. M. Ranjbar, "An Adaptive PMU-Based Wide Area Backup Protection Scheme for Power Transmission Lines," *IEEE Transactions on Smart Grid*, vol. 6, *(3)*, pp. 1550-1559, 2015.

[39] J. Zare, F. Aminifar and M. Sanaye-Pasand, "Communication-Constrained Regionalization of Power Systems for Synchrophasor-Based Wide-Area Backup Protection Scheme," *IEEE Transactions on Smart Grid*, vol. 6, *(3)*, pp. 1530-1538, 2015.

[40] M. K. Jena, S. R. Samantaray and B. K. Panigrahi, "A New Wide-Area Backup Protection Scheme for Series-Compensated Transmission System," *IEEE Systems Journal*, vol. 11, *(3)*, pp. 1877-1887, 2017.

[41] C. W. Potter, A. Archambault and K. Westrick, "Building a smarter smart grid through better renewable energy information," *2009 IEEE/PES Power Systems Conference and Exposition*, Seattle, WA, 2009, pp. 1-5.

[42] M. H. Rehmani, M. Reisslein, A. Rachedi, M. Erol-Kantarci and M. Radenkovic, "Integrating Renewable Energy Resources Into the Smart Grid: Recent Developments in

Information and Communication Technologies," *IEEE Transactions on Industrial Informatics*, vol. 14, *(7)*, pp. 2814-2825, 2018.

[43] W. Yi, Y. Zhang, Z. Zhao and Y. Huang, "Multiobjective Robust Scheduling for Smart Distribution Grids: Considering Renewable Energy and Demand Response Uncertainty," *IEEE Access*, vol. 6, pp. 45715-45724, 2018.

[44] H. S. V. S. Kumar Nunna, Y. Amanbek, B. Satuyeva and S. Doolla, "A decentralized transactive energy trading framework for prosumers in a microgrid cluster," *2019 IEEE PES GTD Grand International Conference and Exposition Asia (GTD Asia)*, Bangkok, Thailand, 2019, pp. 824-830.

[45] D. Westermann and A. John, "Demand Matching Wind Power Generation With Wide-Area Measurement and Demand-Side Management," *IEEE Transactions on Energy Conversion*, vol. 22, *(1)*, pp. 145-149, 2007.

[46] A. Mohsenian-Rad, V. W. S. Wong, J. Jatskevich, R. Schober and A. Leon-Garcia, "Autonomous Demand-Side Management Based on Game-Theoretic Energy Consumption Scheduling for the Future Smart Grid," *IEEE Transactions on Smart Grid*, vol. 1, *(3)*, pp. 320-331, 2010.

[47] P. Centolella, "The integration of Price Responsive Demand into Regional Transmission Organization (RTO) wholesale power markets and system operations," *Energy*, vol. 35, *(4)*, pp. 1568-1574, 2010.

[48] Triki, C., Violi, A. Dynamic pricing of electricity in retail markets. *4OR-Q J Oper Res 7*, 21–36 (2009).

[49] K. Herter, "Residential implementation of critical-peak pricing of electricity," *Energy Policy*, vol. 35, *(4)*, pp. 2121-2130, 2007.

[50] M. G. Molina, "Energy Storage and Power Electronics Technologies: A Strong Combination to Empower the Transformation to the Smart Grid," *Proceedings of the IEEE*, vol. 105, *(11)*, pp. 2191-2219, 2017.

[51] Y. G. Rebours, D. S. Kirschen, M. Trotignon and S. Rossignol, "A Survey of Frequency and Voltage Control Ancillary Services-Part I: Technical Features," *IEEE Transactions on Power Systems*, vol. 22, *(1)*, pp. 350-357, 2007.

[52] U.S. Department of Energy, "Grid Energy Storage". Available: https://www.energy.gov/sites/prod/files/2014/09/f18/Grid%20Energy%20Storage%20December%202013.pdf

[53] P. Denholm *et al*. "Role of energy storage with renewable electricity generation", *Technical Report, NREL/TP-6A2-47187*, United States, January 2010.

[54] Duong Minh Bui, "Simplified and Automated Fault-Current Calculation for Fault Protection System of Grid-Connected Low-Voltage AC Microgrids," *International Journal of Emerging Electric Power Systems*, vol. 18, *(2)*, 2017.

[55] H. C. Ferreira, L. Lampe, J. Newbury, and T. G. Swart, Power Line Communications: Theory and Applications for Narrowband and Broadband Communications over Power Lines. Wiley, 2010.

[56] M. Kuzlu and M. Pipattanasomporn, "Assessment of communication technologies and network requirements for different smart grid applications," *2013 IEEE PES Innovative Smart Grid Technologies Conference (ISGT)*, Washington, DC, 2013, pp. 1-6.

[57] V. Karapanos, S. de Haan and K. Zwetsloot, "Real time simulation of a power system with VSG hardware in the loop," *IECON 2011 - 37th Annual Conference of the IEEE Industrial Electronics Society*, Melbourne, VIC, 2011, pp. 3748-3754.

[58] *Hardware-in-the-Loop (HIL) Simulation*. Available: https://www.mathworks.com/discovery/hardware-in-the-loop-hil.html.

[59] OPAL-RT Academy, "Fundamental Course; OP-101 Real-Time Simulation Fundamentals with RT-LAB software, Models & Hardware ," unpublished.

[60] J. Blanger, P. Venne, and J.-N. Paquin, "The what, where and why of real-time simulation," in *IEEE PES General Meeting*, Minneapolis, MN, USA, 25–29 July 2010.

[61] B. Lundstrom, S. Chakraborty, G. Lauss, R. Bründlinger and R. Conklin, "Evaluation of system-integrated smart grid devices using software- and hardware-in-the-loop," *2016 IEEE Power & Energy Society Innovative Smart Grid Technologies Conference (ISGT)*, Minneapolis, MN, 2016, pp. 1-5.

[62] B. Sparn, D. Krishnamurthy, A. Pratt, M. Ruth and H. Wu, "Hardware-in-the-loop (HIL) simulations for smart grid impact studies," in *2018 IEEE Power & Energy Society General Meeting (PESGM)*, Aug 2018.

[63] G. F. Lauss, M. O. Faruque, K. Schoder, C. Dufour, A. Viehweider and J. Langston, "Characteristics and Design of Power Hardware-in-the-Loop Simulations for Electrical Power Systems," *IEEE Transactions on Industrial Electronics*, vol. 63, *(1)*, pp. 406-417, 2016.

[64] M. Steurer, F. Bogdan, W. Ren, M. Sloderbeck and S. Woodruff, "Controller and Power Hardware-In-Loop Methods for Accelerating Renewable Energy Integration," *2007 IEEE Power Engineering Society General Meeting*, Tampa, FL, 2007, pp. 1-4.

[65] F. R. Adegbohun and K. Y. Lee, "Real-time modeling, simulation and analysis of a grid connected PV system with hardware-in-loop protection," *2017 North American Power Symposium (NAPS)*, Morgantown, WV, 2017, pp. 1-6.

[66] V. K. Vijapurapu, A. K. Srivastava and N. N. Schulz, "Modelling and validation of differential relay using real time digital simulator," *International Journal of Energy Technology and Policy*, vol. 8, *(3-6)*, pp. 305-322, 2012.

[67] Z. Moravej S. Bagheri "Distance Protection closed-loop testing using RTDS" *Energy Equipment and Systems,* vol. 5, no. 2 pp. 197-210, 2017.

[68] C. L. Fortescue, "Method of Symmetrical Co-Ordinates Applied to the Solution of Polyphase Networks," *in Transactions of the American Institute of Electrical Engineers*, vol. XXXVII, no. 2, pp. 1027-1140, July 1918.

[69] Sewilam, Tamer Sayed Abdelhamid Abdelgayed, "Automated Wavelet-Based Fault Detection and Diagnosis for Smart Distribution Systems and Microgrids." *UOIT ProQuest Dissertations & Theses*, Ann Arbor, 2017 http://hdl.handle.net/10155/817.

[70] M. K. Jena, S. R. Samantaray and B. K. Panigrahi, "A New Decentralized Approach to Wide-Area Back-Up Protection of Transmission Lines," *IEEE Systems Journal*, vol. 12, (4), pp. 3161-3168, 2018.

[71] A. Avalos, A. Zamora, O. Escamilla and M. R. A. Paternina, "Real-time Hardware-in-the-loop Implementation for Power Systems Protection," *2018 IEEE PES Transmission & Distribution Conference and Exhibition - Latin America (T&D-LA)*, Lima, 2018, pp. 1-5.

APPENDICES

Appendix A: The IEEE 9-Bus System on MATLAB/Simulink Model

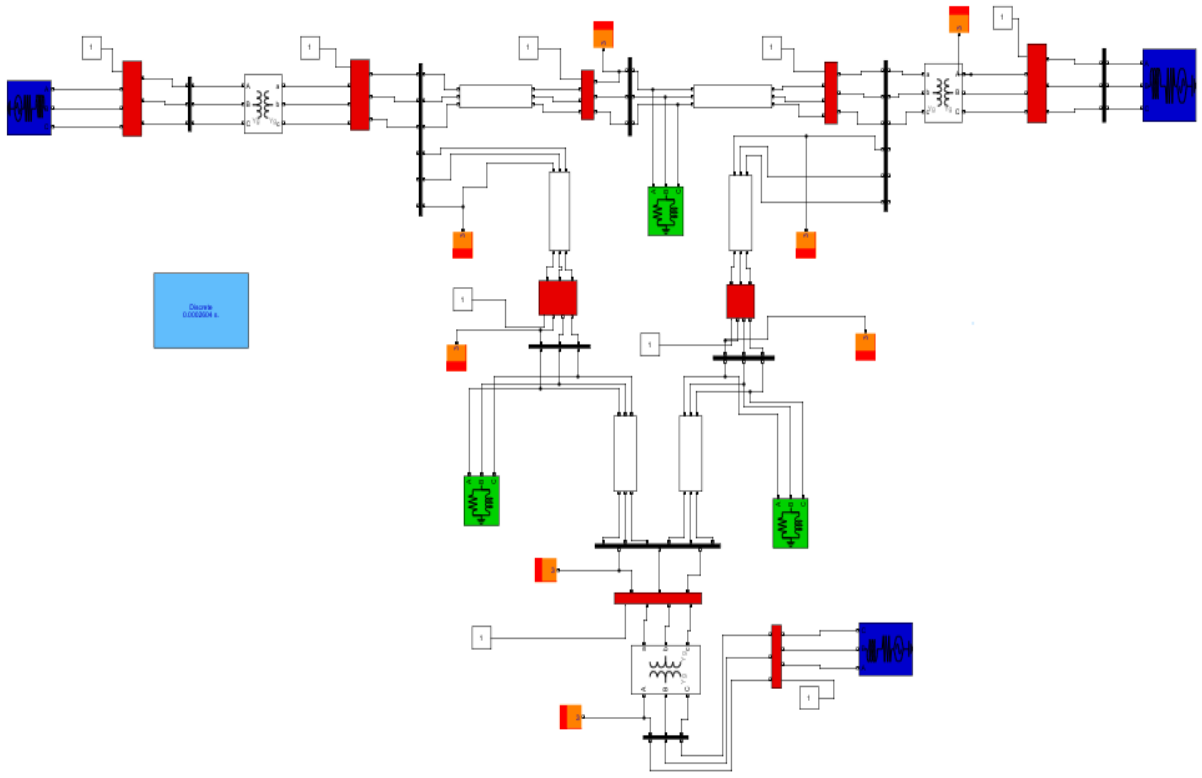

Figure: A.1 IEEE Nine Bus Model on MATLAB/Simulink

Table A.1 Terminal conditions of IEEE 9-bus system

Bus	**V[kV]**	**δ[deg]**	**P[pu]**	**Q[pu]**
1	17.1600	0.0000	0.7163	0.2791
2	18.4500	9.3507	1.6300	0.0490
3	14.1450	5.1420	0.8500	-0.1145

Table A.2 Transmission line characteristics of IEEE 9-bus system

Line		R[pu/m]	X[pu/m]	B[pu/m]
From Bus	To Bus			
4	5	0.0100	0.0680	0.1760
4	6	0.0170	0.0920	0.1580
5	7	0.0320	0.1610	0.3060
6	9	0.0390	0.1738	0.3580
7	8	0.0085	0.0576	0.1490
8	9	0.0119	0.1008	0.2090

Table A.3 Load characteristics of IEEE 9-bus system

Bus	P[pu]	Q[pu]
5	1.25	0.50
6	0.90	0.30
8	1.00	0.35

APPENDIX B: Real-Time Simulation on Opal-RT

B.1 Creating a Model Compatible for OPAL-RT Real-Time Simulation

The OPAL-RT simulator only works with subsystems at the top layer level of a model. Simulink subsystem consists of a set of Simulink blocks that are placed in one single block which is known as a subsystem. This type of groupings helps to simplify the model, establish a hierarchical block diagram and keep blocks of similar functionality together. The objectives of having subsystems in RT-LAB platforms are to differentiate computation subsystems and Graphical User Interface (GUI) Subsystems and to assign different computation subsystems to CPU cores. The grouping of subsystems in Simulink is illustrated in Figure B.1.

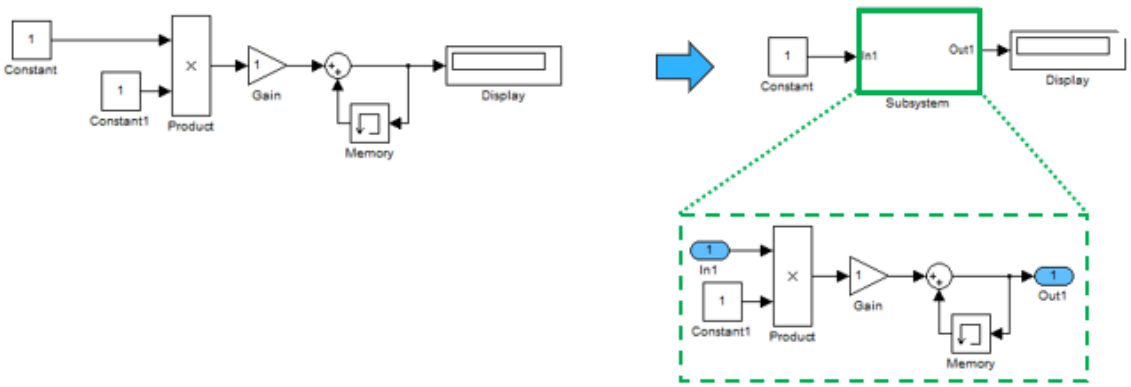

Figure B.1: Creating a subsystem in MATLAB/Simulink

The Simulink blocks in a model for RT-LAB real-time simulation must be grouped into two; a computational subsystem and GUI subsystem. The computation subsystem will be executed in real-time on one CPU core of the OPAL-RT target or machine whiles the GUI subsystem will be viewed on the user's host PC as shown in Figure B.2. The data between the computation subsystem and the GUI subsystem is exchanged asynchronously through a TCP/IP link. The computation blocks can be divided into two subsystems especially for a large model with a lot of computational blocks. In this case, each computation subsystem will be run on a different CPU core of the real-time target. The data between two computation subsystems is exchanged synchronously using shared memory.

The subsystems of the RT-LAB have a naming convention which must be followed in order for successful execution in real-time; the GUI subsystem must have a pre-fix of SC before the name one wants to give the subsystem e.g. ***SC_anyname***. The first or main computational subsystem must have the prefix **SM** and **SS** for any additional computational subsystem added since the computation subsystem can be more than one executed on different CPU cores. Figure B.2 gives a diagrammatic representation of the explanation of subsystems and their execution on OPAL-RT.

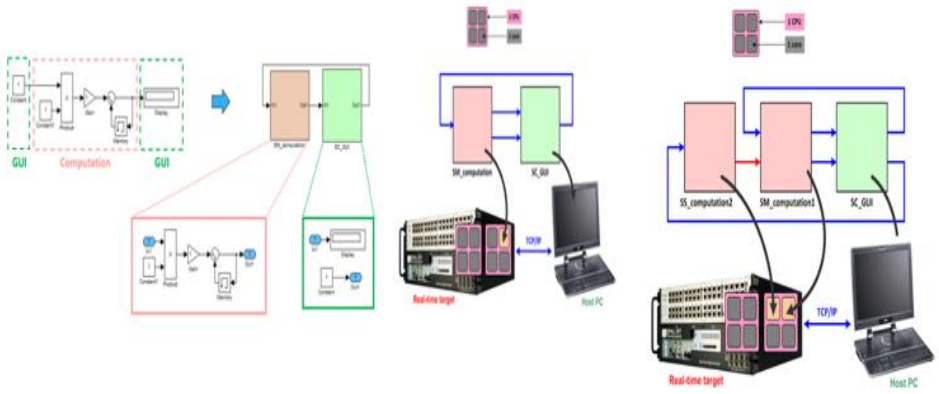

Figure B.2: How the subsystems are executed on the OPAL-RT real-time target [59]

B.1.1 OpComm blocks in RT-LAB Simulation

OpComm blocks are important in RT-LAB simulation because they are used for communication between the subsystems created in the Simulink model. There are two types of communication that happen within the RT-LAB real-time simulation; one is asynchronous communication which happens between a computation subsystem and a GUI subsystem and then synchronous communication between two computation subsystems. Whenever these communications need to be executed, a separate OpComm block is needed for each type of communication. The console or GUI subsystems need at least one OpComm block to receive asynchronous signals from computation subsystems but there can be multiple OpComm blocks with different data acquisition parameters. The computation subsystems need one OpComm block to receive an asynchronous signal from a console and a different OpComm block if it needs to communicate with another computation subsystem. The types of communications using Opal-RT OpComm blocks is shown in Figure B.3.

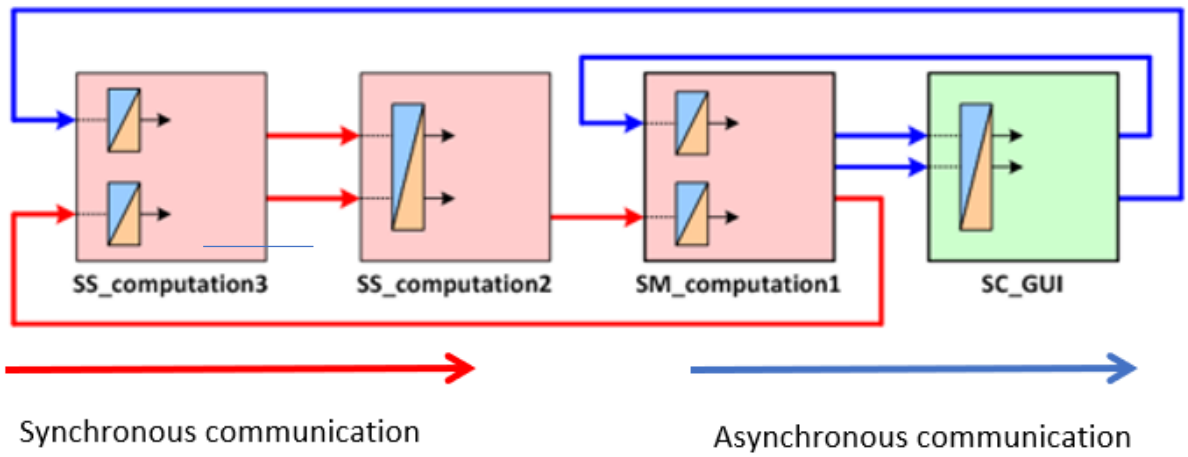

Figure B.3: Using OpComm blocks in RT-LAB Simulations [59]

B.2 Running the Models on the Real-Time Target

In this section, establishing a connection with the real-time target, importing a Simulink model for execution in real-time is discussed and presented.

B.2.1 Making Connections with the real-time target

In order to execute a model on the real-time target, first of all, a TCP/IP connection must be established between the host PC and the target (Figure B.2). This connection is achieved through the RT-LAB software which must be installed on the host PC with a capability of integrating the appropriate MATLAB version onto it. The real-time target has its dedicated ethernet IP address (e.g. 192.168.10.x0x) and hence the host PC must also be assigned an IP address in order to make communication possible (e.g. 192.168.10.xxx). When the connection is established or the target is added to the RT-LAB software as referred by Opal-RT technologies, then the created model can be imported, assign to the target and then executed in real-time. The Figs. B.4 – B.5 shows the real-time target named ***UCT_targets*** in this case being added but disconnected in Figure B.4 and connected in Figure B.5.

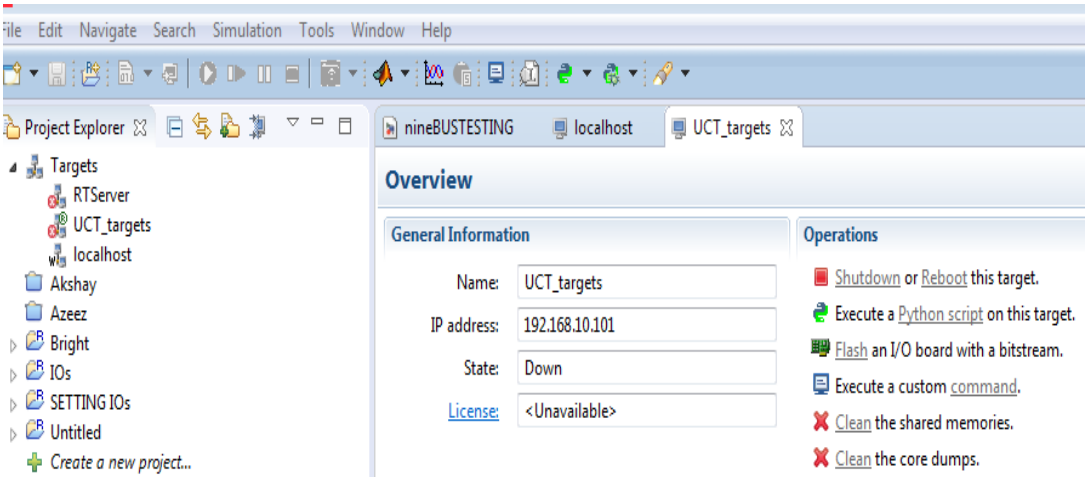

Figure B.4: RT-LAB software with the real-time target disconnected

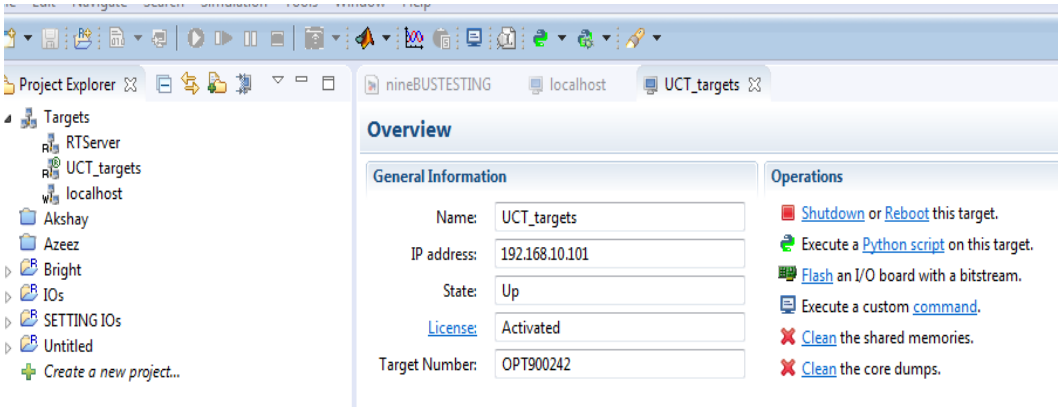

Figure B.5: RT-LAB software with the real-time target connected

B.2.2 Adding an Existing Simulink Models for Execution in Real-Time

The model created in the right form as discussed in the earlier sections may be added to an RT-LAB project for real-time execution after the target is connected. One can create a new project for the model or add it to an existing project if there is already one. There are two ways of adding a Simulink model for execution; first, the model can be imported, in this case, a copy of the model is saved in the RT-LAB software directory and therefore any changes made to the model in the RT-LAB software will not reflect on the original model, this one is recommended. Also, the model can be linked with the RT-LAB software where the original model is used from its directory and therefore there is no copy in the RT-LAB directory.

B.2.3 Editing, Setting, Building, Loading and Executing the Model

When the model is added to a project for execution on the real-time target, there are options for editing and setting execution parameters in order to get the right results. If there is nothing to be edited in the model, then the next thing before building or compiling is setting the development properties. A model that is not intended to send or receive analogue and digitals signals to external hardware, at the execution properties, the real-time simulation mode must be set to software synchronized as shown in Figure B.6. But if the model will send signals for measurement on an oscilloscope or for use in Hardware-in-the-loop testing or receive any signal from external hardware, the simulation mode must be set to hardware synchronized as shown in Figure B.7. At the assignation where we see the subsystem settings shown in Figure B.6 and Figure B.7, the eXtra High Performance (XHP) mode must be set to **OFF** for a software synchronized simulation and **ON** for a hardware synchronized simulation.

When these settings are done correctly then the model is ready for building on the target. When the model is built successfully, a message showing that the building is successful and the time it took to build will be displayed as shown in Figure B.8, for a model built in this project. After the model is successfully built the next step is to load the model and then execute.

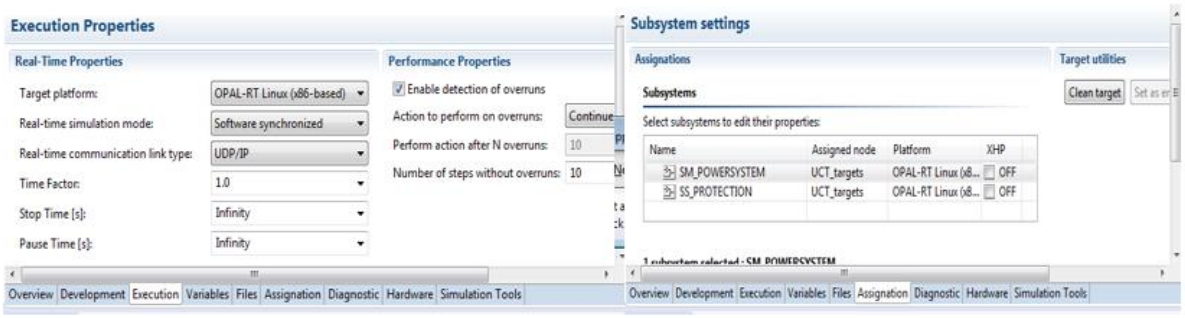

Figure B.6: RT-LAB Settings for a model designed without any input or output signals to an external hardware

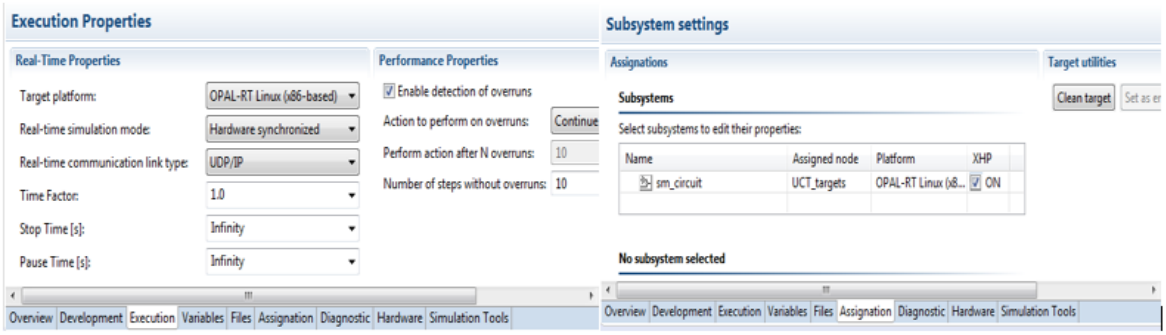

Figure B.7: RT-LAB Settings for a model designed to send or receive signals from an external hardware

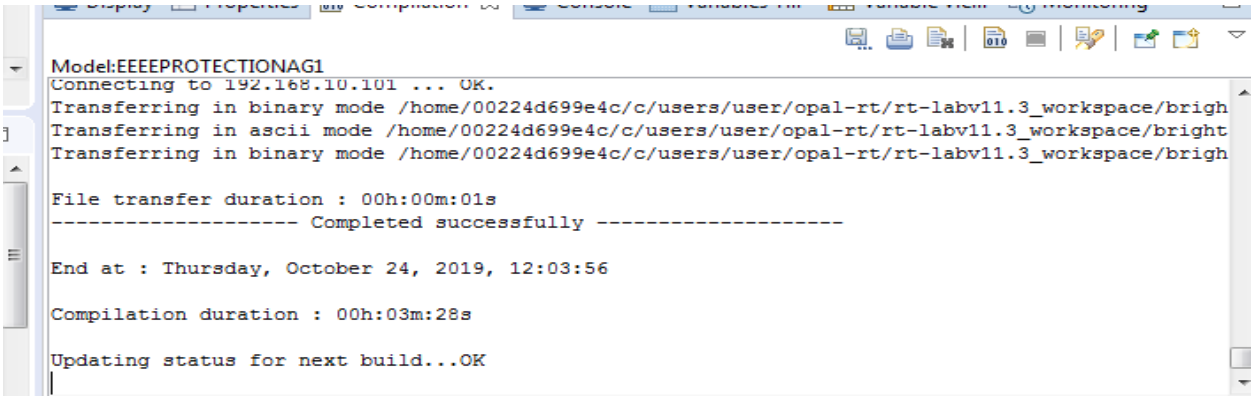

Figure B.8: A build message showing that the model has been built successfully

APPENDIX C: HIL Simulation with Opal-RT and SEL-31A Relay

C.1. Simulink I/O blocks and Model Preparation for HIL Simulation.

To measure the output signals from the real-time target with external hardware, the model created must be hardware synchronized as discussed earlier with the required blocks which are discussed in this section. The first step is that, the model to be executed in real-time and hardware synchronized must be put in a separate folder together with the bitstream (.bin) and the configuration (.conf) files. When these three (the Simulink model, the bitstream, and the configuration) files are in the same folder as shown in Figure C.1, then the model is ready for importing, editing and execution. These extra files are provided by OPAL-RT and they represent the I/O configuration as seen by the specific real-time target's FPGA.

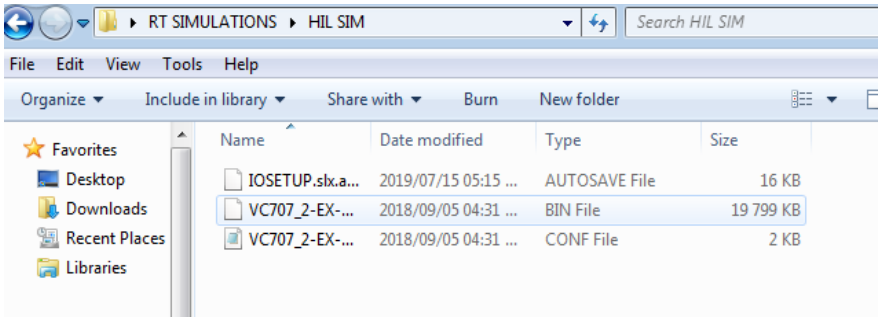

Figure C.1: Folder showing the model with the bitstream and the configuration file

When the model is imported into the RT-LAB environment, it must be edited with the necessary I/O blocks so that the real-time target can output the required signals for measurement or HIL simulation. The first block needed is an OpCtrl block which tells the model that we are going to use ML605 FPGA board in this case; which allows for driving the analog and digital I/O card located in the simulator. OpCtrl block handles synchronization and sets internal parameters. Figure C.2 shows the internal settings required for the OpCtrl block.

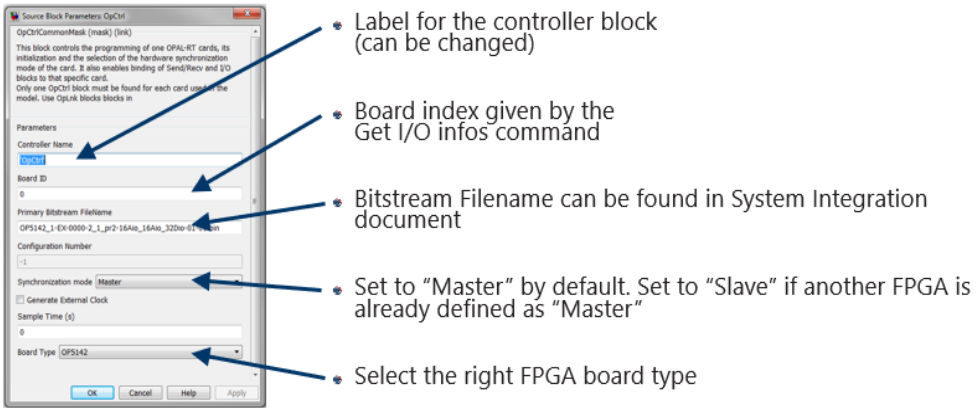

Figure C.2: Setting the requirement of an OpCtrl block [59]

In this project, the signals measured as well as used for HIL simulation are both analog and digital signals, hence the model used analog and digital inputs and outputs (I/Os) blocks. Figure C.3 shows the concept of I/Os as used in OPAL-RT real-time simulation. The Analog IN and Digital IN blocks take electrical signals from external hardware to the users' (simulation) environment, models, algorithms etc. whilst the Analog OUT and Digital OUT blocks send signals out of the

users' environment to external hardware for measurement with an oscilloscope or for HIL simulation using control hardware.

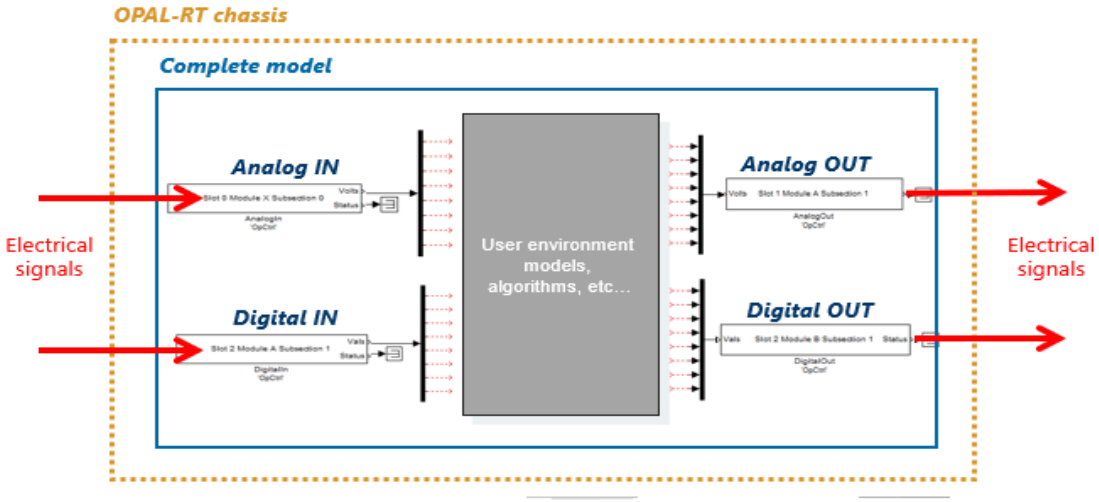

Figure C.3: The concept of Analog/Digital Inputs and Analog/Digital Outputs in OPAL-RT [59]

C.2 Adding an I/O block to the Model

This section discussed how to add Analog Input and Analog Output blocks which are used for this project, the analog is discussed, however, the same concept applies for Digital Inputs and Digital Outputs. The Analog OUT and Analog IN blocks have these internal settings which must match as described here before execution. The controller name should be the same as the OpCtrl block name, the number of channels must be set to 8 and the mux and de-mux blocks must have the same dimensions. The DataIn and DataOut port number for Analog OUT and Analog IN blocks respectively are given in the system description as shown in Figure C.4 for the real-time target used for this project.

AnalogIn block parameters		
Parameters	**CH00-07**	**CH08-15**
Controller Name	OpCtrl	
DataOut Port Number	11	12
Number of channels	8	8
Sample Time (s)	0	0

AnalogOut block parameters		
Parameters	**CH00-07**	**CH08-15**
Controller Name	OpCtrl	
DataIn Port Number	19	20
Number of channels	8	8
Voltage range	[-16 ... 16]	[-16 ... 16]

Figure C.4: The settings for analog I/O blocks parameters as given in the system data used for the project.

Digital Input block parameters				
Parameters	**CH00-07**	**CH08-15**	**CH16-23**	**CH24-31**
Controller Name	OpCtrl			
DataOut Port Number	3	4	5	6
Number of channels	8	8	8	8
Digital Input Type	• Pulse-Width Modulated Input • Static DigitalIn	• Static DigitalIn	• Static DigitalIn	• Static DigitalIn

Digital Output block parameters				
Parameters	**CH00-07**	**CH08-15**	**CH16-23**	**CH24-31**
Controller Name	OpCtrl			
DataIn Port Number	11	12	13	14
Number of channels	8	8	8	8
Digital Output Type	• Pulse-Width Modulated Output • Static DigitalOut	• Static DigitalOut	• Static DigitalOut	• Static DigitalOut

Figure C.5: The settings for digital I/O blocks parameters as given in the system data used for the project.

C.3 Taking Signals Out and Into to the Real-time Simulator

When using I/Os in the simulation, the signals generated may need to be measured, use to test control hardware or you will need to input a signal from hardware into the real-time simulator to control the simulation running in real-time. The user interface for making a connection to external hardware is the DB37 connector, knowing the full pin description of the DB37 connector is paramount to a successful connection to external hardware. These full pin descriptions for analog and digital inputs and outputs are given in the system documentation provided by Opal-RT for the particular target. The analog I/Os have 16 inputs and 16 outputs channels whereas the digital I/Os have 32 inputs and 32 outputs channels. Figure C.6 shows the pin assignment of the DB37

connector, Vuser is a reference voltage that needs to be provided by the user from an external source, this reference voltage is only required for digital out signals.

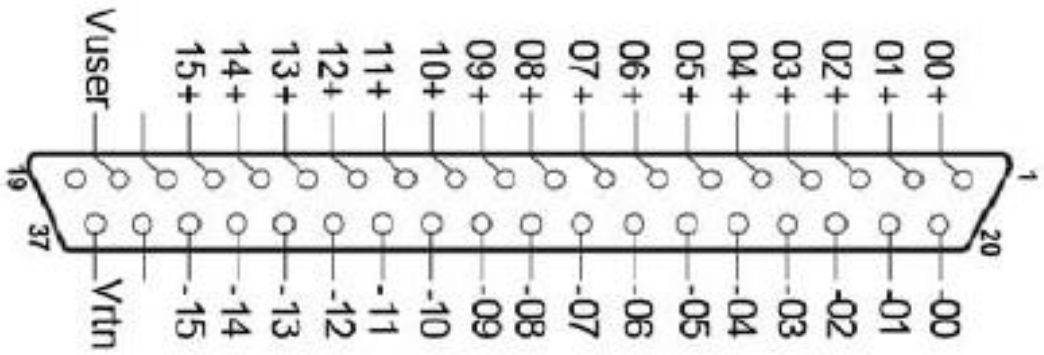

Figure C.6: DB37 connector pin assignment.

C.3.1 Measuring Signals

There are two ways of doing these; one is the loopback method which required using the loopback connector for connection at the rear and the second is using an external scope which requires RJ45 connector at the front panel, both methods can be combined together.

A. Loopback Method

The loopback method involves connecting output channels to input channels at the rear of the target (simulator) so that signals generated by the target can be acquired again by the target and monitored in the model console. Making a loopback connection for analog and digital signals are shown in Figure C.7 and Figure C.8.

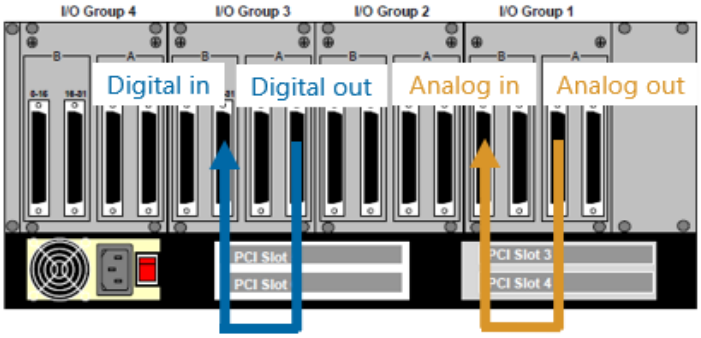

Figure C.7: Making Loopback connection at the rear of the target [59]

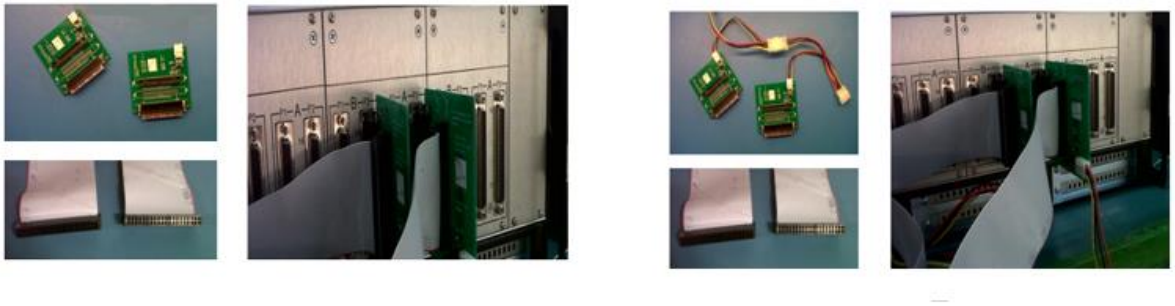

Figure C.8: Loopback connection at the rear of the OPAL-RT Chasis [59]

B. Using an External Scope

The front panel enables the measurement of output and input signals in and out of the simulator. The RJ45 cable, as well as the BNC cable, are used to make the connections as shown in Figure C.9, when using this method, there is a buffer amplifier with a gain of 0.1 which must be taken into consideration.

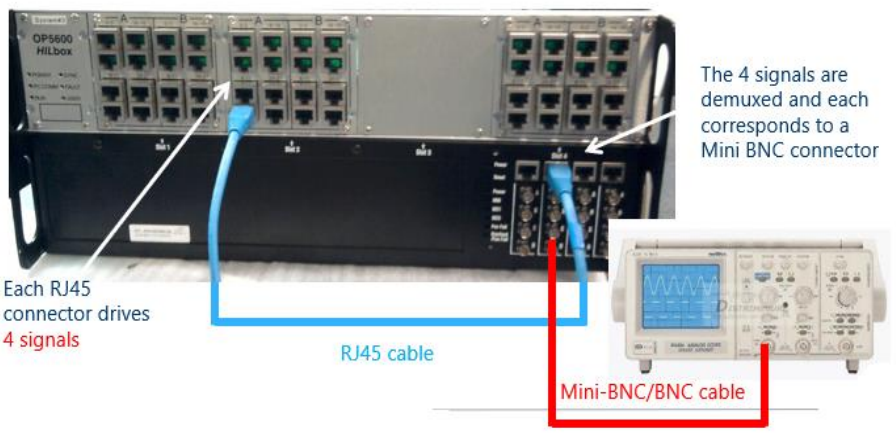

Figure: C.9 Using the scope to measure signals from OPAL-RT [59]

C.3.1 Outputting /Inputting signals to and from an external hardware

To perform hardware-in-the-loop simulation, this aspect of the real-time simulation is important since we need signals to test the control hardware as well as take signals into the simulator to perform actions on the running model. This involves using the PCB board and making the pin connection according to the system description. The pin connections are shown in Figure C.10 - C.12 for analog and digital inputs and outputs signals.

Connector P1 Ch. 0-15			
DB37	Module pin assignment	DB37	Module pin Assignment
1	+AOUT00	20	-AOUT00
2	+AOUT01	21	-AOUT01
3	+AOUT02	22	-AOUT02
4	+AOUT03	23	-AOUT03
5	+AOUT04	24	-AOUT04
6	+AOUT05	25	-AOUT05
7	+AOUT06	26	-AOUT06
8	+AOUT07	27	-AOUT07
9	+AOUT08	28	-AOUT08
10	+AOUT09	29	-AOUT09
11	+AOUT10	30	-AOUT10
12	+AOUT11	31	-AOUT11
13	+AOUT12	32	-AOUT12
14	+AOUT13	33	-AOUT13
15	+AOUT14	34	-AOUT14
16	+AOUT15	35	-AOUT15
17		36	
18	Vuser 1 A*	37	Vrtn 1 A*
19			

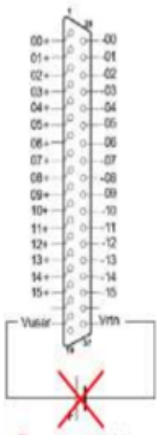

Connector P1 Ch. 0-15			
DB37	Module pin assignment	DB37	Module pin Assignment
1	+AIN00	20	-AIN00
2	+AIN01	21	-AIN01
3	+AIN02	22	-AIN02
4	+AIN03	23	-AIN03
5	+AIN04	24	-AIN04
6	+AIN05	25	-AIN05
7	+AIN06	26	-AIN06
8	+AIN07	27	-AIN07
9	+AIN08	28	-AIN08
10	+AIN09	29	-AIN09
11	+AIN10	30	-AIN10
12	+AIN11	31	-AIN11
13	+AIN12	32	-AIN12
14	+AIN13	33	-AIN13
15	+AIN14	34	-AIN14
16	+AIN15	35	-AIN15
17		36	
18	Vuser 1 A*	37	Vrtn 1 A*
19			

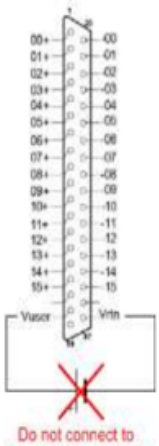

Figure C.10: Analogue 16 channel outputs and inputs connection of the DB37 connector

Connector P1 Ch. 0-15				Connector P2 Ch. 16-31			
DB37	Module pin assignment	DB37	Module pin Assignment	DB37	Module pin Assignment	DB37	Module pin assignment
1	+DOUT00	20	Vrtn 1	1	+DOUT16	20	Vrtn 2
2	+DOUT01	21	Vrtn 1	2	+DOUT17	21	Vrtn 2
3	+DOUT02	22	Vrtn 1	3	+DOUT18	22	Vrtn 2
4	+DOUT03	23	Vrtn 1	4	+DOUT19	23	Vrtn 2
5	+DOUT04	24	Vrtn 1	5	+DOUT20	24	Vrtn 2
6	+DOUT05	25	Vrtn 1	6	+DOUT21	25	Vrtn 2
7	+DOUT06	26	Vrtn 1	7	+DOUT22	26	Vrtn 2
8	+DOUT07	27	Vrtn 1	8	+DOUT23	27	Vrtn 2
9	+DOUT08	28	Vrtn 1	9	+DOUT24	28	Vrtn 2
10	+DOUT09	29	Vrtn 1	10	+DOUT25	29	Vrtn 2
11	+DOUT10	30	Vrtn 1	11	+DOUT26	30	Vrtn 2
12	+DOUT11	31	Vrtn 1	12	+DOUT27	31	Vrtn 2
13	+DOUT12	32	Vrtn 1	13	+DOUT28	32	Vrtn 2
14	+DOUT13	33	Vrtn 1	14	+DOUT29	33	Vrtn 2
15	+DOUT14	34	Vrtn 1	15	+DOUT30	34	Vrtn 2
16	+DOUT15	35	Vrtn 1	16	+DOUT31	35	Vrtn 2
17		36	DGND	17		36	DGND
18	Vuser 1	37	Vrtn 1	18	Vuser 2	37	Vrtn 2
19				19			

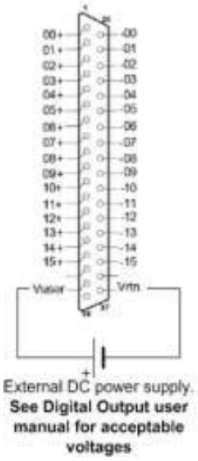

Figure C.11: Digital 32 channel outputs connection of the DB37 connector

Connector P1 Ch. 0-15				Connector P2 Ch. 16-31			
DB37	Module pin assignment	DB37	Module pin Assignment	DB37	Module pin Assignment	DB37	Module pin assignment
1	+DIN00	20	-DIN00	1	+DIN16	20	-DIN16
2	+DIN01	21	-DIN01	2	+DIN17	21	-DIN17
3	+DIN02	22	-DIN02	3	+DIN18	22	-DIN18
4	+DIN03	23	-DIN03	4	+DIN19	23	-DIN19
5	+DIN04	24	-DIN04	5	+DIN20	24	-DIN20
6	+DIN05	25	-DIN05	6	+DIN21	25	-DIN21
7	+DIN06	26	-DIN06	7	+DIN22	26	-DIN22
8	+DIN07	27	-DIN07	8	+DIN23	27	-DIN23
9	+DIN08	28	-DIN08	9	+DIN24	28	-DIN24
10	+DIN09	29	-DIN09	10	+DIN25	29	-DIN25
11	+DIN10	30	-DIN10	11	+DIN26	30	-DIN26
12	+DIN11	31	-DIN11	12	+DIN27	31	-DIN27
13	+DIN12	32	-DIN12	13	+DIN28	32	-DIN28
14	+DIN13	33	-DIN13	14	+DIN29	33	-DIN29
15	+DIN14	34	-DIN14	15	+DIN30	34	-DIN30
16	+DIN15	35	-DIN15	16	+DIN31	35	-DIN31
17		36	DGND	17		36	DGND
18	Vuser 1	37	Vrtn 1	18	Vuser 2	37	Vrtn 2
19				19			

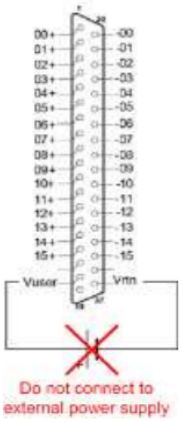

Figure C.12: Digital 32 channel inputs connection of the DB37 connector

APPENDIX D: Analysis of different Types of Faults on a Simple Power Systems

A simulation was carried out to analyze the behavior of different types of faults that occur in the power system and these were tested using power systems of different number of buses. Figure D.1 and Figure D.2 show the power systems simulated and Table D.1 – Table D.2 show the values obtained from the simulations for no fault conditions and fault conditions.

The results in Table D.1 and Table D.2 indicate that the symmetrical faults (L-L-L and L-L-L-G) which are the faults of the highest magnitude that can occur are identical and even have similar values. The fault current is high at the bus closets to the fault and this characteristic is used for overcurrent protection setting in the power system.

Further, across all scenarios considered as shown in Table D.1 to Table D.2, it was observed that using only the variation in current or voltage for fault detection can be sometimes misleading and affect the security and dependability of the protection system. Therefore, in most protection algorithms different parameters are being used for fault detection. These parameters include positive sequence current or voltage magnitude, sequence angle etc.

A. A Two Bus Power System with Fault at One Bus

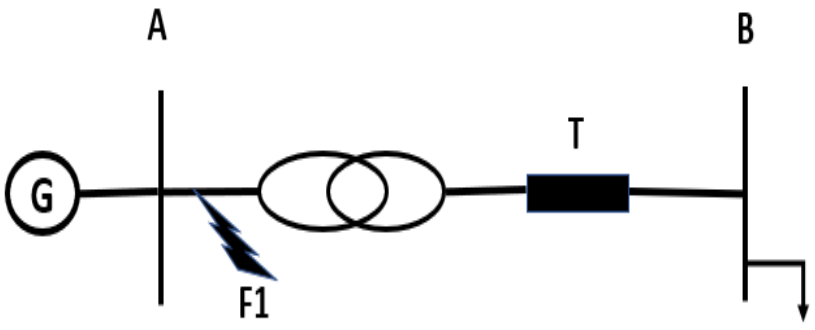

Figure D.1: Two bus power system with fault simulation on bus A only

Table D.1 Voltages and currents of a two-bus power system with no fault and fault conditions

Type of Fault	Voltage (p.u)	Current (p.u)
No fault	1.048	0.8684
L-L(a-b)	0.9875	3.908
L-L(a-c)	0.845	4.509
L-L(b-c)	0.1425	0.894
L-L-L(a-b-c)	0.000194	4.849
L-L-L-G(a-b-c-g)	0.000194	4.849
L-G(a-g)	1.146	1.224
L-L-G(a-b-g)	1.195	3.952

B. A Two Bus Power System with Fault at both Buses

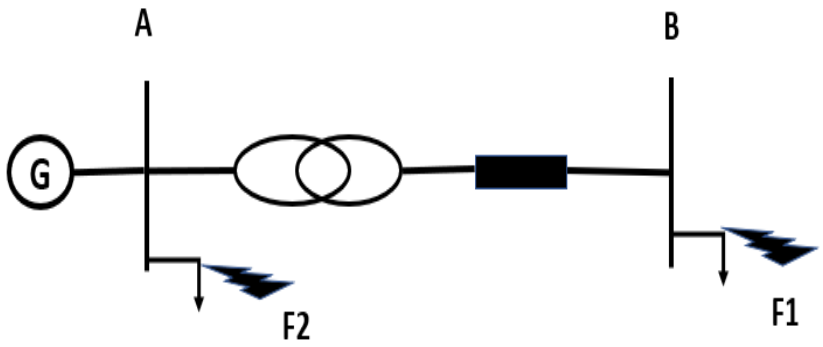

Figure D.2: Two bus power system with fault simulation on both buses

Table D.2: Voltages and currents of a two-bus power system with no fault and fault conditions on both buses

Fault	Bus	No-Fault		L-L-L (a-b-c)		L-L-L-G (a-b-c-g)		L-L (a-b)		L-L (a-c)		L-L (b-c)		L-L-G (a-b-g)		L-G (a-g)	
		V	I	V	I	V	I	V	I	V	I	V	I	V	I	V	I
F1	A	1.048	0.86	1.02	0.81	1.02	0.81	1.1	0.9	1.0	0.85	1.0	0.6	1.1	0.95	1.1	0.96
	B	**0.95**	**0.39**	**4e-5**	**0.46**	**4e-5**	**0.46**	**0.81**	**0.52**	1e-2	0.4	0.83	0.34	0.52	0.52	0.57	0.48
F2	A	1.048	0.86	1.9e-4	4.849	1.9e-4	4.849	0.98	3.9	0.84	4.5	0.142	0.89	1.19	3.9	1.1	1.2
	B	**0.95**	**0.39**	1.7e-4	7e-5	1.7e-4	7e-5	0.81	0.33	1e-2	7e-3	0.83	0.34	0.7	0.32	0.92	0.39